CYTOKINE PROFILES AND VIRAL REPLICATION WITHIN THE THYMUSES OF NEONATALLY FELINE IMMUNODEFICIENCY VIRUS-INFECTED CATS

By

HOLLY MEREDITH KOLENDA-ROBERTS

A DISSERTATION PRESENTED TO THE GRADUATE SCHOOL
OF THE UNIVERSITY OF FLORIDA IN PARTIAL FULFILLMENT
OF THE REQUIREMENTS FOR THE DEGREE OF
DOCTOR OF PHILOSOPHY

UNIVERSITY OF FLORIDA

2006

ACKNOWLEDGMENTS

I would like to thank Dr. Calvin Johnson for creating a wonderful working and learning environment, and for all of his ongoing support and wisdom.

I would like to thank Dr Ayalew Mergia for agreeing to supervise my research and act as my committee chairman after Dr. Johnson's transfer to Auburn University. He helped smooth the transition and provided a supportive environment for the completion of this project.

My deepest appreciation goes to my supervisory committee comprising Dr. Pamela Ginn, Dr. Maureen Goodenow and Dr. Steeve Giguere for their valuable time, interest in the project, professionalism and advice. My sincerest appreciation also goes to Debbie Couch and Sally O'Connell, who have helped me with countless day-to-day issues with a smile and without whom I couldn't have even registered for classes. I would like to thank George Papadi, Abigail Carreño and Peter Nadeau for their support in the lab, advice and technical assistance.

And I would like to thank Janelle Novak, my Siamese twin, for making coming to work fun. My project benefited from our discourse.

TABLE OF CONTENTS

LIST OF TABLES

LIST OF FIGURES

Abstract of Dissertation Presented to the Graduate School
of the University of Florida in Partial Fulfillment of the
Requirements for the Degree of Doctor of Philosophy

CYTOKINE PROFILES AND VIRAL REPLICATION WITHIN
THE THYMUSES OF NEONATALLY FELINE
IMMUNODEFICIENCY VIRUS-INFECTED CATS

By

Holly Meredith Kolenda-Roberts

December 2006

Chair: Ayalew Mergia
Major: Veterinary Medical Sciences

Reported in these studies are immunological, virological and cytological changes within the thymuses of cats infected with feline immunodeficiency virus (FIV) at birth, an important animal model for human immunodeficiency virus infection.

The objective of the first study was to identify the genetic sequences encoding the cytokine mRNAs of interest. Elucidation of the five investigated cytokine sequences was successful, and results were verified against known sequences in other species.

Cytokine sequences were used to design primers and probes for use in the next experiment. Real-time reverse transcription-polymerase chain reaction (RT-PCR) was used to assess changes in mRNA expression that occurs *in vivo* at acute, intermediary and chronic stages of neonatal FIV infection when compared to age-matched controls. The concurrent proviral load and viral gene expression were measured. Compiled cytokine and viral data were analyzed with the corresponding necropsy data from the experimental

animals to find correlations between pathological changes to the immune system and the relative levels of cytokines. A loss of mRNA expression of interleukin (IL)-4, IL-7, interferon (IFN)-α and IFN-γ was observed in chronic infection, and the decreases in IL-7, IFN-α and IFN-γ were positively correlated with the loss of thymocytes observed with FIV infection. Levels of IFN-γ were positively correlated with viral gene expression.

The loss of IFN-α expression, a molecule with antiviral properties, was further investigated. A major cell producer of IFN is the plasmacytoid dendritic cell (PDC), so immunohistochemistry (IHC) was performed in order to detect this cell in thymus samples. It was determined that this cell type is present in inflammatory germinal centers of the infected thymuses, and that they harbor FIV gag RNA, which may result in lytic infection, functional loss and decreased IFN-α mRNA expression.

Attempts to productively infect fetal thymocytes with FIV in order to evaluate potential protective effects of IFN-α treatment were unsuccessful. This supported our IHC analysis of thymuses for viral protein, which showed that only mature cells within germinal centers and the thymic medulla were infected. This study indicates that further FIV research regarding thymic PDC, IL-7 and IFN expression is warranted.

CHAPTER 1
INTRODUCTION

Human Immunodeficiency Virus

In 2005, it was estimated that over 40 million people globally were infected with human immunodeficiency virus (HIV), including 2 million children (UNAIDS/WHO, 2005). There were approximately 700,000 new infections and 570,000 deaths in children in 2005. The rates of infection, disease spread and mortality continue to exceed predictions. While the introduction of highly active retroviral therapy (HAART) has improved individual disease progression, overall mortality has leveled off after improvements noted in 1996-1997. The production of a successful vaccine for HIV remains elusive, and further investigation of the pathogenesis of the disease is being used to further elucidate potential therapeutic targets.

Most pediatric HIV cases are a result of vertical transmission from infected women, and can occur *in utero*, during birth or after the ingestion of infected milk, with the greatest number occurring during the peripartum/neonatal period (Khoury, 2001). Pediatric infection occurs at a time of immunological immaturity, with a third of cases having rapidly progressive disease. Children have a higher incidence of neurologic abnormalities, cardiomyopathy, and pulmonary complications including lymphoid interstitial pneumonia. As the course of infection is related to degree of immunological development and the resulting host response to infection, a greater understanding is needed of the age-related factors impacting lentiviral pathogenesis.

Animal Models for HIV Infection

One of the preeminent goals in HIV research is to develop a suitable animal model for infection, where infection can be controlled and tissues can be obtained for study throughout the course of infection. HIV, feline immunodeficiency virus (FIV) and simian immunodeficiency virus (SIV) all belong to the lentivirus genus of retroviruses. Clinical disease associated with these agents is characterized by progressive deterioration of the host immune function, ultimately leading to acquired immunodeficiency syndrome (AIDS) (Levy, 2006). The similarities between the viruses and their clinical courses have prompted the use of SIV (Haigwood, 2004; Kimata, 2006) and FIV (Willett BJ, 1997; Burkhard, 2003) as animal models of AIDS pathogenesis. Both viruses exhibit tropism for many cells of the immune system, including the $CD4^+$ subset of T lymphocytes which are responsible for much of the cell signaling and initiation of the acquired immune response. As the number of $CD4^+$ cells dwindles within the course of infection, the host becomes susceptible to opportunistic infections and degenerative disorders, ultimately leading to the death of the host. As the use of the primate model can be cost prohibitive, and primate experiments are generally limited in the number of animals available for study, FIV therefore offers an attractive alternative.

Neonatal FIV Infection

In an experimental animal model such as the cat, tissue is available for examination, timing of inoculation is known in relation to the disease course, the effects of the virus in relation to stage of parturition are identifiable and uninfected littermates are available as a control for environmental and maternal effects. In experiments with the Petaluma strain of FIV, neonatally infected animals exhibited a persistent generalized lymphadenopathy, a more profound neutropenia, a persistent decrease in CD4+/CD8+ T

lymphocyte ratio, and decreased CD4+ T cell count when compared to cats infected as adults (George, 1993). When compared to age-matched controls, other experiments using the Petaluma stain appear to produce variable effects. In one study infection caused decreases in CD4+ cells and increases in CD8+ T cells, but weight gain in kittens was not impaired (Power, 1998). However, Johnston et al. did not measure significant decreases in CD4+ T cell counts though the same strain was used (2002). The highly pathogenic molecular clone JSY3 (derived from the NCSU-1 strain) produces a reduction in CD4+ T cell numbers and CD4+/CD8+ T cell ratio (Orandle, 2000; Norway, 2001) that is partially abrogated with an inactivating mutation of the ORF-A gene (Norway, 2001). Similar changes in CD4+ T cells and CD4+/CD8+ T cell ratios were observed with pFIV-PPR (Phipps, 2000).

The Thymus

The thymus is the major site of production for the mammalian immune system's T lymphocytes, which are the major cellular target for the lentiviruses. Replacement of these cells as they are lost in the course of infection is by cell division within the periphery and *de novo* production by the thymus. As recent thymic emigrants (RTEs) display novel genetic rearrangements for the T cell receptors (TCRs), these cells maintain the repertoire by which the immune system can respond to diverse foreign antigens. Therefore one of the major factors in the progression of disease is the loss of the thymus's ability to replace lymphocytes during immunosuppression. The thymus and the impact of HIV infection has been extensively reviewed, and it has been shown that the thymus is directly infected by the lentivirus, resulting in thymocyte depletion and varying degrees of inflammation (Ye, 2004; Hazra, 2005; Meissner, 2003; de la Rosa, 2003; Robertson, 2003; al Harthi, 2002). Treatment of HIV infection with highly active

antiretroviral therapy (HAART) does not fully restore thymic function and normal numbers of circulating T cells. Recovery of circulating CD4+ T cells in response to successful viral suppression with HAART appears dependent on thymic function (Fernandez, 2006). The pathogenesis of the thymic infection is an important component to consider when intending to promote immune reconstitution.

At birth, the human thymus is active, generating the cohort of T cells for the developing immune system. The thymus continues to increase in size until puberty, after which it undergoes progressive involution (Aspinall, 2000). Newly produced T cells contain excised loops of DNA (TCR rearrangement excision circles, TRECs) that are generated during the genetic rearrangements necessary for surface T cell receptor (TCR) expression (Steffens, 2000). Compared to uninfected children, vertically infected HIV-positive children were shown to have lower levels of TRECs in peripheral blood mononuclear cells (PBMC), indicating impaired thymic output, and this decrease was not directly related to viral load (Correa, 2002). As children tend to have higher viral loads and faster disease progression, it has been suggested that these trends may be related to thymic dysfunction and early involution (Ye, 2004). As overall direct viral infection of thymocytes is low, the pathogenetic mechanisms behind thymic infection need to be better understood.

Thymic FIV Infection

As in its overall immune pathophysiology, FIV exhibits similar effects within the thymus of neonatal cats as HIV has been shown to cause in the thymus of children, and adequately models this disease process. Neonatal thymus infection with FIV results in a reduction of thymus-body weight ratio, selective depletion of CD4+CD8+ thymocytes, cortical atrophy, infiltrations of B cells, formation of lymphoid follicles and deformation

of the thymic architecture (Orandle, 1997; Orandle, 2000; Norway, 2001; Johnson, 2001). Interestingly, these changes were not ameliorated with effective antiretroviral therapy in juvenile cats (Hayes, 2000) or with a mutation of the ORF-A gene that yielded lower viral replication and a lower thymic proviral load (Norway, 2001), suggesting that host factors and inflammatory processes may be significant factors in the disease process and thymic disruption. Thymic infection was associated with the emergence of CD8+ T cells expressing $CD8\alpha^{+}\beta^{low}$ and $CD8\alpha^{+}\beta^{neg}$ phenotypes (Orandle, 2000; Crawford, 2001), but these cells were not found to correlate with reduction in viral load (Crawford, 2001). Immunohistochemistry of thymic samples showed significant staining for IgG outside of lymphoid follicles that did not correlate with positive staining for a B cell marker, suggesting that thymocytes are coated with antibody (Orandle, 1997). Infection was associated with a 10-fold increase in the expression of interferon (IFN)-γ mRNA within PBMC and within thymic samples in perivascular areas, along the corticomedullary junction and adjacent to lymphoid follicles (Orandle, 2000). As with HIV, the overall number of FIV expressing cells within the thymus was low, and the lowest incidence of productive infection correlated with the most severe histologic lesions (Johnson, 2001).

Cytokines

Cytokines are chemical mediators that are released by cells that result in altered cell function in the target population. A highly regulated combination of cytokines is elaborated by cells of the immune system and used to coordinate the overall response to foreign antigen. HIV infection has been shown to cause a significant impact on host cytokine profiles. These changes are believed to be associated with the increased programmed cell death (apoptosis) within uninfected T cells (Badley, 1997), chronic immune system stimulation (McCune, 2001), defective cell-mediated immunity, and

impairment of the immune system's regenerative capacity (Neben, 1999) that have been observed in HIV infected people. Modified cytokine production is likely involved in all of the aforementioned pathologic features, whether secondary to the disease process or acting as an inciting mechanism.

Thymopoiesis is dependent on a sensitive microenvironment and is regulated by direct cellular interactions and paracrine cytokine production. Many cytokines used in the immune response by mature cells are used for alternate functions within the thymus, such as thymocyte selection and to promote cell survival. The thymus is a primary lymphoid organ that normally contains relatively few mature lymphocyte populations and active germinal centers, and the introduction of inflammatory processes impacts the cytokine milieu, thymopoiesis and viral replication.

Goals of Study

The purpose of this research was to identify immunological factors that impact FIV infection within the neonatal thymus. A greater understanding of FIV thymic immunopathogenesis would allow for potential manipulation of cytokines in a way that would promote thymopoiesis and immune reconstitution, while not contributing to increased viral replication.

In the following chapters, thymic cytokines will be discussed in detail (Chapter 2). Several objectives were developed for this research project and are addressed in the following chapters: 1. Discovery of mRNA sequences for interleukin (IL)-7, IL-4, IL-15, interferon (IFN)-α, and IFN-γ (Chapter 3); 2. Measurement of interleukin (IL)-7, IL-4, IL-15, interferon (IFN)-α, and IFN-γ mRNA expression levels within the thymus of neonatally FIV-infected animals and age-matched controls at 3 time points correlating with acute and chronic infection (Chapter 4); 3. Determination of cytokine alterations

which correlate with changes in viral load and replication, influx of inflammatory cells and thymocyte depletion (Chapter 5); 4. Demonstration of changes in inflammatory cell populations, interferon production and viral distribution using immunohistochemistry (Chapter 6); 5. Assessment of FIV infection of cultured thymocytes (Chapter 7). The hypothesis of this study is that alterations in cytokine mRNA expression occur as a result of FIV infection of the pediatric thymus, and that these changes correlate with changes in FIV viral replication, local inflammatory cell populations and T cell production by the thymus.

CHAPTER 2
LITERATURE REVIEW

Cytokines are chemical mediators used to influence cell survival and function. Many of the cytokines used by the thymus have alternate functions when elaborated in the periphery and within secondary lymphoid organs. Changes in the local production of these molecules have a potential impact on further T cell production, the ability of the immune system's inflammatory cell populations to successfully combat the viral infection, and viral replication itself.

Interleukin-7

Interleukin (IL)-7 has been proven to have multiple effects on immune system cells. In peripheral lymph nodes of mice, increased IL-7 production has been shown to cause marked increases in the numbers of immature B cells ($B220^{+}Ig^{-}$, which differentiate into antibody-secreting cells) and T cells (particularly cytotoxic $CD8^{+}$ cells, which are responsible for direct cellular killing in target cells such as virus-infected cells) (Mertsching, 1995). In addition to cytotoxic T cells, IL-7 causes proliferation of natural killer cells, which are also responsible for direct cell killing of virus-infected cells (Or, 1998). Within the thymus (the site of development and selection of immature T cells) IL-7 appears to have multiple effects on maturing T cells. If added very early in T cell development ($CD3^{-}CD4^{-}CD8^{-}$ cells), IL-7 causes an increased expression of a high-affinity receptor for another cytokine, IL-2, an inducer of T-cell proliferation (Morrissey, 1994). Within the thymus IL-7 has also been shown in mice to cause expansion of newly differentiated and selected $CD4^{+}$ and $CD8^{+}$ thymocytes (Hare, 2000).

Studies of HIV patients have revealed that as the circulating $CD4^+$ cell count drops, the concentration of plasma IL-7 increases in proportion to the cell loss (Napolitano, 2001). In children infected with HIV, IL-7 levels were higher in HIV-infected children, and higher IL-7 levels were associated with lower CD4+ T cell counts and lower TREC values (Resino, 2005). In addition, increased plasma IL-7 levels in pediatric infection appeared to correlate with the emergence of more virulent strains of HIV (Resino, 2005; Kopka, 2005).

Immunohistochemistry of patient lymph nodes revealed strong expression of IL-7 by dendritic cells of depleted parafollicular T cell areas (Napolitano, 2001). The authors proposed that cells such as these "sensed" a drop in the lymphocyte population within the periphery, and that IL-7 was produced to stimulate thymopoiesis in a compensatory feedback loop. However, it has also been shown that the receptor for IL-7 (IL-7Rα) is downregulated on T cells with HIV infection, and loss of the receptor was associated with increased plasma IL-7 concentrations and decreased numbers of CD4+ T cells (Rethi, 2005). *In vitro*, reduced receptor expression correlated with decreased Bcl-2 expression and decreased cell survival in these cells. IL-7 has also been shown to augment Fas-mediated apoptosis in HIV-infected CD4+ and CD8+ T cells (Lelievre, 2005).

Ongoing studies are investigating the utility of IL-7 as a treatment modality. Preliminary studies using SIV-infected macaques undergoing antiviral therapy have shown increases numbers of memory and newly generated T cells in response to injection with IL-7 without a corresponding increase in viral load (Beq, 2006). However, conflicting data would suggest IL-7 may promote viral replication. Napolitano, et al.

showed increased viral load associated with increased plasma IL-7. In support of this finding, others that have found IL-7 actually augments infection of thymocytes and fetal thymic organ culture *in vitro* (Pedroza-Martins, 2002; Uittenbogaart, 2000). IL-7 was shown to be a potent reactivator of HIV replication in latently HIV-infected CD4+ T lymphocytes (Wang, 2005). In addition, with thymocyte depletion, it is likely that IL-7 is relatively increased in the thymic microenvironment. As an excess of IL-7 has been shown to expand double negative (DN) CD4-CD8- populations while inhibiting the production of double positive (DP) CD4+CD8+ thymocytes (DeLuca, 2002). Overabundance of this cytokine may be contributing to the decrease in the DP thymocytes seen in lentivirus infection. Further study is necessary to determine the overall impact and efficacy of IL-7 in the treatment of HIV.

Interleukin-4

IL-4 is another multifunctional cytokine utilized by the immune system, and it exhibits varying effects within the peripheral immune system and the thymus. Within the thymus, IL-4 exposure causes direct changes in the phenotype of responsive cells, inducing expression of CD45RA on a variety of thymocyte subpopulations (Uittenbogaart, 1990). IL-4 was shown to be as effective as IL-7 in promoting conversion of intermediate $CD4^{+}8^{-}$ thymocytes into $CD4^{-}8^{+}$ cells, and IL-2, -4, and -15 were as effective as IL-7 in promoting functional competence as measured by proliferative responses to CD3 + CD28 stimulation (Yu, 2003).

Within the periphery, IL-4 is one of the major cytokines responsible for polarizing the immune system in response to antigen toward humoral or cellular immunity. Production of IL-4 causes CD4+ T-cell differentiation to the Th2 phenotype (as opposed to the Th1, involved in cellular immune responses), and these cells in turn produce more

IL-4 (Santana, 2003). One of the key immunological observations in HIV infections is the shift from a Th1 response to a Th2 response, characterized by increased numbers of IL-4-secreting cells (Klein, 1997), which is clearly unsuitable for ongoing viral infection and the maintenance of the critically important cell-mediated immunity. IL-4 was found to be produced by CD8+ T cells in HIV-infected patients undergoing HAART with high viremia, and levels were increased with the presence of opportunistic infections (Sindhu, 2006; Rodrigues, 2005). And, as mentioned previously, studies on viral replication in thymocyte cultures and fetal thymic organ culture showed that IL-4, by itself or particularly in conjunction with IL-7, increased HIV viral replication (Pedroza-Martins, 2002; Uittenbogaart, 2000). Using thymic and liver implants in mice with severe combined immunodeficiency (SCID-hu model), infection with HIV was not associated with changes in IL-4 mRNA production (Koka, 2003). Interference with IL-4 production using anti-sense IL-4 DNA suppressed viral replication of simian-human immunodeficiency virus (SHIV, hybridized viral strain) in CD4+ T cells, macrophages and *in vivo* in macaques (Dhillon, 2005).

Interleukin-15

Interleukin-15 is a cytokine closely related to IL-2, which is commonly used in laboratories for preservation and proliferation of lymphocytes in culture systems. IL-2 and IL-15 are structurally similar, share two receptor subunits (IL-2Rβ and the common γ chain) and has been shown to share many immune system functions. IL-15 is believed to act as a regulator of CD8+ T cell homeostasis, and studies have shown IL-15 deficiency can result in a decreased magnitude of CD8+ T cell expansion with stimulation, resulting in fewer memory cells (Prlic, 2002). IL-15 is also believed to be responsible for basal proliferation of CD8+ memory cells necessary for maintenance of these cells within the

host. IL-15 has been shown to be important for expression of the antiapoptotic protein Bcl-2 in CD8 T cells, suggesting IL-15 may also help with CD8+ T cell survival. So while IL-2 is involved in elimination of T cells through activation-induced cell death (AICD), IL-15 serves to prevent apoptosis (Waldmann, 2002). Where IL-15 stimulates the persistence of memory CD8+ T cells, IL-2 inhibits their expression. As further research such as this emerges regarding IL-15, it will potentially be considered a more suitable cytokine to stimulate immune reconstitution in AIDS patients. As cell-mediated immune responses (largely CD8+ T cell-mediated) are critical in the long-term control of HIV, understanding the role of IL-15 in the immunopathology of AIDS will need to be elucidated.

In vitro studies with human peripheral blood mononuclear cells has shown that treatment with the Nef protein of HIV causes early up-regulation of IL-15 by monocytes in response to an infectious agent, and this production of IL-15 inhibited subsequent antibody production (Giordani, 2000). In contrast to these findings, blood levels of IL-15 were decreased in HIV-infected people (Ahmad, 2003). Stimulated PBMCs from untreated HIV patients and patients with HAART failure showed significantly impaired IL-15 production when compared to healthy donors or HAART-responsive patients (d'Ettorre, 2002). While there was not increased viral replication in PBMCs treated with IL-15, the combination of IL-15 and IL-2 together did result in significant increases in viral production. In HIV patients with pulmonary infiltration by CD8+ T cells (lymphocytic alveolitis), IL-15 was implicated in up-regulation of interferon-γ and tumor necrosis factor-α (inflammatory cytokines), infiltration and proliferation of T cells within the lung and up-regulation of accessory, co-stimulatory B7 molecules CD80 and CD86

on alveolar macrophages (Agostini, 1999). In addition, compartmentalization of CD8+ T cells within the enlarged lymph nodes of SIV-infected monkeys corresponded to increased RNA expression of IL-7 and IL-15 within these tissues (Caufour, 2001). Treatment of SIV-infected macaques with IL-15 resulted in 3-fold expansion of NK cells and a 2-fold increase in CD8+ T cells, particularly the effector memory subset, with no concurrent increase in plasma viremia (Mueller, 2005).

Interferon-γ

Bacteria, protozoa and perhaps viruses trigger monocytes/macrophages to produce IL-12, which in turn promotes T cell activation and IFN-γ production. IFN-γ is considered a "pro-inflammatory" cytokine that is produced by activated T lymphocytes (CD4+ and CD8+) and natural killer cells (Young, 2006). It is considered important to both the innate and adaptive immune systems, and plays a particularly important role in activating macrophages and neutrophils. IFN-γ promotes T and B cell proliferation, MHC I and II expression, causes augmentation of NK cell lytic function and suppresses IL-4 responses. IFN-γ is one of the cytokines measured to identify a Th1 response (cell-mediated immunity), in contrast to IL-4 and a Th2 response (Corthay, 2006). IFN-γ plays a role in expression of NF-κB, and is considered a necessary component of several inflammatory and autoimmune conditions. However, IFN-γ can also cause apoptosis in certain populations of cells (hepatocytes, B lymphocytes, monocytes/macrophages, activated T cells, tumor cells) and inhibit production of other pro-inflammatory cytokines, IL-1 and IL-8, conferring it anti-inflammatory and regulatory functions as well (Muhl, 2003). In this way, IFN-γ may down-regulate the activated immune system and aid in resolving inflammation.

Initial infection by lentiviruses induces an expansion of virus-specific, IFN- γ-producing CD8+ T cells that corresponds to a decline in plasma viremia. However, in chronic infection HIV-specific CD8+ T cells were shown to have decreased ability to generate IFN- γ, even though CTL numbers remained adequate, and this dysfunction was not corrected when HAART therapy was instituted (Onlamoon, 2004). Serum IFN- γ levels were found to be reduced in chronically HIV-infected individuals as compared to controls, though values tended to be higher if concurrent opportunistic infections were present (Sindhu, 2006). NK cells from patients with progressive HIV infection demonstrated lower IFN- γ production in response to a CpG oligodeoxynucleotide (Saez, 2005). HIV-specific IFN- γ production by CD 4+ T cells was associated with lower plasma viral RNA and proviral load in peripheral blood mononuclear cells (PBMCs), and this response, in combination with IgG2 antibody production, was the best predictor for longterm nonprogressors to disease (Martinez, 2005). It has been suggested that HIV-infected children have decreased IFN- γ-producing CD8 T cell responses, and that this may contribute to persistent high levels of viral replication after neonatal infection (Buseyne, 2005).

Macrophages in HIV patients exhibit deficiencies in oxidative burst activity and phagocytosis. *In vitro* these effects can be counteracted by treatment with IFN-γ, and treatment of HIV-infected patients with IFN-γ results in decreased incidence of opportunistic infections (Murphy, 1988; Reed, 1992; Kedzierska, 2003). IFN-γ is currently being investigated as a treatment modality for opportunistic infections in HIV patients.

Interferon-α

Type I interferons, such as IFN-α, are produced when cells are exposed to viral products, particularly dsRNA. The interferons are secreted, and binding to the IFN receptor triggers the Jak/STAT pathway of intracellular signaling (Cebulla, 1999). This, in turn, induces the transcription of IFN-stimulated genes (ISG). Interferons as a group can induce more than 300 cellular proteins, which depends on the IFN signal and the target cell type. Through IFN-triggered 2-5(A) synthetase activity, RNaseL produces antiviral and anticellular effects, often influencing apoptosis (Samuel, 2001). Activation of ISG56, which encodes for P56, results in the binding of translation initiation factor eIF-3, blocking protein synthesis. PKR has been shown to have many functions, which ultimately affect cell functions, cell growth and apoptosis. Induction of the P200 family of genes causes decreased transcription of rRNA and impairs cell proliferation. So, many of the effects of interferons are directly aimed at viral replication (Sen, 2001). Type I interferons (IFN-α/β) work in conjunction with IL-12 and Type II interferons (IFN-γ) to suppress Th2 cells (Durbin, 2000). IFN-α has also been shown to support the differentiation of cytotoxic T lymphocytes and induce CTL responses (von Hoegen, 1995).

IFN-α is produced during HIV infection, and increased IFN levels correlate with diminished levels of virus and rises in CD4+ T cell count (Poli, 1991). In culture systems, type I interferons have been shown to inhibit different stages of the HIV life cycle, and IFN-α strongly inhibits FIV replication in feline PBMC (Tanabe, 2001). HIV-1 has been shown to be able to block IFN-induced function through the Tat protein, which competitively binds PKR, and TAR RNA can block PKR activation (Sen, 2001). In HIV infection, the progressive loss of IFN-α highly correlates with disease progression

and the onset of opportunistic infections. Observations of HIV in the natural course of disease showed loss of interferon generation and low CD4+ T cell counts are required for opportunistic infections to occur. Preclinical and early clinical trials are underway using IFN-α to treat HIV (Jablonowski, 2003). Also, IFN-α is being investigated for use as a multiple cytokine therapeutic modality, particularly to counteract the increases in replication seen with use of proliferation-inducing cytokines. *In vitro*, combination treatment of IFN-α and IL-7 strongly inhibited HIV replication while preserving T cell numbers, increasing T cell proliferation and IFN-γ production (Audige, 2005).

Interferon-Producing Cells

Recently, it was determined that the professional Type I IFN-producing cell type (IPC) is the previously identified plasmacytoid dendritic cell (Siegal, 1999). The hematological origin of these cells has been controversial, and it was determined that these cells express CD4 and MHC class II, and are negative for other lineage markers such as CD3 (T cells), CD19 (B cells), CD14 (monocytes), CD56 (NK cells) and CD11c (monocyte-derived type 1 dendritic cells). Manipulation and isolation of these cells was made difficult by their rarity (0.01% to 0.05% of PBMC) and rapid apoptosis in culture. These cells were found to be recruited in significant numbers to inflamed lymph nodes, and can be found in T cell areas and within germinal centers (Cella, 1999). IPCs are triggered by viruses and other pathogens, more specifically by CpG oligonucleotide binding to toll-like receptor (TLR) 9 (Colonna, 2002).

In vitro, IPCs have been shown to become directly and productively infected with the HIV virus, and HIV infection triggers IFN-α secretion and decreases viable cell numbers (Yonezawa, 2003; Loré, 2005; Schmitt, 2006). Interaction with HIV viral

components triggers immature IPCs to mature, exhibit more cytoplasm with dendritic processes and express CD80 and CD86 (Yonezawa, 2003). IPC are induced to replicate the HIV virus upon ligation of CD40L, and can infect naïve T cells in *trans* (Fong, 2002; Loré, 2005). Chronically HIV-infected patients have decreased numbers of IPCs in the peripheral blood, and lower CD4+ T cell counts correlated with decreased numbers of IPCs (Feldman, 2001). The progressive loss of functional IPCs in the circulation is correlated with increased viral load and the development of opportunistic infections and disease (Feldman, 2001; Siegal, 2003). Long-term survivors (at least ten years without signs of disease) were shown to have increased IPC number and function when compared to HIV-infected subjects with progressive disease or AIDS (Soumelis, 2001). Given the very recent developments characterizing this cell type, data concerning IPC infection with SIV or FIV is currently unavailable, since species-specific reagents remain to be generated.

CHAPTER 3
DETERMINATION OF FELINE CYTOKINE SEQUENCES

Introduction

The ultimate objective of the study was identify significant changes in cytokine profiles within thymic tissue, therefore, identification of the sequences for the relevant cytokine mRNA was essential for future work. Most of the cytokines of interest in this study did not have published sequences in a review of GenBank at the onset of this project, so primers and probes for the cytokine sequences could not be developed for real time reverse transcription-polymerase chain reaction (RT-PCR) experiments. In the present experiment, we report the full length complementary DNA (cDNA) sequences for feline IL-4, IL-7, IL-15, IFN-γ and IFN-α.

Materials and Methods

Primer Design

Oligonucleotide primers were designed based on consensus DNA sequences that were currently available for other species in order to amplify the cytokine sequences using the polymerase chain reaction (PCR). When possible, a nested PCR reaction was desired in order to reduce nonspecific sequence amplification. So, for IFN-γ, IL-4 and IL-15, a set of primers (forward 1/reverse 1) was designed at a distance outside the coding region for a first round of PCR, then followed by a second reaction using forward 2/reverse 2 primers that included start and stop codon sequences. IL-7 and IFN-α were amplified using a single set of primers. Desired amplification products would include the entire coding region that was present in the mRNA. In addition, an oligonucleotide probe

was designed that would anneal within the coding region. Expected product lengths were also predicted: IFN-α (538 base pairs, bp), IFN-γ (515 bp), IL-4 (406 bp), IL-15 (499 bp), and IL-7 (835 bp).

Table 3-1. Oligonucleotide primers and probes used for nested PCR protocols.

IFN-α forward	ATG GCG CTG CCC TCT TCC TTC TTG GTG GCC
IFN-α probe	CTG GGA CAA ATG AGG AGA CTC
IFN-α reverse	TCA TTT CTC GCT CCT TAA TCT TTT CTG CAA
IFN-γ forward 1	CTA CTG ATT TCA ACT TCT
IFN-γ forward 2	GAA ACG ATG AAT TAC ACA AGT TTT
IFN-γ probe	CAT TTT GAA GAA CTG GAA A
IFN-γ reverse 1	CAA ATA TTG CAG GCA GGA
IFN- γ reverse 2	CAA CCA TTA TTT CGA TGC TCT ACG
IL-4 forward 1	TGC ATC GTT AGC KTC TCC T
IL-4 forward 2	TTA ATG GGT CTC ACC TCC CAA CTG ATT CC
IL-4 probe	ACT TCT TGG AAA GGC TAA A
IL-4 reverse 1	TTA GAK TCT ATA TAT AYT WTA T
IL-4 reverse 2	GCT TCA ATG CCT GTA GTA TTT CTT CTG CAT
IL-7 forward	AAC TCC GCG GAA GAC CAG GGT
IL-7 probe	ATT TTA TTC CAA CAA GTT TT
IL-7 reverse	TTC AGT AAC TTC CAG GAG GCA TTC
IL-15 forward 1	TGG ATG GAT GGC WGC TGG AA
IL-15 forward 2	GAG TAA TGA GAA TTT CGA AAC CAC ATT TGA
IL-15 probe	GGC ATT CAT GTC TTC ATT TTG G
IL-15 reverse 1	CTT CAT TTC YAA GAG TTC AT
IL-15 reverse 2	TGC AAT CAA GAA GTG TTG ATG AAC ATT TGG

Synthesis of cDNA

Total RNA was extracted from frozen thymic tissue from a SPF kitten using a RNeasy Mini kit (QIAGEN, Valencia, CA, USA). RNA yield was quantified by spectrophotometry at an absorbance of 260nm. One microgram samples of extracted RNA were used to generate complementary DNA (cDNA) in a 20 µl synthesis reaction using random hexamer primers (First Strand cDNA Synthesis Kit, Roche, Indianapolis, IN, USA).

Amplification of Cytokine Sequences

PCR amplification of each cytokine was performed in 50 µl reaction mixtures containing 0.1 µg of cDNA, 0.2 µM of deoxynucleotide mixture, 5 µl reaction buffer (1.5 mM $MgCl_2$), 0.2 µM of each oligonucleotide primer and 2.5 U of Taq DNA polymerase (Roche Applied Science, Indianapolis, IN, USA). After an initial denaturation cycle at 94ºC for 1 minute, PCR amplification was carried out at 92ºC for 30 seconds, 55ºC for 30 seconds, and 72ºC for 90 seconds for 30 cycles. A final elongation step was performed at 72ºC for 5 minutes, then the samples were cooled to 4ºC.

Construction and Use of a Plasmid Containing Cytokine Sequence Inserts

The commercially available pCR-Blunt II-TOPO plasmid (Invitrogen, Carlsbad, CA, USA) was selected for its suitability for accepting blunt ended PCR products. The 6µl cloning reaction was performed according to manufacturer's instructions and contained 1 µl salt solution (1.2 M NaCl, 0.06 M $MgCl_2$), 1µl TOPO vector and 4 µl of fresh PCR product. The reaction mixture was gently mixed, incubated at room temperate for 5 minutes and then cooled on ice. A vial of One Shot Chemically Competent *E. coli* cells (Invitrogen, Carlsbad, CA, USA) was thawed on ice, 4 µl of the plasmid reaction mixture was added and allowed to incubate on ice for 5 minutes. Cells were then heat-shocked in a 42ºC water bath for 30 seconds, then the tubes were returned to the ice. A 250 µl aliquot of room temperature SOC medium (2% tryptone, 0.5% yeast extract, 10 mM NaCl, 2.5 mM KCl, 10 mM $MgCl_2$, 10 mM $MgSO_4$, 20 mM glucose) was added, and the tubes were then incubated at 37ºC for one hour. A 125 µl sample of this solution was spread on a pre-warmed selective Luria-Bertani (LB) plates (with kanamycin, 50 µg/ml). Plates were incubated at 37ºC overnight then screened for bacterial colonies.

To screen colonies for the plasmids which contained cytokine sequences, direct inoculation of PCR reaction mixtures with bacteria was performed using a sterile toothpick. Two PCR reactions were prepared using the forward and reverse primers, and using the probe oligonucleotide as a forward primer in conjunction with the reverse primer. PCR was performed in 50 µl reaction mixtures containing 0.2 µM of deoxynucleotide mixture, 5 µl reaction buffer (1.5 mM $MgCl_2$), 0.2 µM of each oligonucleotide primer and 2.5 U of Taq DNA polymerase (Roche Applied Science, Indianapolis, IN, USA). After an initial denaturation cycle at 94ºC for 1 minute, PCR amplification was carried out at 92ºC for 30 seconds, 55ºC for 30 seconds, and 72ºC for 90 seconds for 30 cycles. A final elongation step was performed at 72ºC for 5 minutes, then the samples were cooled to 4ºC. PCR products were visualized by electrophoresis in 1% agarose gel stained with ethidium bromide.

Colonies were considered positive for the appropriate cytokine sequence if two PCR reactions gave bands of the expected size when amplified. Positive colonies were used to inoculate 10 ml of LB broth. After incubation of the broth overnight at 37ºC, bacteria were harvested by centrifugation at 6000 x *g* and 4ºC for15 minutes. Plasmid DNA was isolated and purified using the QIAGEN Plasmid Mini kit (Qiagen, Santa Clarita, CA, USA). Plasmid DNA samples were sent to the Genome Sequencing Service Laboratory, University of Florida. Sequence data was used to perform a nucleotide-nucleotide search through the Basic Local Alignment Search Tool (BLAST), available from the National Center for Biotechnology Information (NCBI).

Results

Plasmid Construction

Amplified DNA was cloned into the pCR-Blunt II-TOPO plasmid. Transformation reactions produced a very low yield of number of colonies produced (0-3 colonies per plate). PCR screening reactions using direct inoculation from bacterial colonies gave ample amplification, and positive colonies were identified containing inserts for IFN-γ, IFN-α, IL-4, IL-7 and IL-15 as shown in Figures 3-1, 3-2, 3-3 and 3-4.

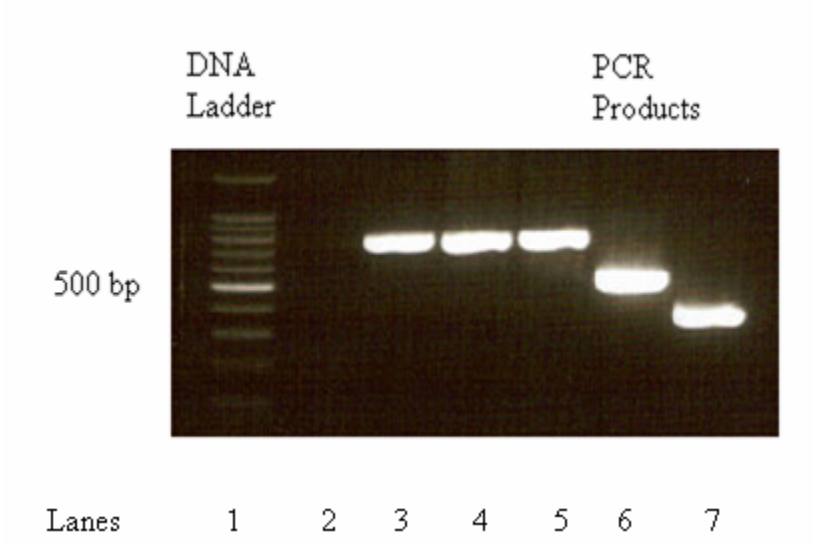

Figure 3-1. Ethidium bromide-stained agarose gel of polymerase chain reaction products from colonies transformed with plasmid containing a feline IFN-γ insert. Lanes 3-5: Vector-specific M13 primers. Lane 6, IFN-γ forward/reverse primers. Lane 7, IFN-γ probe/reverse primers.

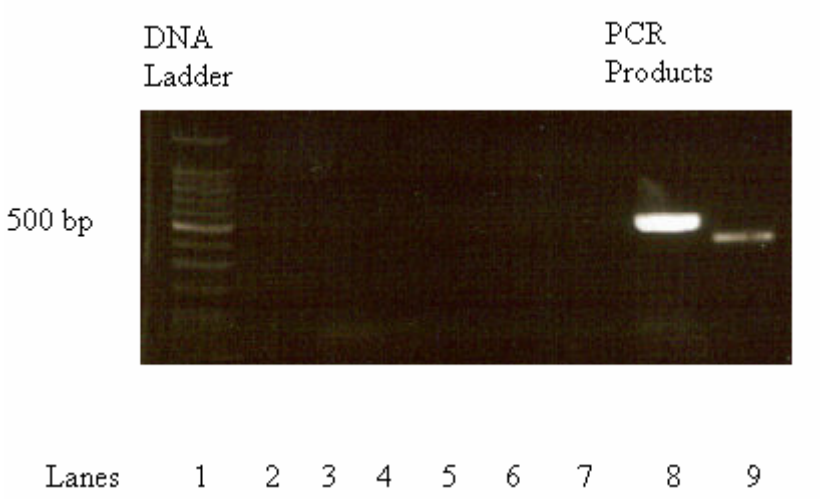

Figure 3-2. Ethidium bromide-stained agarose gel of polymerase chain reaction products from colonies transformed with plasmid containing a feline IFN-α insert. Lane 8, IFN-α forward/reverse primers. Lane 9, IFN-α probe/reverse primers.

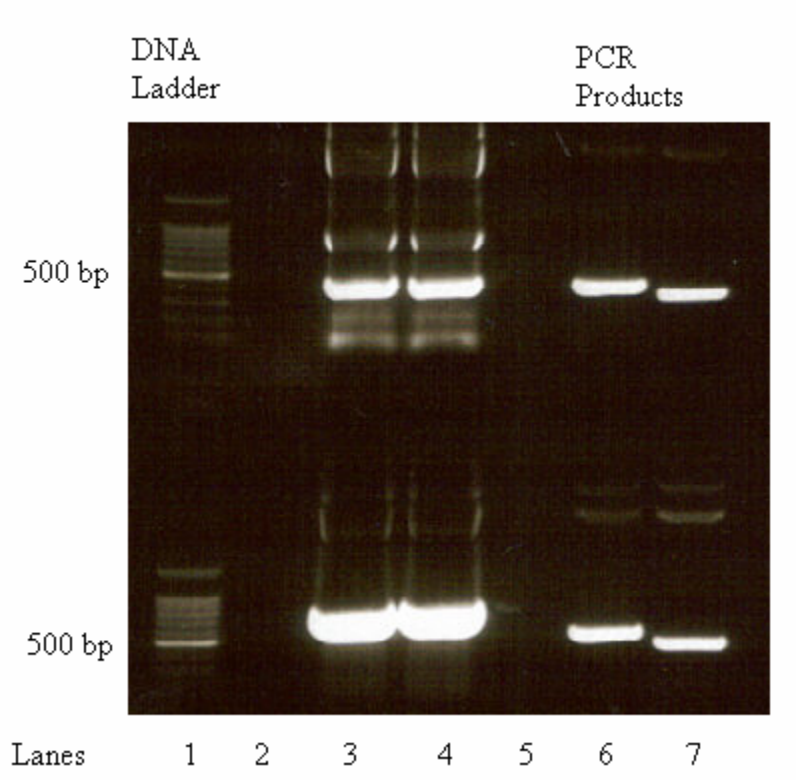

Figure 3-3. Ethidium bromide-stained agarose gel of polymerase chain reaction products from colonies transformed with plasmid containing feline IL-4 and IL-15 inserts. Row 1: Lanes 3-4: Vector-specific M13 primers. Lane 6, IL-4 forward/reverse primers. Lane 7, IL-4 probe/reverse primers. Row 2: Lanes 3-4: Vector-specific M13 primers. Lane 6, IL-15 forward/reverse primers. Lane 7, IL-15 probe/reverse primers.

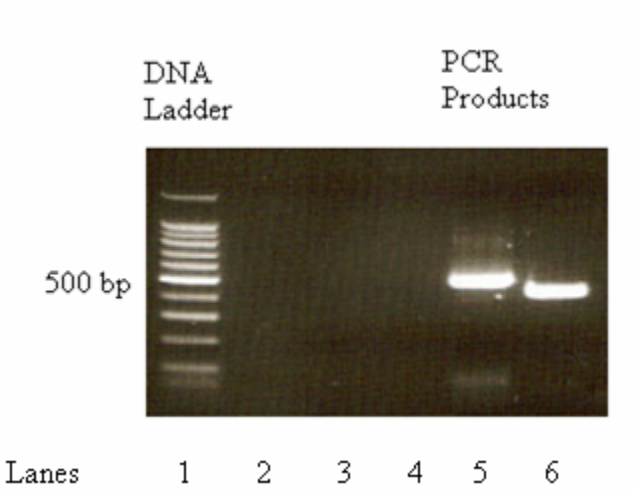

Figure 3-4. Ethidium bromide-stained agarose gel of polymerase chain reaction products from colonies transformed with plasmid containing a feline IL-7 insert. Lane 5, IL-7 forward/reverse primers. Lane 6, IL-7 probe/reverse primers.

Feline Cytokine cDNA sequences

Sequences were obtained for all 5 of the investigated cytokines, as shown in Figures 3-5, 3-6, 3-7, 3-8 and 3-9.

```
  1 CAGAATTCGC CCTTGAAACG ATGAATTACA CAAGTTTTAT TTTCGCTTTC
 51 CAGCTTTGCA TAATTTTGTG TTCTTCTGGT TATTACTGTC AGGCCATGTT
101 TTTTAAAGAA ATAGAAGAGC TAAAGGGATA TTTTAATGCA AGTAATCCAG
151 ATGTAGCAGA TGGTGGGTCG CTTTTCGTAG ACATTTTGAA GAACTGGAAA
201 GAGGAGAGTG ATAAAACAAT AATTCAAAGC CAAATTGTCT CCTTCTACCT
251 GAAAATGTTT GAAAACCTGA AAGATGATGA CCAGCGCATT CAAAGGAGCA
301 TGGACACCAT CAAGGAAGAC ATGCTTGATA AGTTGTTAAA TACCAGCTCC
351 AGTAAACGGG ATGACTTCCT CAAGCTGATT CAAATCCCTG TGAATGATCT
401 GCAGGTCCAG CGCAAAGCAA TAAATGAACT CTTCAAAGTG ATGAATGATC
451 TCTCACCAAG ATCTAACCTG AGGAAGCGGA AAAGGAGCCA GAATCTGTTT
501 CGAGGCCGTA GAGCATCGAA ATAATGGTTG AAGGGCGAAT TCCAGCACA
```

Figure 3-5. Full length nucleotide sequence of the feline IFN-γ cDNA. The start and stop codons of the open reading frame are highlighted in bold/red.

```
  1 GTGTGCTGGA ATTCGCCCTT ATGGCGCTGC CCTCTTCCTT CTTGGTGGCC
 51 CTGGTGGCGC TGGGCCGCAA CTCCGTCTGC TCTCTGGGCT GTGACCTGCC
101 TCAGACCCAC GGCCTGCTGA ACAGGAGGGC CTTGACGCTC CTGGGACAAA
151 TGAGGAGACT CCCTGCCAGC TCCTGTCAGA AGGACAGGAA TGACTTCGCC
201 TTCCCCCAGG ACGTGTTCGG TGGAGACCAG TCCCACAAGG CCCAAGCCCT
251 CTCGGTGGTG CACGTGACGA ACCAGAAGAT CTTCCACTTC TTCTGCACAG
301 AGGCGTCCTC GTCTGCTGCT TGGAACACCA CCCTCCTGGA GGAATTCTGC
351 ACGGGACTTG ATCGGCAGCT GACCCGCCTG GAAGCCTGTG TCGTGCAGGA
401 GGTGGGGGAG GGAGAGGCTC CCCTCACGAA CGAGGACTCC CTCCTGAGGA
451 ACTACTTCCA AAGACTCTCC CTCTACCTGC AAGAGAAGAA ATACAGCCCT
501 TGTGCCTGGG AGATCGTCAG AGCAGAAATC ATGAGATCCT TGTATTCGTC
551 AACAGCCTTG CAGAAAAGAT TAAGGAGCGA GAAATGAAAG GGCGAATTCT
601 GCAGATAT
```

Figure 3-6. Full length nucleotide sequence of the feline IFN-α cDNA. The start and stop codons of the open reading frame are highlighted in bold/red.

```
  1 CTTCCGGCTC CGCCCTTTTA ATGGGTCTCA CCTCCCAACT GATTCCAGCT
 51 CTGGTCTGCT TACTAGCATT TACCAGCACC TTCGTCACGG CCAGAACTTC
101 AATAATACGT TGAAAGAGAT CATCAAAACG TTGAACATCC TCACAGCGAG
151 AAACGACTCG TGCATGGAGC TGGCCGTCAT GGACGTCTTG GCAGCCCCTA
201 AGAACACAAG TGACAAGGAA ATCTTCTGCA GAGCCACAAC CGTGCTCCGG
251 CAGATCTATA CACATCACAA CTGCTCCACC AAATTCCTCA AAGGACTCGA
301 CAGGAACCTC AGCAGCATGG CAAACAGGAC CTGTTCCGTG AATGAAGACA
351 AGAAGTGTAC ACTGAAAGAC TTCTTGGAAA GGCTAAAAGC GATCATGCAG
401 AAGAAATACT ACAGGTATTG AAGCAAGGGC GAATTCTGCA GATAT
```

Figure 3-7. Full length nucleotide sequence of the feline IL-4 cDNA. The start and stop codons of the open reading frame are highlighted in bold/red.

```
  1 CAGTGTGCTG GAATTCGCCC TTGCCCATGT TCCATGTTTC TTTTAGGTAT
 51 ATCTTTGGAA TTCCTCCCCT GATCCTTGTT CTGTTGCCAG TAGCATCATC
101 TGATTGTGAT ATTGAAGGTA AAGACGGAAG AGAATATCAG CACATTCTAA
151 TGATCAGCAT CAATTACTTG GACACCATGA TAAAAAATCG TACCAATTGC
201 CCGAATAATG AACCTAACGT TTTTAAAAAA CATGCATGTG ATGATAATAA
251 GGAAGCTGTG TTTTTATATC GTGCTGCTCA CAAGTTGAAG CACTTTGTCA
301 AAGTGAATAA CAGTGAGGAA TTCAATCTCC ACTTATCAAG AGTTTCACAG
351 GGCATGTTAC AGTTGTTGAA CTGTACCCCC AAGGAAGACA GCAAATCTTT
401 AAAGGAACAG AGAAAACAGA AGAGCTTGTG TTTTCTAGGG ATACTACTAC
451 AAAAGATAAA AACTTGTTGG AATAAAATTT TGAGGGGCAC TAAAGAACAC
501 TGAAAAATAT GGAGAAGGGC GAATTCT
```

Figure 3-8. Full length nucleotide sequence of the feline IL-7 cDNA. The start and stop codons of the open reading frame are highlighted in bold/red.

```
  1 AGTGTGCTGG AATTCGCCCT TGAGTAATGA GAATTTCGAA ACCACATTTG
 51 AGAAGTACTT CCATCCAGTG CTACTTGTGT TTACTTCTGA ACAGCCATTT
101 TTTAACTGAA GCTTGCATTC CTGTCTTCAT TTTGAGCTGT ATCAGTGCAG
151 GTCTTCCTAA AACAGAGGCA AACTGGCAGG ATGTAATAAG TGATTTGAAA
201 ATAATTGACA AGATTATTCA ATCCTTACAT ATCGATGCCA CTTTATATAC
251 TGAAAGTGAT GTTCATCCCA ATTGCAAAGT AACAGCGATG AAGTGCTTTC
301 TCCTGGAGTT ACATGTTATT TCGCTTGAGT CCAAAAATGA GACCATTCAT
351 CAAACAGTAG AAAACATTAT TATCCTGGCA AACAGTGGTT TATCTTCTAA
401 CAGGAATATA ACTGAAACAG GATGCAAAGA ATGTGAGGAA CTGGAGGAAA
451 AGAACATTAA AGAATTTCTG CAGAGTTTTG TACATATTGT ACAAATGTTC
501 ATCAACACTT CTTGATTGCA AAGGGCGAAT TCTGCAGATAT
```

Figure 3-9. Full length nucleotide sequence of the feline IL-15 cDNA. The start and stop codons of the open reading frame are highlighted in bold/red.

Basic Local Alignment Search Tool (BLAST) comparisons were made for the sequenced cytokines. The nucleotide sequence obtained for feline IFN-γ is 100% identical to reported sequences for the feline cytokine (Argyle, 1995). The feline sequence exhibits 89% homology to that of the dog (*Canis familiaris*), 88% homology to the Eurasian badger (*Meles meles*), and 83-84% homology to horse (*Equus caballus*), the steer (*Bos taurus*), the Bactrian camel (*Camelus bactrianus*) and the sheep (*Ovis aries*), and 80% homology to the pig (*Sus scrofa*).

The idenitifed IFN-α nucleotide sequence exhibited 96-99% similarity to several different reported feline IFN-α sequences (Nagai, 2004). The feline sequence also has 81-87% homology to that of the horse IFN-α, 78% homology to the dog, and 82-91% homology to various fragments of human interferon sequences.

The feline IL-4 nucleotide sequence demonstrates 98% homology to reported feline IL-4 sequences (Schijns, 1995, direct PubMed submission). Feline IL-4 cDNA exhibits 88% homology to canine IL-4, 84% homology to the bovine sequence, 82% homology to the pig and the horse, and 80% to the Bactrian camel.

The nucleotide sequence for feline IL-7 cDNA has not been previously reported. The feline IL-7 sequence was most homologous to that of the pig and the sheep (87%), followed by the steer (86%), the rhesus monkey (*Macaca mulatta*) (85%), and humans (84%).

The sequence for feline IL-15 cDNA exhibits 98% homology to sequences from a recent report (Dean, 2005). It also demonstrates homology to the IL-15 sequences of the horse (89%), human (88%), the steer (87%) and the dog (87%).

Discussion

The cDNA sequences for feline cytokines were successfully amplified by PCR, cloned using a bacterial plasmid system and confirmed by DNA sequencing. The full length transcripts are isolated in plasmid-containing bacteria for rapid access in any future experiments by our laboratories that require expression of the feline protein.

CHAPTER 4
MEASUREMENT OF FIV GAG MESSENGER RNA AND DNA, AND IL-4, IL-7, IL-15, IFN-ALPHA AND INTERFERON-GAMMA MESSENGER RNA LEVELS IN THE THYMUSES OF CATS NEONATALLY INFECTED WITH FIV

Introduction

Cytokine expression tends to be low in tissues and cell samples under investigation, and real-time reverse-transcription (RT)-PCR has proven to be the most sensitive, reproducible, rapid and accurate technique available for mRNA quantitation. As tissue samples are often too small to evaluate cytokines at the protein level, real-time RT-PCR using fluorogenic probes has become the standard method of choice in investigating tissue cytokine profiles (Blaschke, 2000; Giulietti, 2001; Rajeevan, 2001; Yin, 2001; Overbergh, 2003). While mRNA expression in the tissues may not definitively reflect the ultimate cytokine protein levels, analyses comparing mRNA expression relative to tissue protein content have demonstrated good correlation (Blaschke, 2000; Hein, 2001).

Using the previously derived cDNA sequences for the feline cytokines (Chapter 3) and sequence map for JSY3 (the molecular clone of FIV used in the infected animal groups), primers and probes were generated for use in a real-time RT-PCR protocol. Real-time RT-PCR was used to determine the RNA levels for IL-4, IL-7, IL-15, IFN-α, IFN-γ and FIV *gag*, and the proviral load of FIV *gag* DNA. The current chapter describes cytokine changes that exist for the different age groups and as a result of FIV infection; Chapter 5 discusses the statistical correlations between the cytokine changes and the changes that were observed in thymus cell subpopulations and viral levels.

Materials and Methods

Quantitative Real-Time PCR for Feline Cytokine mRNA.

Cats with acute (6-8 weeks), 12 week, and chronic (>16 weeks) neonatal FIV infection (infected at birth) were identified from previous studies. Total RNA was extracted from thymic samples, which had been frozen at -80˚C (RNeasy Midi Kit, Qiagen Inc., Valencia, CA). RNA concentration and purity was determined by UV spectrophotometer (A_{260}/A_{280}). RNA samples were treated with DNase I (Sigma, St. Louis, MO, USA). One microgram samples of extracted RNA were used to generate complementary DNA (cDNA) in a 20 µl synthesis reaction using random hexamer primers (First Strand cDNA Synthesis Kit, Roche, Indianapolis, IN, USA). Feline G3PDH was selected as the housekeeping gene for normalization of cytokine mRNA content. The cytokine primers, feline G3PDH primers, and corresponding Taqman probes were designed using Primer Express software (PE Applied Biosystems, Foster City, CA) (Table 4-1). Real-time RT-PCR analyses were conducted using the PRISM 7700 Sequence Detection System (PE Applied Biosystems, Foster City, CA), utilizing a 25-µl reaction volume of PCR Universal Master Mix (PE Applied Biosystems, Foster City, CA) containing ˜100-200 ng of cDNA , 900 nM of each *gag* and G3PDH primer, and 125 nM of the TaqMan probes. The standard curve was generated by PCR on serial dilutions of a thymic cDNA sample from a selected 6 week-old, FIV-infected animal. All samples and the serial dilutions of the standards were assayed in triplicate. For all samples, target quantity was determined from the standard curve and divided by the target quantity of a calibrator, a 1×sample. All other quantities were expressed as an *n*-fold difference relative to the calibrator, and the same calibrator thymic sample was used

for all cytokine experiments. The relative feline cytokine gene transcription products were expressed as the ratio of cytokine mRNA to G3PDH mRNA content.

Quantitative Real-Time PCR for FIV Provirus.

Genomic DNA was extracted (QIAamp DNA Mini Kit, Qiagen Inc., Valencia, CA) from thymic samples. Resulting DNA concentration and purity was determined by UV spectrophotometer (A_{260}/A_{280}). The *gag* primers, feline G3PDH primers, and corresponding Taqman probes were designed using Primer Express software (PE Applied Biosystems, Foster City, CA) (Table 4-1). PCR analyses were conducted using the PRISM 7700 Sequence Detection System (PE Applied Biosystems, Foster City, CA), utilizing a 25-µl reaction volume of PCR Universal Master Mix (PE Applied Biosystems) containing ~100-200 ng of DNA, 900 nM of each *gag* and G3PDH primer, and 125 nM of the TaqMan probes. The standard curve was generated by PCR on serial dilutions of a cDNA containing the JSY3 *gag* sequence and feline G3PDH. All samples and the serial dilutions of the standards were assayed in triplicate. For all samples, the target quantity was determined from the standard curve and divided by the target quantity of a calibrator, a 1×sample. All other quantities were expressed as an *n*-fold difference relative to the calibrator. The relative FIV provirus content was expressed as the ratio of FIV *gag* DNA to G3PDH DNA content.

Quantitative Real-Time PCR for FIV Transcription.

Total RNA was extracted (RNeasy Midi Kit, Qiagen Inc., Valencia, CA) from thymic samples. RNA concentration and purity was determined by UV spectrophotometer (A_{260}/A_{280}). Reverse transcription was performed by use of the TaqMan Reverse Transcription Reagents (PE Applied Biosystems, Foster City, CA) utilizing ~0.5 µg RNA and 3' reverse *gag* specific primer with the following cycling

conditions: 75°C for 5 min, 42°C for 1 hour, 95°C for 5 minutes, and 4°C for 5 minutes. Real-time RT-PCR analyses were conducted using the PRISM 7700 Sequence Detection System (PE Applied Biosystems, Foster City, CA), utilizing a 25-µl reaction volume of PCR Universal Master Mix (PE Applied Biosystems, Foster City, CA) containing ~100-200 ng of cDNA , 900 nM of each *gag* and G3PDH primer, and 125 nM of the TaqMan probes. The standard curve was generated by PCR on serial dilutions of a cDNA containing the JSY3 *gag* sequences and feline G3PDH. All samples and the serial dilutions of the standards were assayed in triplicate. For all samples, target quantity was determined from the standard curve and divided by the target quantity of a calibrator, a 1×sample. All other quantities were expressed as an *n*-fold difference relative to the calibrator. The relative FIV *gag* gene transcription products were expressed as the ratio of FIV *gag* RNA to G3PDH mRNA content.

Table 4-1. Primers and probes used for real-time RT-PCR.

IL-4 forward primer	TTC ACG GAA CAG GTC CTG TTT
IL-4 reverse primer	TGC TCC ACC AAA TTC CTC AAA
IL-4 probe	6FAM-CCA TGC TGC TGA GGT TCC TGT CGA-TAMRA
IL-7 forward primer	GCC CTG TGA AAC TCT TGA TAA GTG
IL-7 reverse primer	TCG TGC TGC TCA CAA GTT GAA
IL-7 probe	6FAM-AGA TTG AAT TCC TCA CTG TTA TTC ACT TTG ACA AAG TG-TAMRA
IL-15 forward primer	AAC TGA AGC TTG CAT TCC TGT CT
IL-15 reverse primer	TCC TGC CAG TTT GCC TCT GT
IL-15 probe	6FAM-CAT TTT GAG CTG TAT CAG TGC AGG TCT TCC TAA-TAMRA
IFN-alpha forward primer	TCC GGT GGA GAC CAG TCC C
IFN-alpha reverse primer	TTC TGG TTC GTC ACG TGC A
IFN-alpha probe	6FAM-CAA GGC CCA AGC CCT CTC GGT G-TAMRA
IFN-gamma forward primer	ATG ATG ACC AGC GCA TTC AA
IFN-gamma reverse primer	TTT ACT GGA GCT GGT ATT TAA CAA CTT ATC
IFN-gamma probe	6FAM-AGC ATG GAC ACC ATC AAG GAA GAC ATG C-TAMRA
FIV gag forward primer	AGCCCTCCACAGGCATCTC
FIV gag reverse primer	TGGACACCATTTTTGGGTCAA
FIV gag probe	6FAM-ATT CAA ACA GCA AAT GGA GCA CCA CAA TAT G-TAMRA
G3PDH forward primer	CCATCAATGACCCCTTCATTG
G3PDH reverse primer	TGACTGTGCCGTGGAATTTG
G3PDH probe	6FAM-CTC AAC TAC ATG GTC TAC ATG TTC CAG TAT GAT TCC-TAMRA

Statistical Analysis

Cytokine mRNA expression was analyzed for differences between the different age groups, and between infected animals as compared to the age matched controls. SAS PROC GLM was used to conduct the one-way ANOVA analysis; the least squares means were calculated and pair-wise group comparisons were conducted using SAS 9.1 (SAS Institute, Inc., Cary, NC). Values were considered statistically significant for analyses where $P < 0.05$.

Results

Interleukin (IL)-4

IL-4 mRNA levels were measured at three time points after neonatal infection with a pathogenic molecular clone of FIV (JSY3) (Table 4-2). Cytokine expression values were compared over time and against age-matched controls. *P* values from the comparisons are summarized in Table 4-3. Arithmetic means with the corresponding standard deviations are graphically represented in Figure 4-1.

The only group of animals demonstrating statistically significant differences in IL-4 expression was the uninfected >16-week-old control group. Uninfected >16-week-old cats had higher IL-4 mRNA expression than the infected animals ($P = 0.01$), but also expressed IL-4 at a higher level than younger animals that weren't infected. This suggests that IL-4 becomes more active within the thymus as the animal matures to the subadult age group, and that this activity level is suppressed by pathogenic FIV infection (3.8-fold less IL-4 expression in infected animals).

Table 4-2. Relative IL-4 mRNA concentration in thymic samples, as expressed as *n*-fold difference to a calibrator sample.

	Animal group	Arithmetic mean with standard deviation
1	6-8-week-old cats, uninfected (n=5)	0.77 ± 0.37
2	6-8-week-old cats, FIV-infected (JSY3) (n=5)	0.7 ± 0.26
3	12-week-old cats, uninfected (n=2)	1.94 ± 0.91
4	12-week-old cats, FIV-infected (JSY3) (n=5)	2.53 ± 0.97
5	>16-week-old cats, uninfected (n=3)	$6.59 \pm 8.08_a$
6	>16-week-old cats, FIV-infected (JSY3) (n=8)	1.74 ± 1.23

a: Statistically significant difference from infected and uninfected 6-8-week-old groups, 12-week-old infected cats, and >16-week-old infected cats ($P < 0.05$).

Table 4-3. P values from pairwise comparison of IL-4 levels, animal groups 1-6 from Table 4-2.

	1	2	3	4	5	6
1		0.96	0.59	0.29	0.005	0.44
2	0.96		0.57	0.27	0.005	0.41
3	0.59	0.57		0.79	0.06	0.99
4	0.29	0.27	0.79		0.04	0.29
5	0.005	0.005	0.06	0.04		0.01
6	0.44	0.41	0.99	0.68	0.01	

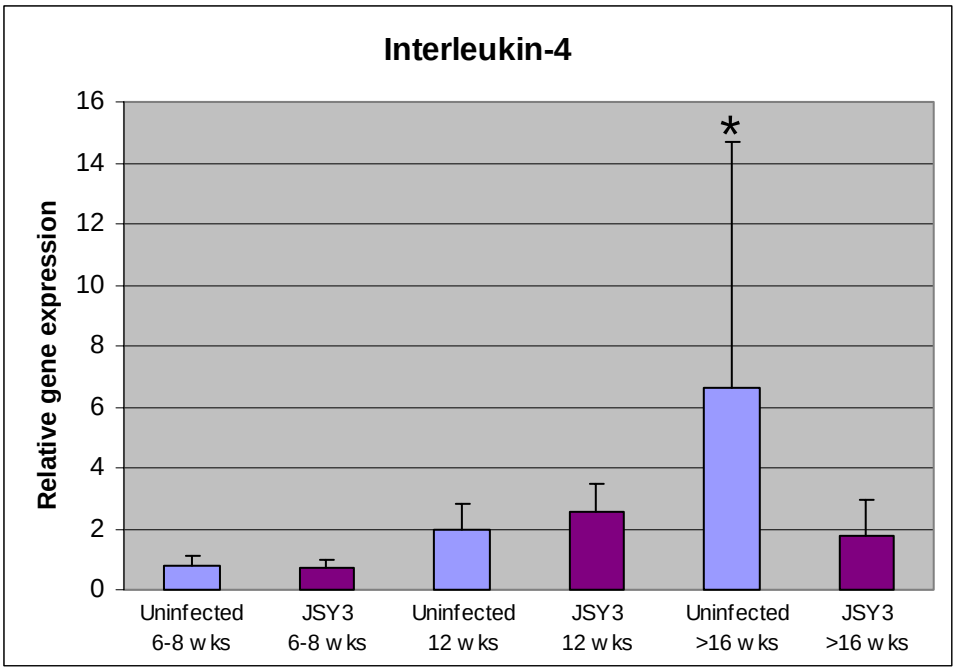

Figure 4-1. Measurement of relative IL-4 mRNA expression in thymic samples of FIV-infected (viral molecular clone, JSY3) cats and age matched controls. (*) denotes statistically significant from infected and uninfected 6-8-week-old groups, 12-week-old infected cats, and >16-week-old infected cats ($P < 0.05$).

Interleukin-7

IL-7 mRNA levels were measured at three time points after neonatal infection with a pathogenic molecular clone of FIV (JSY3) (Table 4-4). Cytokine expression values were compared over time and against age-matched controls. *P* values from the comparisons are summarized in Table 4-5. Arithmetic means with the corresponding standard deviations are graphically represented in Figure 4-2.

IL-7 mRNA exhibited a similar pattern of expression as IL-4 in the animal groups examined. Older (>16 weeks) uninfected animals showed a higher level of expression of IL-7 than younger animals and cats infected with FIV (6.3-fold more IL-7 is present in uninfected controls). This findings suggest that IL-7 is upregulated within that thymus as the animals mature, but that this effect is suppressed with FIV infection ($P = 0.003$).

Table 4-4. Relative IL-7 mRNA concentration in thymic samples, as expressed as *n*-fold difference to a calibrator sample.

	Animal group	Arithmetic mean
1	6-8-week-old cats, uninfected (n=5)	2.24 ± 2.88
2	6-8-week-old cats, FIV-infected (JSY3) (n=5)	0.79 ± 0.54
3	12-week-old cats, uninfected (n=2)	1.09 ± 0.4
4	12-week-old cats, FIV-infected (JSY3) (n=5)	2.52 ± 1.93
5	>16-week-old cats, uninfected (n=3)	8.02 ± 8.42[a]
6	>16-week-old cats, FIV-infected (JSY3) (n=8)	1.27 ± 1.17

a: statistically significant difference from all other animal groups in study ($P < 0.05$)

Table 4-5. *P* values from pairwise comparison of IL-7 levels, animal groups 1-6 from Table 4-4.

	1	2	3	4	5	6
1		0.4	0.66	0.88	0.02	0.59
2	0.4		0.84	0.32	0.003	0.68
3	0.66	0.84		0.58	0.02	0.92
4	0.88	0.32	0.58		0.02	0.49
5	0.02	0.003	0.02	0.02		0.003
6	0.59	0.68	0.93	0.49	0.003	

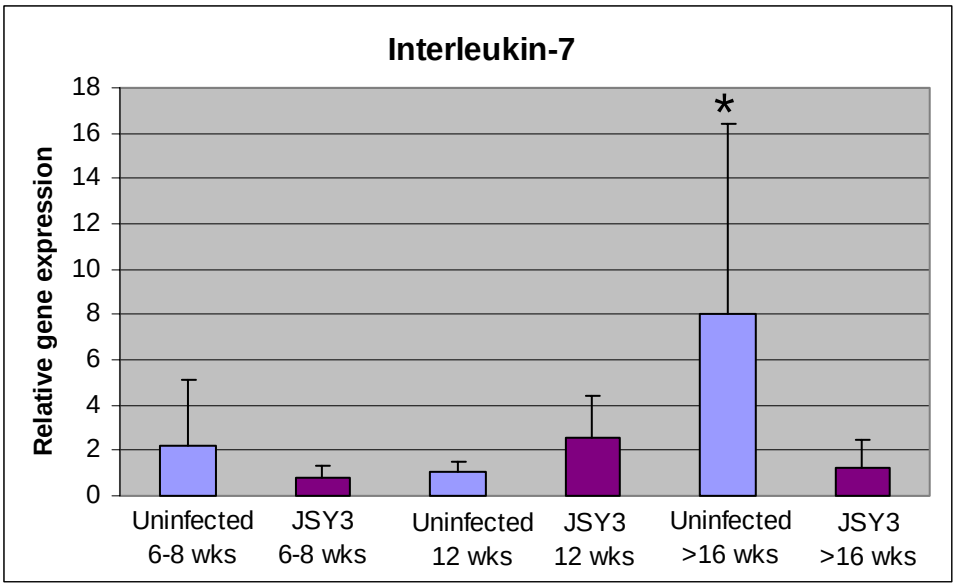

Figure 4-2. Measurement of relative IL-7 mRNA expression in thymic samples of FIV-infected (viral molecular clone, JSY3) cats and age matched controls. (*) denotes statistically significant differences from all other animal groups in study ($P < 0.05$).

Interleukin-15

IL-15 mRNA levels were measured at three time points after neonatal infection with a pathogenic molecular clone of FIV (JSY3) (Table 4-6). Cytokine expression values were compared over time and against age-matched controls. *P* values from the comparisons are summarized in Table 4-7. Arithmetic means with the corresponding standard deviations are graphically represented in Figure 4-3.

IL-15 was slightly upregulated in FIV-infected animals at 12 weeks of age as compared to infected 6-8-week-old infected animals ($P = 0.004$) and >16-week-old infected animals ($P = 0.06$). However, this appears to be due to a physiological trend for IL-15 upregulation at this age, as IL-15 levels are not statistically different from 12-week-old age-matched control cats ($P = 0.36$). IL-15 mRNA expression in infected animals also does not differ significantly from age-matched controls at other time points (6-8 weeks, $P = 0.59$; >16 weeks, $P = 0.12$).

Table 4-6. Relative IL-15 mRNA concentration in thymic samples, as expressed as *n*-fold difference to a calibrator sample.

	Animal group	Arithmetic mean
1	6-8-week-old cats, uninfected (n=5)	1.26 ± 0.74
2	6-8-week-old cats, FIV-infected (JSY3) (n=5)	1.56 ± 0.78
3	12-week-old cats, uninfected (n=2)	2.93 ± 0.51
4	12-week-old cats, FIV-infected (JSY3) (n=5)	3.77 ± 1.95
5	>16-week-old cats, uninfected (n=3)	1.4 ± 0.43
6	>16-week-old cats, FIV-infected (JSY3) (n=8)	2.33 ± 0.96

Table 4-7. *P* values from pairwise comparison of IL-15 levels, animal groups 1-6 from Table 4-6.

	1	2	3	4	5	6
1		0.59	0.07	0.001	0.87	0.04
2	0.59		0.15	0.004	0.77	0.13
3	0.07	0.15		0.36	0.12	0.66
4	0.001	0.004	0.36		0.006	0.06
5	0.87	0.77	0.12	0.006		0.12
6	0.04	0.13	0.66	0.06	0.12	

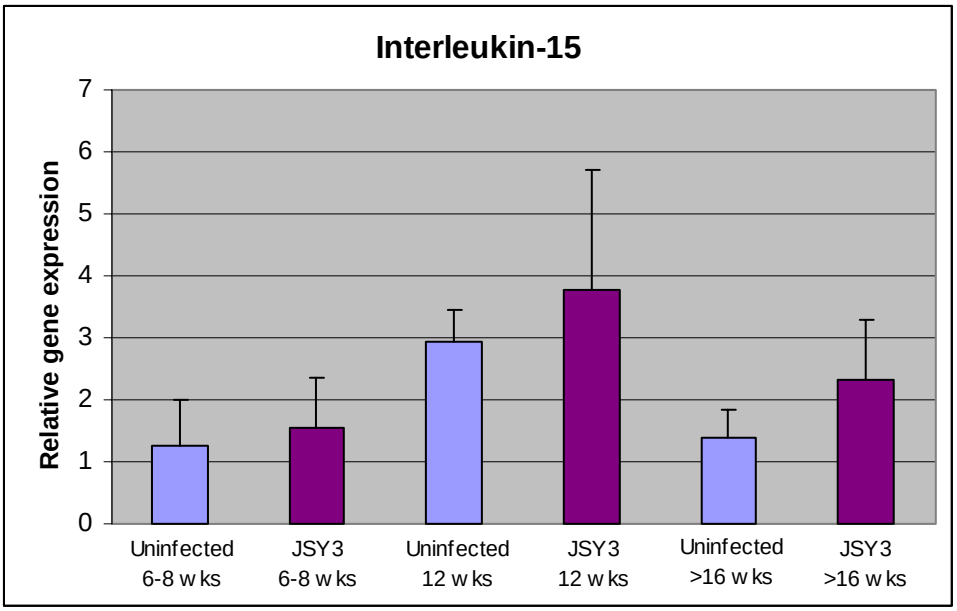

Figure 4-3. Measurement of relative IL-15 mRNA expression in thymic samples of FIV-infected (viral molecular clone, JSY3) cats and age matched controls. (*) denotes statistically significant differences from all other animal groups in study ($P < 0.05$).

Interferon (IFN)-γ

IFN-γ mRNA levels were measured at three time points after neonatal infection with a pathogenic molecular clone of FIV (JSY3) (Table 4-8). Cytokine expression values were compared over time and against age-matched controls. *P* values from the comparisons are summarized in Table 4-9. Arithmetic means with the corresponding standard deviations are graphically represented in Figure 4-4.

Again, mRNA levels for IFN-γ demonstrates a physiological upregulation at the >16 week time point similar to the trends observed for IL-4 and IL-7. IFN-γ values are statistically higher in >16-week-old animals than all other animal groups (Tables 4-9). This heightened expression level is abrogated by infection with FIV ($P = 0.01$), and infected animals express IFN-γ at a level 4.5 times less than uninfected controls.

Table 4-8. Relative IFN-γ mRNA concentration in thymic samples, as expressed as *n*-fold difference to a calibrator sample.

	Animal group	Arithmetic mean
1	6-8-week-old cats, uninfected (n=5)	3.22 ± 5.89
2	6-8-week-old cats, FIV-infected (JSY3) (n=5)	2.12 ± 2.08
3	12-week-old cats, uninfected (n=2)	1.14 ± 1.38
4	12-week-old cats, FIV-infected (JSY3) (n=5)	4.11 ± 1.78
5	>16-week-old cats, uninfected (n=3)	13.07 ± 15.14[a]
6	>16-week-old cats, FIV-infected (JSY3) (n=8)	2.9 ± 1.91

a: statistically significant difference from all other animal groups in study ($P < 0.05$)

Table 4-9. *P* values from pairwise comparison of IFN-γ levels, animal groups 1-6 from Table 4-8.

	1	2	3	4	5	6
1		0.7	0.66	0.8	0.02	0.94
2	0.7		0.88	0.52	0.01	0.72
3	0.66	0.88		0.52	0.03	0.68
4	0.8	0.52	0.52		0.04	0.72
5	0.02	0.01	0.03	0.04		0.01
6	0.94	0.72	0.68	0.72	0.01	

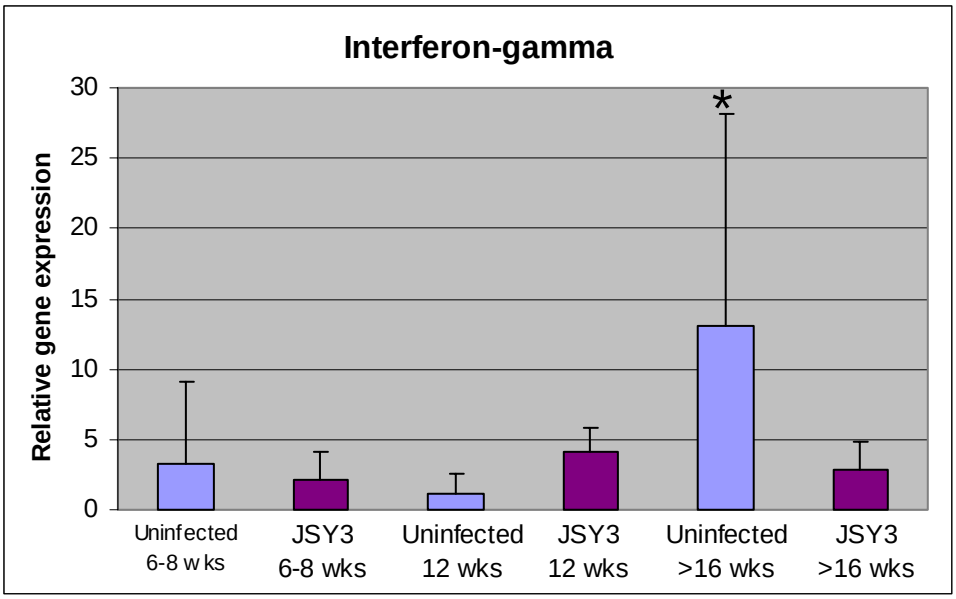

Figure 4-4. Measurement of relative IFN- γ mRNA expression in thymic samples of FIV-infected (viral molecular clone, JSY3) cats and age matched controls. (*) denotes statistically significant differences from all other animal groups in study ($P < 0.05$).

Interferon-α

IFN-α mRNA levels were measured at three time points after neonatal infection with a pathogenic molecular clone of FIV (JSY3) (Table 4-10). Cytokine expression values were compared over time and against age-matched controls. *P* values from the comparisons are summarized in Table 4-11. Arithmetic means with the corresponding standard deviations are graphically represented in Figure 4-5.

The pattern of mRNA expression observed for IFN-α was similar to that of IL-4, IL-7 and IFN-γ, both over time and in response to infection. Uninfected animals greater than 16 weeks of age demonstrated a higher cytokine expression level than all other animal groups (Tables 4-10 and 4-11). Chronically infected animals (>16-week-old cats) exhibited 148.7-fold less thymic IFN-α mRNA expression than uninfected age-matched

controls ($P = 0.0003$). Pair-wise comparisons of all others groups were not statistically significant.

Table 4-10. Relative IFN-α mRNA concentration in thymic samples, as expressed as *n*-fold difference to a calibrator sample.

	Animal group	Arithmetic mean
1	6-8-week-old cats, uninfected (n=5)	306.24 ± 608.32
2	6-8-week-old cats, FIV-infected (JSY3) (n=5)	2.74 ± 1.99
3	12-week-old cats, uninfected (n=2)	35.04 ± 31.08
4	12-week-old cats, FIV-infected (JSY3) (n=5)	302.12 ± 641.95
5	>16-week-old cats, uninfected (n=3)	1773.81 ± 1533.36[a]
6	>16-week-old cats, FIV-infected (JSY3) (n=8)	11.93 ± 31.94

a: statistically significant difference from all other animal groups in study ($P < 0.05$)

Table 4-11. *P* values from pairwise comparison of IFN-α levels, animal groups 1-6 from Table 4-10.

	1	2	3	4	5	6
1		0.43	0.59	0.99	0.003	0.4
2	0.43		0.95	0.44	0.0005	0.98
3	0.59	0.95		0.6	0.004	0.96
4	0.99	0.44	0.6		0.003	0.41
5	0.003	0.0005	0.004	0.003		0.0003
6	0.4	0.98	0.96	0.41	0.0003	

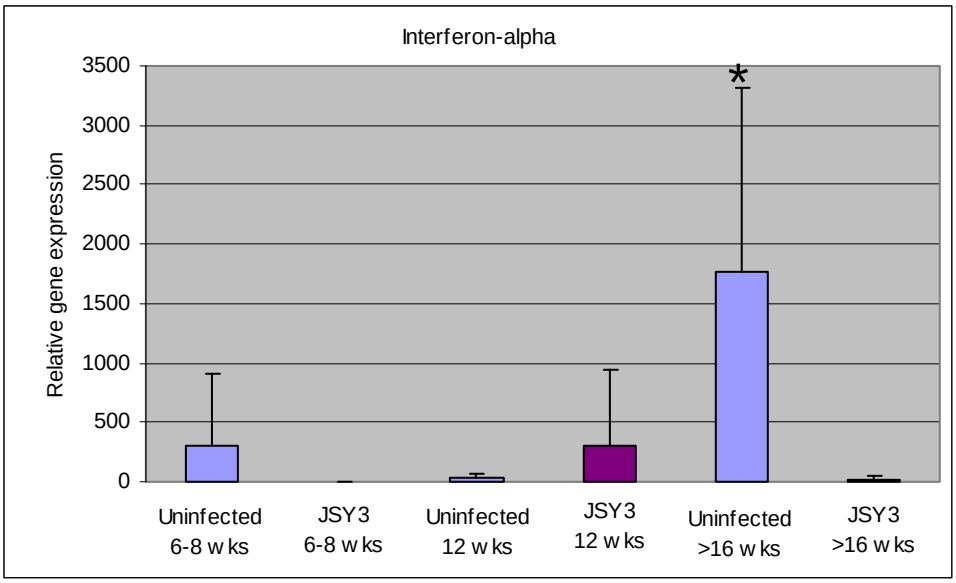

Figure 4-5. Measurement of relative IFN-α mRNA expression in thymic samples of FIV-infected (viral molecular clone, JSY3) cats and age matched controls. (*) denotes statistically significant differences from all other animal groups in study ($P < 0.05$).

Viral Transcription (FIV *gag* RNA) and Proviral Load (FIV *gag* DNA)

FIV *gag* RNA and DNA levels were measured for all thymus samples from the previous cytokine studies, using the same real time RT-PCR protocol. Arithmetic means with standard deviations are tabulated in Table 4-12 and graphically represented in Figures 4-6 (RNA) and 4-7 (DNA). All cats from age-matched control groups had undetectable levels of *gag* RNA and DNA, as expected for uninfected animals.

There was a great deal of variability for levels of FIV *gag* RNA between cats of the same age group, exemplified by large standard deviation values. The trend of higher viral gene expression levels over time was present but not statistically significant (one-way ANOVA, $P = 0.64$). While overall the variability in proviral load in cats of older age groups was lower than viral gene expression, statistically significant changes in thymic *gag* content were not observed (one-way ANOVA, $P = 0.85$).

Table 4-12. Relative viral *gag* RNA expression and viral DNA loads within feline thymic samples as measured with real time RT-PCR.

	Animal group	Arithmetic mean *gag* RNA	Arithmetic mean *gag* DNA
1	6-8-week-old cats, uninfected (n=2)	ND	ND
2	6-8-week-old cats, FIV-infected (JSY3) (n=5)	5.19 ± 6.27	0.21 ± 0.44
3	12-week-old cats, uninfected (n=2)	ND	ND
4	12-week-old cats, FIV-infected (JSY3) (n=2)	9.15 ± 12.94	0.005 ± 0.005
5	>16-week-old cats, uninfected (n=3)	ND	ND
6	>16-week-old cats, FIV-infected (JSY3) (n=7)	11.57 ± 13.31	0.02 ± 0.03

ND = Not detected, value of 0

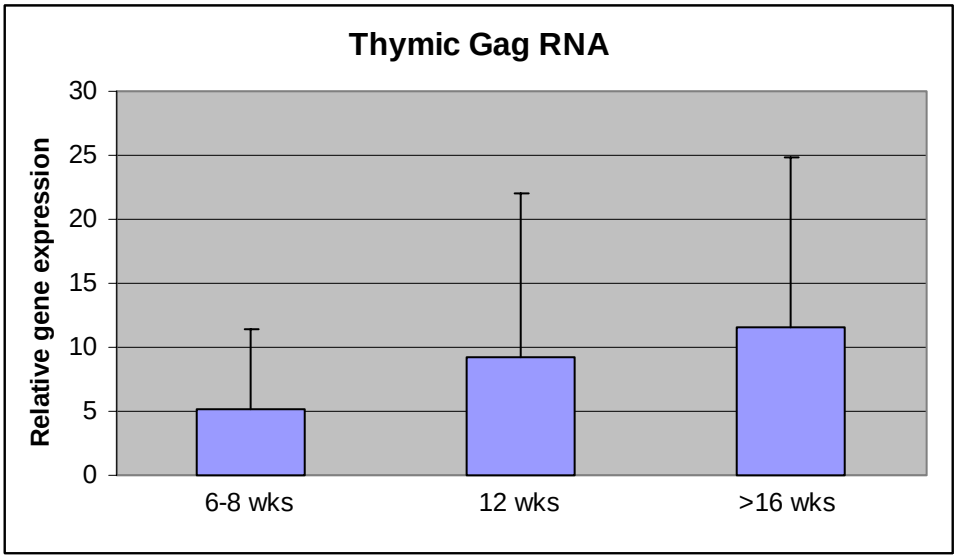

Figure 4-6. Measurement of relative viral *gag* RNA expression by real time RT-PCR in thymic samples of FIV-infected (viral molecular clone, JSY3) cats at 3 time points after neonatal infection.

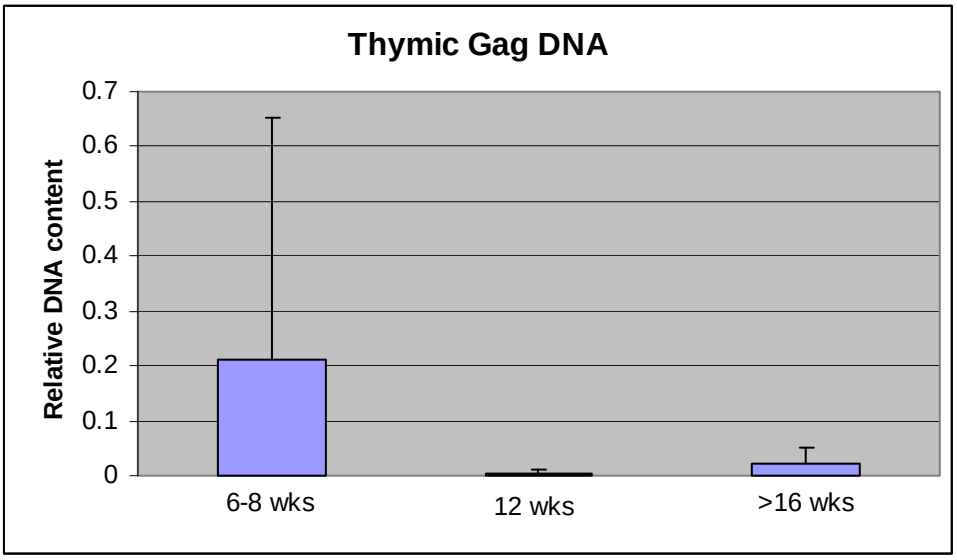

Figure 4-7. Measurement of relative viral *gag* DNA content by real time RT-PCR in thymic samples of FIV-infected (viral molecular clone, JSY3) cats at 3 time points after neonatal infection.

Discussion

Of the cytokines evaluated in the present study, four of the five (IL-4, IL-7, IFN-γ and IFN-α) demonstrated a physiologic upregulation by 16 weeks of age as compared to the 6-8-week and 12-week age groups. This peak in normal cytokine activity was depressed in the course of FIV infection, and for IL-4, IL-7 and IFN- γ there was a 4-6 fold difference in mRNA expression between the uninfected and infected animals. A similar but much more pronounced pattern also existed for IFN- α, with uninfected animals exhibiting a 149-fold greater expression of IFN-α transcripts than FIV-infected animals.

For the fifth cytokine, IL-15, there was a slight, non-statistically significant physiologic increase in expression levels around 12 weeks of age when compared to the 6-8-week and >16-week-old uninfected animal groups. While the values for IL-15 were

higher for infected animals at every time point, none of the groups reached statistical significance for the virally-induced increases.

The cytokines of this study are known to be elaborated by a diverse host of immune system cells. While IL-4 and IFN-γ are generally synthesized by activated T cells in the process of the immune response, IL-7 is generated by dendritic cells/stromal cells, IFN-α by virus-infected cells and at much higher levels by plasmacytoid dendritic cells (PDC; also referred to as interferon-producing cells, IPC) and IL-15 is produced by monocyte/macrophages, dendritic cells and stromal cells. Therefore, the observed increases in most cytokine activity do not appear to be as a result of a change in a single thymic cellular subpopulation, and these findings may reflect a generalized increase in thymopoietic activity in this age group. The particularly robust increase in IFN-α expression after 16 weeks of age could potentially reflect an expansion in the thymic subpopulation of Type II dendritic cells (PDC) and a rise in intrathymic innate immunity.

As mentioned previously, four of the five cytokines were decreased in infected animals over 16 weeks of age, reflecting a suppression of the peak in physiological cytokine activity that was observed in the age-matched control animals. This may reflect a viral influence on overall mRNA expression in multiple cell types, and the lack of IL-15 inhibition could indicate that the monocyte/macrophage cell lineage is not as susceptible to this virally-induced mRNA suppression at this stage in thymic FIV infection. The correlations between cytokine levels and thymic cellular subpopulations, and the ramifications of cytokine changes on viral replication, are examined in Chapter 5.

CHAPTER 5
IMPACT OF CYTOKINE CHANGES ON FIV REPLICATION AND THYMIC CELLULAR COMPOSITION

Introduction

As published previously, neonatal infection of the thymus with FIV results in a reduction of thymus-body weight ratio, selective depletion of CD4+CD8+ thymocytes, cortical atrophy, infiltrations of B cells, formation of lymphoid follicles and deformation of the thymic architecture (Orandle, 1997; Orandle, 2000; Norway, 2001; Johnson, 2001). Archival tissue from these experiments was selected for pursuit of the present study. At the time of tissue collection, flow cytometry had been performed with antibodies against the cell markers CD4 and CD8, which vary in surface expression on thymocytes depending on their level of T cell maturation. "Double-negative" (CD4-CD8-) thymocytes represent the most immature cell population, are present within the superficial cortex, and represent recent emigrants from the bone marrow into the thymus. "Double-positive" (DP) ,or CD4+CD8+, thymocytes comprise the bulk of the normal developing thymocyte pool, move progressively throughout the thymic cortex to the medulla, and have not yet been restricted to a more mature lineage of single-positive (SP) CD4+ or CD8+ cells. SP CD4+ and CD8+ T cells are the population of cells ready to emigrate from the thymus after thymopoiesis is complete, or can indicate an influx of inflammatory cells from an ongoing infectious disease such as FIV infection.

Several pathogenic indicators have been shown to reflect the impact of FIV on the thymus. FIV infection induces cortical atrophy largely through the depletion of the main

thymocyte subpopulation, DP thymocytes. The mechanism for this cell loss is unclear. Previous studies have indicated a low incidence of direct infection of thymocytes by FIV (Woo, 1997; Hayes, 2000; Norway; 2001), so it appears that the unknown cause of cell death is due to alterations in the thymic microenvironment or indirect viral effects, such as apoptosis triggered by the viral envelope (Sutton, 2005). A relative increase in SP CD8+ cells and cells staining with a B cell marker correlates with the inflammatory infiltration of the tissue and the formation of germinal centers that are apparent upon histological evaluation.

As these tissues were available from experiments that had been used to characterize the thymic pathogenesis of FIV infection, they were a good choice for regression analysis. Changes in cell populations already identified in infected tissue could be potentially correlated to alterations found in the cytokine profile and lead to a better understanding of the impact of cytokines and viral replication on thymopoiesis.

Materials and Methods

Profile of Thymocyte Subpopulations.

The feline thymic tissue used for this cytokine research had been evaluated in previous studies investigating FIV pathogenesis in the thymus (Orandle, 1997; Crawford, 2001; Norway, 2001). Necropsy data and the results from flow cytometry experiments were compiled in order to establish larger groups than previously published, and to compare the changes in cell populations to the cytokine levels.

Statistical Analysis

Absolute cell counts and percentages of total thymocytes were used to identify the subpopulations of thymocytes. Comparisons between animal groups for cell numbers were conducted using Sigma Stat 3.0 (SPSS Inc., Chicago, IL). Changes in cytokine

levels and viral loads and replication were subjected to regression analysis. Pairwise Pearson's correlations of the cellular data with cytokine levels and viral parameters were performed with SAS 9.1 (SAS Institute, Inc., Cary, NC). Tables were generated for values when $P < 0.1$, and correlations were considered statistically significant for analyses where $P < 0.05$.

Results

Enumeration of Thymocyte Subpopulations.

The cell populations present in thymic tissue for infected animals and age-matched controls at 6-8 week, 12 week and >16 week age time points are summarized in Tables 5-1 through 5-4, and graphically represented in Figures 5-1 through 5-9. At 6-8 weeks of age, reductions in the total thymocyte number ($P = 0.11$) and increase in IgG+ cells ($P = 0.06$) due to FIV infection were not statistically significant. However, when looking at the individual cellular subsets within the tissue, a reduction in the major thymocyte population, double-positive (DP) CD4+CD8+ cells, is observed both as a percentage of total thymocytes ($P = 0.04$) and in absolute cell numbers ($P = 0.05$). The absolute number of immature DN thymocytes was unaffected with infection (P = 0.86). As an overall percentage of total thymocytes, single-positive (SP) CD4+ cells is unaffected ($P = 0.37$); but absolute numbers of CD4+ cells are in fact decreased ($P = 0.03$). An increase in SP CD8+ cells is observed as a percentage of total thymocytes ($P = 0.04$), but not when actual absolute numbers of CD8+ cells is calculated ($P = 0.64$).

For 12-week-old animals, total thymocyte numbers ($P = 0.095$) and DP thymocytes ($P = 0.095$) were decreased, but this trend did not reach statistical significance. This was also true when the decrease in DP thymocytes ($P = 0.095$) and increase in SP CD4+ thymocytes ($P = 0.1$) were examined as a percentage of total thymocytes, but the

percentage of SP CD8+ cells was significantly higher in infected animals ($P = 0.003$). Again, changes in DN thymocytes ($P = 0.71$) and IgG+ cells ($P = 0.38$) were not observed. There were no observed differences in the numbers of SP CD4+ thymocytes ($P = 0.90$), and change in the absolute numbers of SP CD8+ thymocytes were not statistically significant ($P = 0.095$).

In animals >16 weeks of age, the loss of the absolute number of total thymocytes ($P = 0.06$), DP thymocytes ($P = 0.06$) and DN thymocytes ($P = 0.09$) approaches but did not achieve statistical significance. The absolute numbers of SP CD4+ thymocytes ($P = 0.94$), SP CD8+ thymocytes ($P = 0.89$), and numbers of IgG+ cells ($P = 0.22$) were unchanged. When evaluated as a percentage of total thymocytes, DP CD4+CD8+ thymocytes were decreased ($P = 0.04$), SP CD4+ thymocytes were increased ($P = 0.07$) and the increase in SP CD8+ thymocytes was not significant ($P = 0.12$).

Table 5-1. Historical data for absolute total thymocyte counts and absolute number of total thymocytes, double-negative thymocytes and IgG+ cells (B cells) in thymus samples from animals infected with JSY3, a pathogenic molecular clone of FIV, and age-matched control animals at three different time points.

	Animal group	Total thymocytes ($x10^9$) (arithmetic mean with standard deviation)	Absolute number of DN thymocytes ($x10^9$) (arithmetic mean with standard deviation)	Absolute number of IgG+ cells ($x10^9$) (arithmetic mean with standard deviation)
1	6-8-week-old cats, uninfected (n=5)	8.64 ± 4.24	0.772 ± 0.441	0.05 ± 0.03
2	6-8-week-old cats, FIV-infected (JSY3) (n=4)	3.51 ± 3.01	0.724 ± 0.334	1.16 ± 1.44
3	12-week-old cats, uninfected (n=2)	17.75 ± 7.04	1.21 ± 0.414	0.3 ± 0.05
4	12-week-old cats, FIV-infected (JSY3) (n=5)	8.52 ± 1.7	1.1 ± 0.309	1.14 ± 0.81
5	>16-week-old cats, uninfected (n=2)	37.59 ± 18.97	4.47 ± 2.74	0.16 ± 0.12
6	>16-week-old cats, FIV-infected (JSY3) (n=7)	10.5 ± 6.02	1.99 ± 1.26	0.96 ± 0.8

Table 5-2. Historical data for absolute number of double-positive CD4+CD8+ thymocytes and the percentage of total thymocytes exhibiting the CD4+CD8+ phenotype in thymus samples from animals infected with JSY3, a pathogenic molecular clone of FIV, and age-matched control animals at three different time points.

	Animal group	Absolute number of CD4+CD8+ thymocytes ($x10^9$) (arithmetic mean with standard deviation)	% of total thymocytes CD4+CD8+ (arithmetic mean with standard deviation)
1	6-8-week-old cats, uninfected (n=5)	6.63 ± 3.4	0.764 ± 0.055
2	6-8-week-old cats, FIV-infected (JSY3) (n=4)	$1.92 \pm 2.2_a$	$0.448 \pm 0.278_a$
3	12-week-old cats, uninfected (n=2)	15.6 ± 6.22	0.876 ± 0.003
4	12-week-old cats, FIV-infected (JSY3) (n=5)	5.06 ± 1.21	0.594 ± 0.093
5	>16-week-old cats, uninfected (n=2)	2.96 ± 1.42	0.793 ± 0.023
6	>16-week-old cats, FIV-infected (JSY3) (n=7)	5.15 ± 4.17	$0.395 \pm 0.233_a$

a: animal groups with statistically significant cell counts from age-matched control groups ($P<0.05$)

Table 5-3. Historical data for absolute number of CD4+ thymic cells and the percentage of total thymic cells exhibiting the CD4+ phenotype in thymus samples from animals infected with JSY3, a pathogenic molecular clone of FIV, and age-matched control animals at three different time points.

	Animal group	Absolute number of CD4+ cells ($x10^9$) (arithmetic mean with standard deviation)	% of total thymic cells CD4+ (arithmetic mean with standard deviation)
1	6-8-week-old cats, uninfected (n=5)	0.285 ± 0.108	0.04 ± 0.02
2	6-8-week-old cats, FIV-infected (JSY3) (n=4)	$0.138 \pm 0.023_a$	0.06 ± 0.04
3	12-week-old cats, uninfected (n=2)	0.501 ± 0.407	0.03 ± 0.01
4	12-week-old cats, FIV-infected (JSY3) (n=5)	0.472 ± 0.214	0.05 ± 0.02
5	>16-week-old cats, uninfected (n=2)	0.647 ± 0.549	0.02 ± 0.01
6	>16-week-old cats, FIV-infected (JSY3) (n=7)	0.671 ± 0.361	0.07 ± 0.04

a: animal groups with statistically significant cell counts from age-matched control groups ($P<0.05$)

Table 5-4. Historical data for absolute number of CD8+ thymic cells and the percentage of total thymic cells exhibiting the CD8+ phenotype in thymus samples from animals infected with JSY3, a pathogenic molecular clone of FIV, and age-matched control animals at three different time points.

	Animal group	Absolute number of CD8+ cells ($x10^9$) (arithmetic mean with standard deviation)	% of total thymic cells CD8+ (arithmetic mean with standard deviation)
1	6-8-week-old cats, uninfected (n=5)	0.95 ± 0.7	0.099 ± 0.03
2	6-8-week-old cats, FIV-infected (JSY3) (n=4)	0.73 ± 0.62	$0.225 \pm 0.105_a$
3	12-week-old cats, uninfected (n=2)	0.48 ± 0.01	0.029 ± 0.012
4	12-week-old cats, FIV-infected (JSY3) (n=5)	1.89 ± 0.71	$0.219 \pm 0.048_a$
5	>16-week-old cats, uninfected (n=2)	2.87 ± 1.49	0.076 ± 0.001
6	>16-week-old cats, FIV-infected (JSY3) (n=7)	2.68 ± 1.73	0.296 ± 0.169

a: animal groups with statistically significant cell counts from age-matched control groups ($P<0.05$)

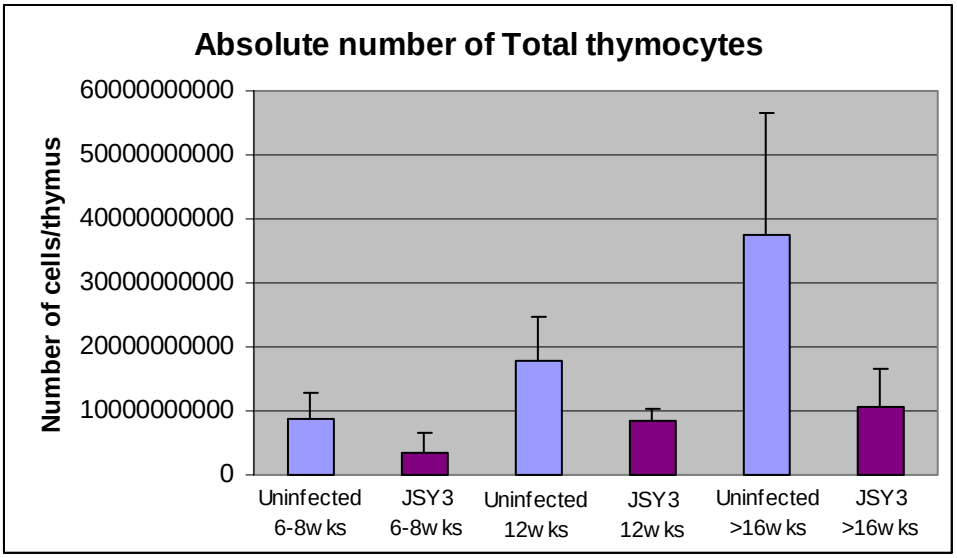

Figure 5-1. Historical flow cytometry results from previous published experiments: absolute numbers of total thymocytes present in thymus samples from animals infected with JSY3, a pathogenic molecular clone of FIV, and age-matched control animals at three different time points.

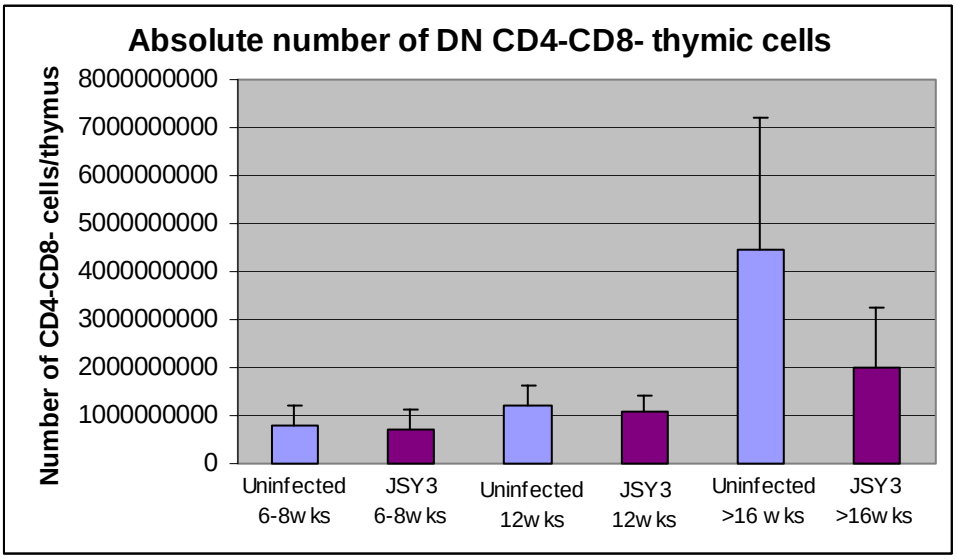

Figure 5-2. Historical flow cytometry results from previous published experiments: absolute numbers of double-negative (DN) CD4-CD8- cells present in thymus samples from animals infected with JSY3, a pathogenic molecular clone of FIV, and age-matched control animals at three different time points.

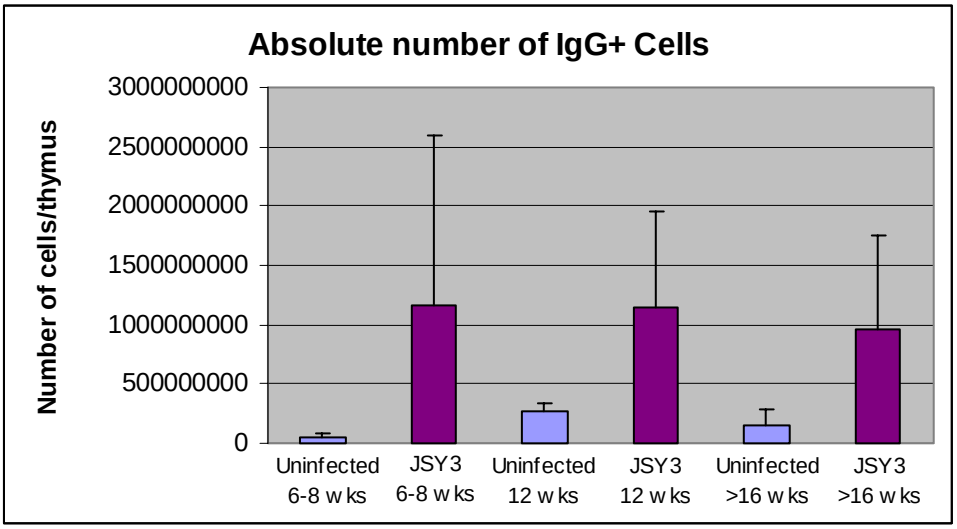

Figure 5-3. Historical flow cytometry results from previous published experiments: absolute numbers of IgG+ cells (B cells) present in thymus samples from animals infected with JSY3, a pathogenic molecular clone of FIV, and age-matched control animals at three different time points.

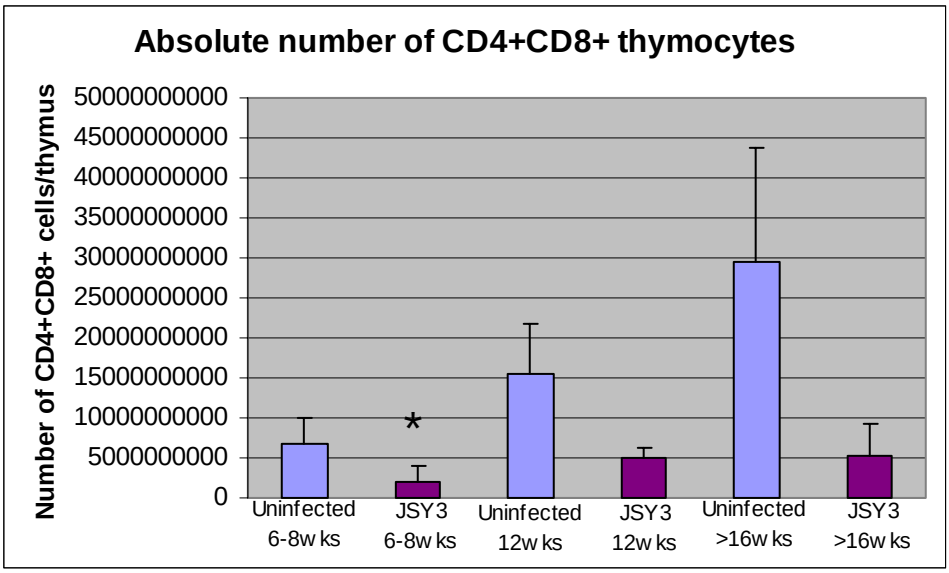

Figure 5-4. Historical flow cytometry results from previous published experiments: absolute numbers of CD4+CD8+ thymocytes present in thymus samples from animals infected with JSY3, a pathogenic molecular clone of FIV, and age-matched control animals at three different time points. (*) denotes statistically significant differences from all other animal groups in study ($P < 0.05$).

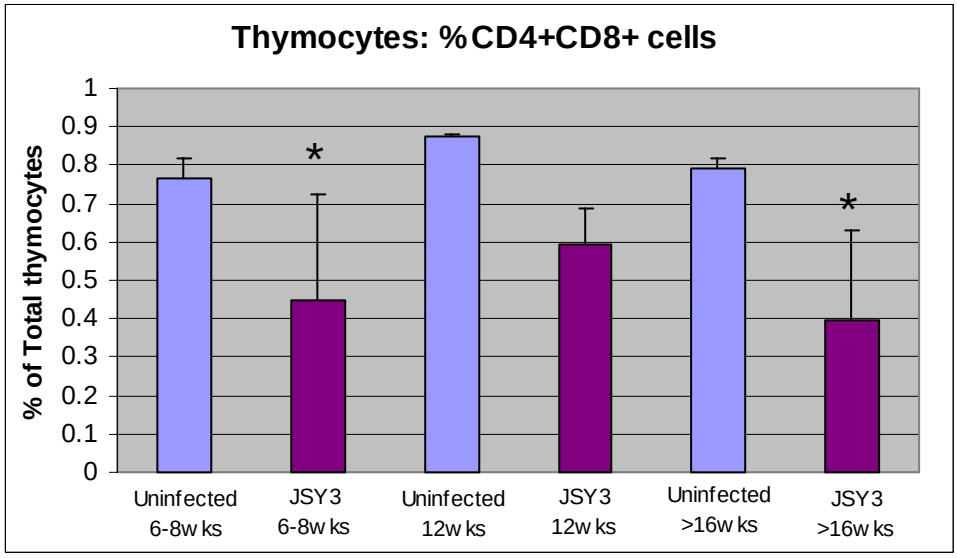

Figure 5-5. Historical flow cytometry results from previous published experiments: percentage of CD4+CD8+ thymocytes present in thymus samples from animals infected with JSY3, a pathogenic molecular clone of FIV, and age-matched control animals at three different time points. (*) denotes statistically significant differences from all other animal groups in study ($P < 0.05$).

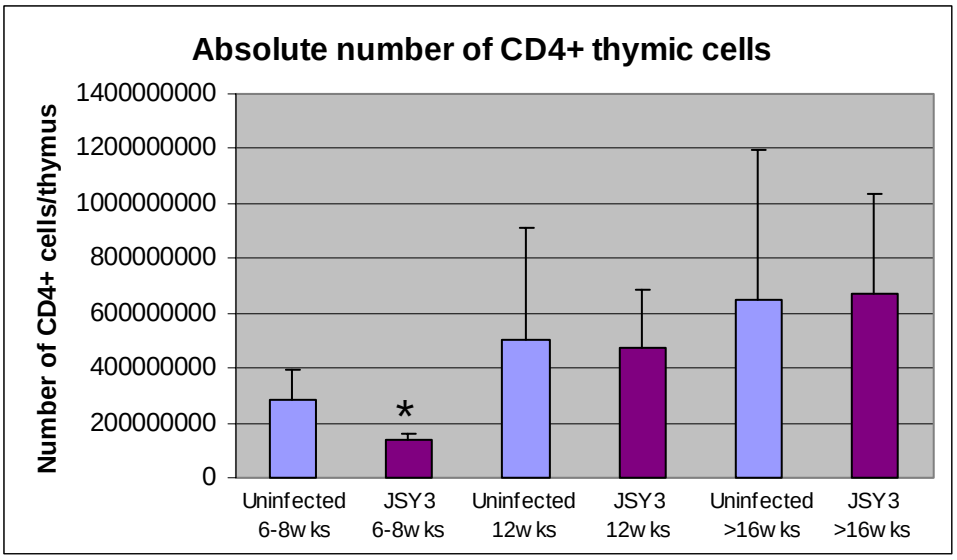

Figure 5-6. Historical flow cytometry results from previous published experiments: absolute numbers of single-positive (SP) CD4+ cells present in thymus samples from animals infected with JSY3, a pathogenic molecular clone of FIV, and age-matched control animals at three different time points. (*) denotes statistically significant differences from all other animal groups in study ($P < 0.05$).

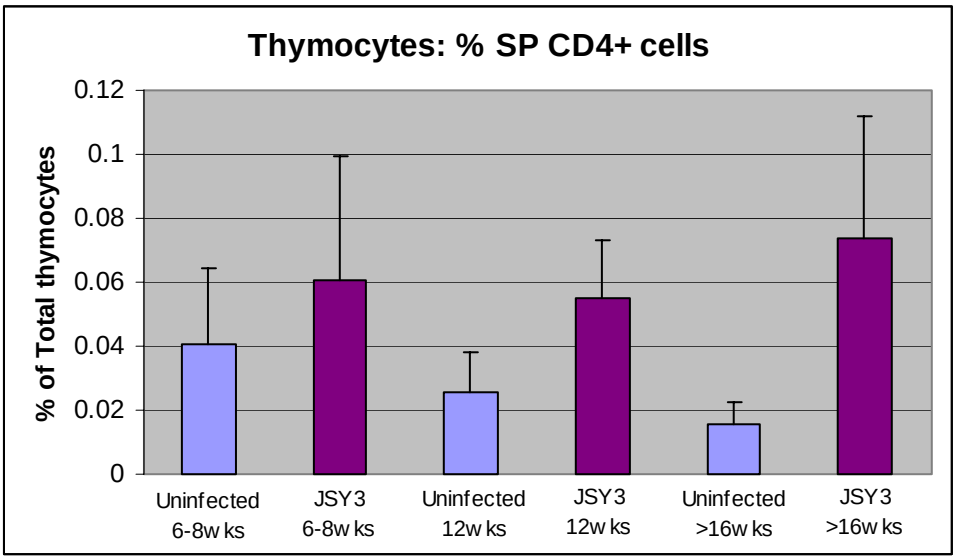

Figure 5-7. Historical flow cytometry results from previous published experiments: percentage of single-positive (SP) CD4+ cells present in thymus samples from animals infected with JSY3, a pathogenic molecular clone of FIV, and age-matched control animals at three different time points.

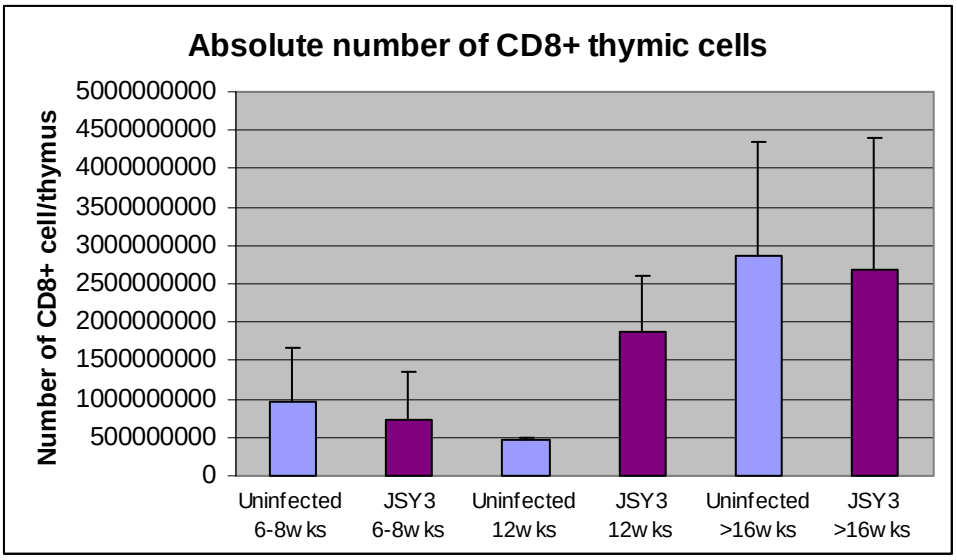

Figure 5-8. Historical flow cytometry results from previous published experiments: absolute numbers of single-positive (SP) CD8+ cells present in thymus samples from animals infected with JSY3, a pathogenic molecular clone of FIV, and age-matched control animals at three different time points.

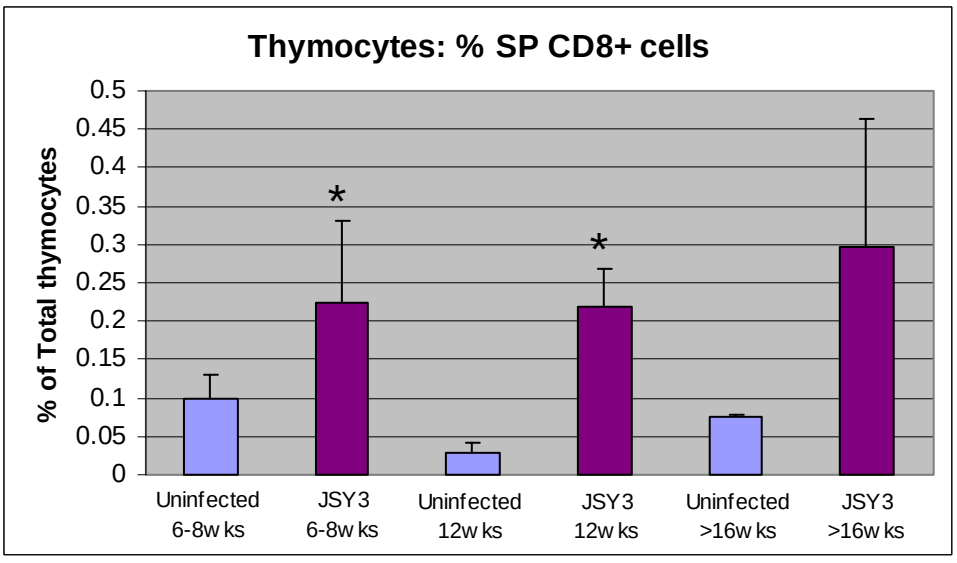

Figure 5-9. Historical flow cytometry results from previous published experiments: percentage of single-positive (SP) CD8+ cells present in thymus samples from animals infected with JSY3, a pathogenic molecular clone of FIV, and age-matched control animals at three different time points. (*) denotes statistically significant differences from all other animal groups in study ($P < 0.05$).

Peripheral Blood Counts

Total white blood cell counts (total WBC) and numbers of CD4+ and CD8+ T cells in the peripheral blood are compiled in Table 5-5. Cell count data is graphically represented in Figures 5-10 through 5-12. At 6-8 weeks of age, the WBC ($P = 0.91$) and CD4+ T cell count ($P = 0.41$) are unchanged, and the increase in circulating CD8+ T cells is not statistically significant ($P = 0.08$). By the 12-week time point, WBC are statistically unchanged ($P = 0.2$), as is the CD4+ cell count ($P = 0.57$) and the numbers of CD8+ cells ($P = 0.3$). At >16 weeks of age, again the WBC ($P = 0.97$) and CD8+ T cell number ($P = 0.95$) remains unaffected, and the changes in CD4+ T cells are not statistically significant ($P = 0.08$).

Table 5-5. Historical data for absolute number of total white blood cells, CD4+ T cells and CD8+ T cells within peripheral blood samples from animals infected with JSY3, a pathogenic molecular clone of FIV, and age-matched control animals at three different time points.

	Animal group	Total WBC (arithmetic mean with standard deviation)	CD4+ cells ($x10^9$) (arithmetic mean with standard deviation)	CD8+ cells ($x10^9$) (arithmetic mean with standard deviation)
1	6-8-week-old cats, uninfected (n=5)	8718 ± 1157	619 ± 696	266 ± 236
2	6-8-week-old cats, FIV-infected (JSY3) (n=4)	9800 ± 4761	1096 ± 835	670 ± 353
3	12-week-old cats, uninfected (n=2)	6915 ± 1478	1214 ± 567	487 ± 201
4	12-week-old cats, FIV-infected (JSY3) (n=5)	13788 ± 6186	879 ± 682	953 ± 528
5	>16-week-old cats, uninfected (n=2)	9050 ± 4596	1441 ± 1062	500 ± 228
6	>16-week-old cats, FIV-infected (JSY3) (n=7)	8919 ± 3668	586 ± 411	517 ± 325

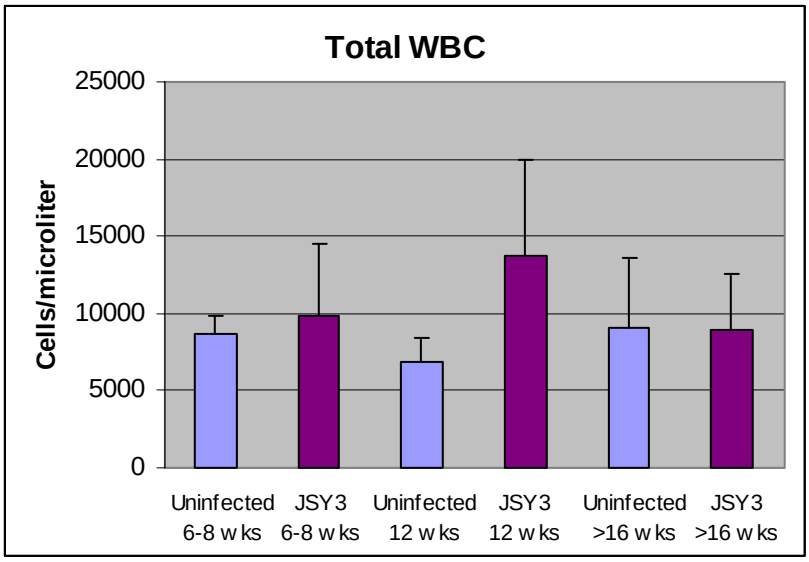

Figure 5-10. Historical flow cytometry results from previous published experiments: absolute numbers of white blood cells present in peripheral blood samples from animals infected with JSY3, a pathogenic molecular clone of FIV, and age-matched control animals at three different time points.

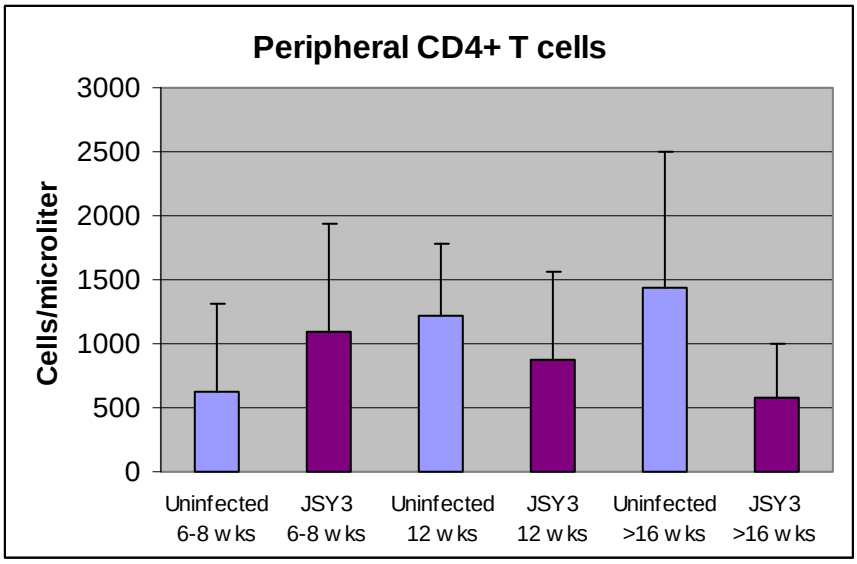

Figure 5-11. Historical flow cytometry results from previous published experiments: absolute numbers of single-positive (SP) CD4+ cells present in peripheral blood samples from animals infected with JSY3, a pathogenic molecular clone of FIV, and age-matched control animals at three different time points.

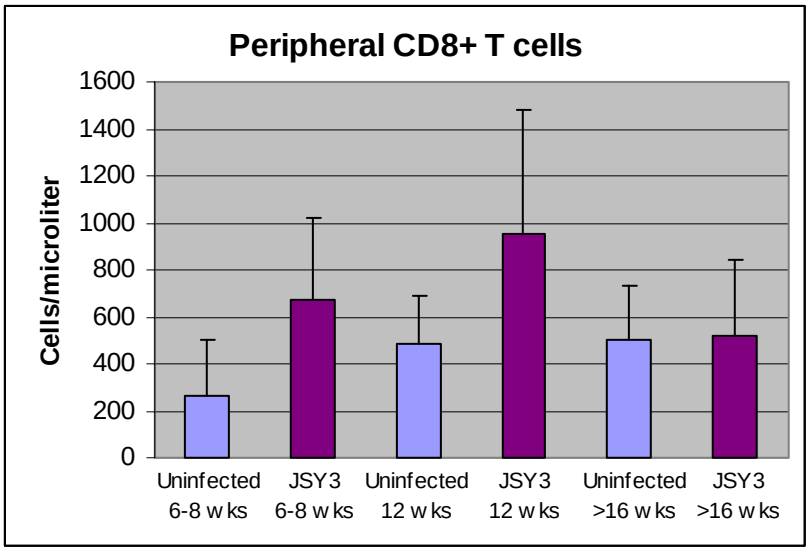

Figure 5-12. Historical flow cytometry results from previous published experiments: absolute numbers of single-positive (SP) CD8+ cells present in thymus samples from animals infected with JSY3, a pathogenic molecular clone of FIV, and age-matched control animals at three different time points.

Pairwise Correlations of Lymphocyte Subsets to Viral and Cytokine Parameters

A summary of Pearson's pairwise correlations with a *P* value less than 0.1 are compiled in Table 5-6. In Chapter 4, it was determined that IL-4, IL-7, IFN-α and IFN-γ exhibited similar expression patterns. The regression analysis confirms a strong positive correlation between the expression levels of IL-7, IFN-α and IFN-γ ($P < 0.001$). Expression of these cytokines was associated with increased absolute numbers of thymocytes, DP CD4+CD8+ thymocytes and DN CD4-CD8- thymocytes. IL-4 was correlated with increased numbers of SP CD4+ cells within the thymus ($P = 0.002$) and SP CD8+ T cells within the peripheral circulation ($P = 0.03$). Expression of IL-15 weakly associated with percentage of CD8+ cells within the thymus ($\rho = 0.363$, $P = 0.068$), and highly correlated with numbers of CD8+ T cells circulating within the peripheral blood ($P = 0.005$). No cytokine or cellular data appeared to correlate with proviral load/*gag* DNA levels. However, *gag* RNA/viral gene expression was increased

with elevated numbers of SP CD8+ cells within the thymus ($P = 0.001$) and IFN-γ expression ($P = 0.012$). *Gag* RNA was less strongly but positively associated with the presence of IgG+ cells within the thymus ($\rho = 0.525$, $P = 0.08$) and IL-15 expression ($\rho = 0.513$, $P = 0.07$).

Table 5-6. Summary of Pearson's pairwise correlations of historical necropsy data, measured cytokine values and viral parameters. All comparisons with $P<0.1$ are listed.

Variable 1	Variable 2	Rho (ρ)	*P* value
%CD4+CD8+ thymocytes	IFN-α	0.335	0.095
%CD4+ thymocytes	IL-7	-0.362	0.069
%CD4+ thymocytes	IFN-α	-0.438	0.025
%CD8+ thymocytes	IL-15	0.363	0.068
Absolute # total thymocytes	IL-7	0.792	<0.001
Absolute # total thymocytes	IFN-γ	0.766	<0.001
Absolute # total thymocytes	IFN-α	0.769	<0.001
Absolute # CD4+CD8+ thymocytes	IL-7	0.8	<0.001
Absolute # CD4+CD8+ thymocytes	IFN-γ	0.74	<0.001
Absolute # CD4+CD8+ thymocytes	IFN-α	0.789	<0.001
Absolute # of CD4+ thymocytes	IL-4	0.586	0.002
Absolute # of CD8+ thymocytes	IFN-γ	0.434	0.03
Absolute # of CD8+ thymocytes	*gag* RNA	0.812	0.001

Absolute # of CD4-CD8- thymocytes	IL-7	0.652	<0.001
Absolute # of CD4-CD8- thymocytes	IFN-γ	0.699	<0.001
Absolute # of CD4-CD8- thymocytes	IFN-α	0.602	0.001
IgG+ cells	IL-15	0.367	0.072
IgG+ cells	*gag* RNA	0.525	0.08
Total WBC (peripheral blood)	IL-15	0.55	0.004
CD8+ T cells (peripheral blood)	IL-4	0.43	0.03
CD8+ T cells (peripheral blood)	IL-15	0.537	0.005
IL-7	IFN-γ	0.952	<0.001
IL-7	IFN-α	0.949	<0.001
IL-15	*gag* RNA	0.513	0.07
IFN-γ	IFN-α	0.892	<0.001
IFN-γ	*gag* RNA	0.671	0.012

Discussion

This compiled data represents a greater number of overall animals than previous reports and is broken down into distinct age brackets/phases of infection for analysis. The earlier studies reported a reduction of DP CD4+CD8+ thymocytes and in increase in the percentage of SP CD8+ cells in thymuses of infected animals (Orandle, 1997; Orandle 2000; Johnson, 2001; Norway, 2001). Similar findings were found in the current investigation: specifically, statistically significant changes were observed in decreased

absolute numbers of DP thymocytes at weeks 6-8, the decreased percentages of DP thymocytes at weeks 6-8 and >16 weeks, and in the increased percentage of total thymic cells that are CD8+ at weeks 6-8 and 12. Significant changes in total thymocyte number, absolute numbers of DN thymocytes and IgG+ cells were not observed.

The correlation in expression levels of IL-7, IFN-α and IFN-γ was observed in Chapter 4 and confirmed here with regression analysis. Expression of these cytokines appeared to be associated with improved indicators of thymus composition, namely increased overall number of thymocytes, and, more specifically, increased numbers of the immature DP thymocytes and DN thymocytes. Levels of IL-15 were not significantly associated with increased inflammatory infiltrates, germinal center formation, the percentage of CD8+ cells and numbers of IgG+ (B cells) within the thymus. No cytokine influences on proviral load were observed, but viral *gag* gene expression was positively associated with inflammatory infiltrates (CD8+ cells) and IFN-γ expression. It is not clear, however, whether increased viral expression induces more pronounced inflammation, or if the influx of inflammatory cells is responsible for the increase in viral activity.

Decreases in endogenous thymic production of IFN-α proved to be the most pronounced cytokine change observed. As there was a marked peak in IFN-α mRNA production in the older animals that was abrogated by infection with FIV, further experiments were undertaken to determine a potential source of the IFN production (Chapter 6) and the effects of IFN-α on viral replication in thymocytes (Chapter 7). It was proposed that an interferon-producing cell type such as the Type II/plasmacytoid

dendritic cell might exist in the thymus of cats that could potentially be infected directly by FIV or undergo viral-induced impairment of IFN-producing function.

CHAPTER 6
DETECTION OF FIV-INFECTED CELLS AND IFN-PRODUCING CELLS WITHIN THE THYMUS OF NORMAL AND FIV-INFECTED CATS

Introduction

Historically, one limitation in the manipulation and study of plasmacytoid dendritic cells (PDCs)/interferon-producing cells (IPCs) was the lack of a specific cellular surface expression marker. Isolation of IPCs required depleting peripheral blood mononuclear cells (PBMCs) of cells bearing lineage specific molecules, including CD3 (T cells), CD19 (B cells), CD14 (monocytes) and CD56 (NK cells). Remaining cells were enriched for IPCs by selecting for CD11c-negative/CD123-bright cells, to remove the monocyte-derived type 1 dendritic cells (Siegal, 1999). A PDC-specific marker was eventually discovered, blood dendritic cell antigen-2 (BDCA-2) (Dzionek, 2000). Characterization of this molecule revealed it as a novel type II C-type surface lectin (Dzionek, 2001). A recombinant human dendritic cell lectin (rhDLEC) was developed and commercially developed antibodies recently became available, facilitating the study of this rare cell type.

The thymus has been shown to harbor a subset of resident PDC, however, their function within the normal thymus remains unclear (Fohrer, 2004). While most of these cells were observed to be of an immature phenotype, some PDC expressed markers indicative of activation and may contribute to a late stage of negative thymocyte selection. In the context of HIV infection, *in vitro* experiments using a thymic culture system have shown that thymic PDCs respond to viral infection with IFN-α production

(Gurney, 2004). The amount of interferon produced suppressed viral production, but at a suboptimal level and could be enhanced by the addition of CpG oligonucleotides to the culture system. While PDCs only comprised 0.2% of the lymphoid cells of the thymus, depletion of these cells from the thymic culture enhanced viral replication 2-110 fold.

Previous reports indicated that anti-human DLEC antibodies did not cross-react with PDC from the peripheral blood of the rhesus macaque (Chung, 2005). The current study sought to test the binding capacity of a polyclonal anti-human DLEC-derived antibody against feline thymic PDCs using a peroxidase-based immunohistochemistry protocol and provide preliminary data to characterize this cell type.

Materials and Methods

Single-Label Immunohistochemistry

Archival tissue selected from seven 6-8-week-old kittens (acute FIV infection) and six >16-week-old kittens (chronic FIV infection) that had been inoculated at birth with JSY3, a FIV molecular clone that exhibits thymic pathogenicity (Orandle, 1997; Norway, 2001; Johnson, 2001). Uninfected thymus samples from two 6-8-week-old kittens and four >16-week-old kittens served as age-matched controls. 5 µm frozen sections of thymic tissue were removed from -80ºC and immediately fixed in ice cold ethanol for 5 minutes and rinsed in room temperature PBS buffer. Sections were incubated at room temperature for 30 minutes with blocking solution of 1% normal horse serum and blotted, followed by a 30 minute incubation with10µg/mL of either anti-rhDLEC polyclonal antibody (R&D Systems, Minneapolis, MN, USA), a polyclonal anti-human IFN-α antibody (PBL Biomedical Laboratories, Piscataway, NJ, USA) or a monoclonal antibody against FIV p24 *gag* protein (clone PAK3-2C1; Custom Monoclonals International, West Sacramento, CA.). Negative control slides from infected and

uninfected thymus sections underwent an additional blocking step and did not receive primary antibody. All slides were developed and stained using the Vectastain Universal Elite® ABC Kit (Vector Laboratories Inc., Burlingame, CA) and visualized with diaminobenzidine chromagen enhanced with nickel. Sections were then rinsed in water and counterstained with Harris's hematoxylin. Slides were examined microscopically, and measurements of total visualized thymic area were made at a 40X objective magnification using the Image J NIH software program (http://rsb.info.nih.gov/ij/download.html). The results were reported as the number of positively-staining cells identified per unit of designated area.

Double-Label Immunohistochemistry

Tissue sections from several acutely and chronically infected kittens were chosen based on the quality of the tissue sections during previous single-label immunohistochemistry experiments. 5 µm thymic samples were removed from -80ºC and immediately fixed in ice cold ethanol for 5 minutes and rinsed in room temperature PBS buffer. Sections were incubated at room temperature for 30 minutes with blocking solution of 1% normal horse serum and blotted, followed by a 30 minute incubation with10µg/mL of anti-rhDLEC polyclonal antibody (R&D Systems, Minneapolis, MN, USA). Negative control slides did not receive an incubation with the primary antibody and underwent an additional 30 minute blocking step. All slides were developed and stained using the Vectastain Universal Elite ABC Kit (Vector Laboratories Inc., Burlingame, CA) and visualized with diaminobenzidine chromagen enhanced with nickel. Slides were incubated again with blocking solution for 30 minutes, then incubated with a second primary antibody, either polyclonal anti-human IFN-α antibody (PBL Biomedical Laboratories, Piscataway, NJ, USA) or a monoclonal antibody against

FIV p24 *gag* protein (clone PAK3-2C1; Custom Monoclonals International, West Sacramento, CA.). Negative slides remained in blocking solution and did not receive primary antibody. Slides were developed and stained using the Vectastain Universal Elite ABC Kit (Vector Laboratories Inc., Burlingame, CA) and visualized with Vector VIP Substrate (Vector Laboratories Inc., Burlingame, CA). Slides were examined via light microscopy for positively-staining cells.

Statistical Analysis

The numbers of cells present per unit area were analyzed for differences between the groups of FIV-infected animals and the age-matched control cats. SAS PROC GLM was used to conduct the one-way ANOVA analysis, and the least squares means were calculated and pair-wise group comparisons were conducted using SAS 9.1 (SAS Institute, Inc., Cary, NC).

Results

Initial immunohistochemical slides exhibited mild homogenous brown extracellular background staining within the germinal centers/lymphoid follicles, particularly in test samples using lymph nodes. However, attempts to incorporate a step to quench endogenous peroxidase activity resulted in abrogation of antibody staining and were discontinued. The low level of brown background stain did not impair the evaluation of the dark black cellular staining in antigen-positive cells.

Pathologic changes in thymic sections from infected animals included variable loss of cortical thymocytes, but overall the cortices were well populated and the corticomedullary junctions were clearly visible. Formation of germinal centers was a prominent feature within the infected tissues, and formed either within the medullary areas or abutting the cortical surface.

Single-Label Immunohistochemistry

Single-label immunohistochemistry experiments using the anti-rhDLEC antibody in uninfected thymuses stained a very small number of medium-sized to large, ovoid cells scattered along the corticomedullary junction, as shown in Figure 6-1. In samples from infected animals, these cells were still present, but the majority of DLEC+ cells were found to be present within the inflammatory germinal centers that developed as a result of viral infection (Figure 6-2).

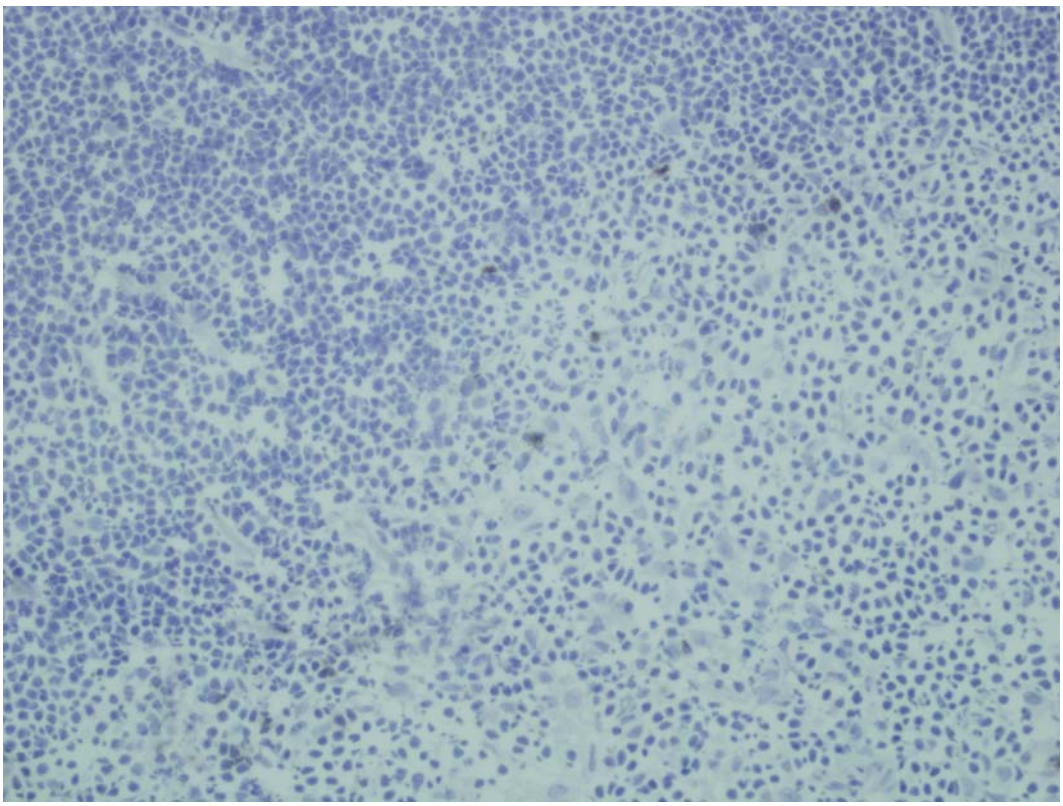

Figure 6-1. 40X. Single-label immunohistochemistry with a polyclonal antibody against human BDCA-2 (DLEC) performed on thymic sections from a 16-week-old, uninfected kitten. Scattered, black-staining DLEC+ cells are present along the junction between the cortex (more densely cellular area along the top and left of the figure) and the medulla.

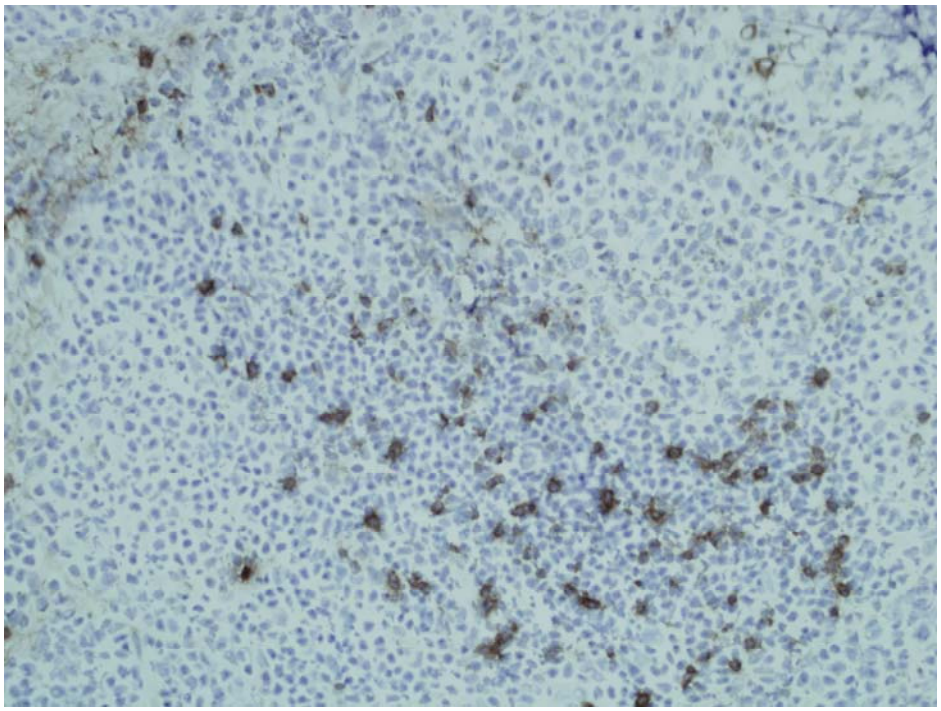

Figure 6-2. 60X. Single-label immunohistochemistry with a polyclonal antibody against human BDCA-2 (DLEC) performed on thymic sections from an 8-week-old kitten infected with FIV. DLEC+ cells are clustered within a germinal center that formed along the thymic corticomedullary junction.

Single-label immunohistochemistry experiments using the anti-human IFN-α antibody resulted in a similar number and distribution of positively staining cells when compared to those using the anti-rhDLEC antibody. In uninfected animals, small numbers of positive cells were present along the corticomedullary junction, but in addition, there was faint positive staining of endothelial cells (Figure 6-3). In infected animals, cells were present in qualitatively higher numbers and were present along the corticomedullary junction and within germinal centers (Figure 6-4).

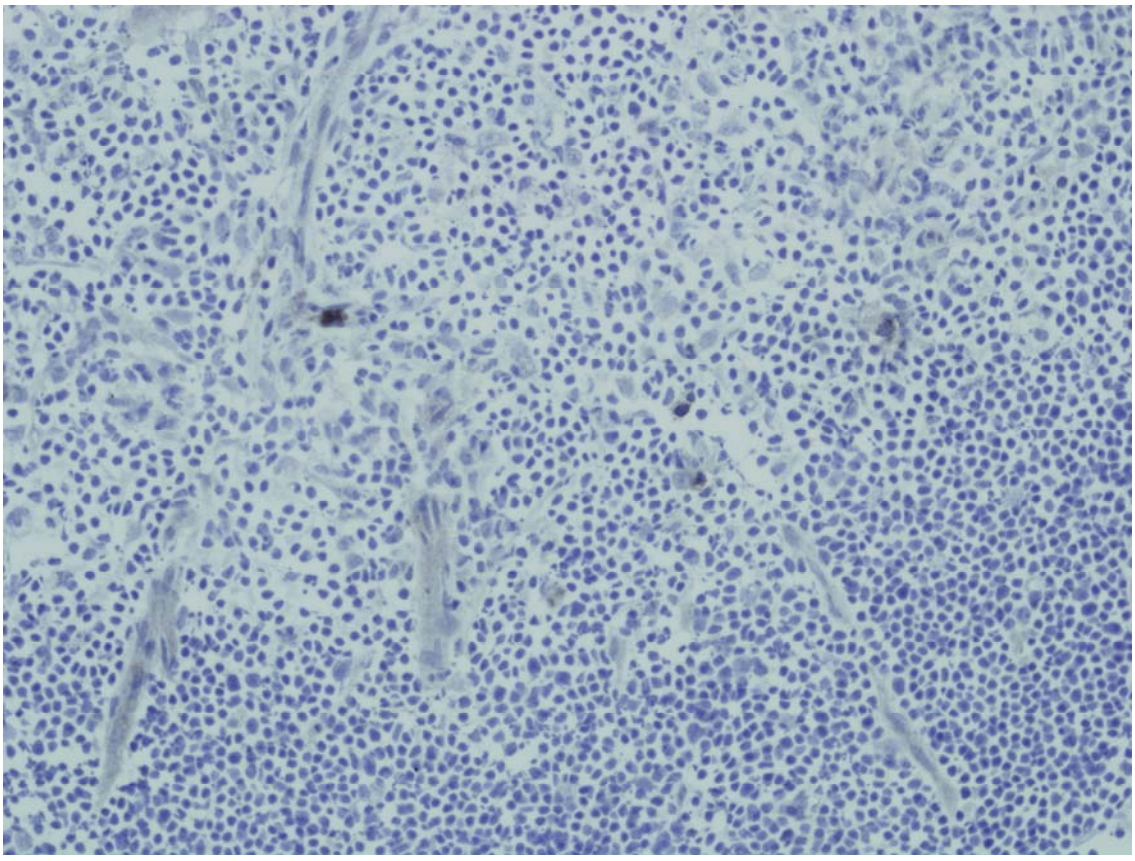

Figure 6-3. 40X. Single-label immunohistochemistry with an antibody against IFN-α performed on thymic sections from a 16-week-old, uninfected kitten. Scattered, black-staining IFN+ cells are present along the junction between the cortex (more densely cellular area along the bottom of the figure) and the medulla. Endothelial cells also exhibit faint positive staining.

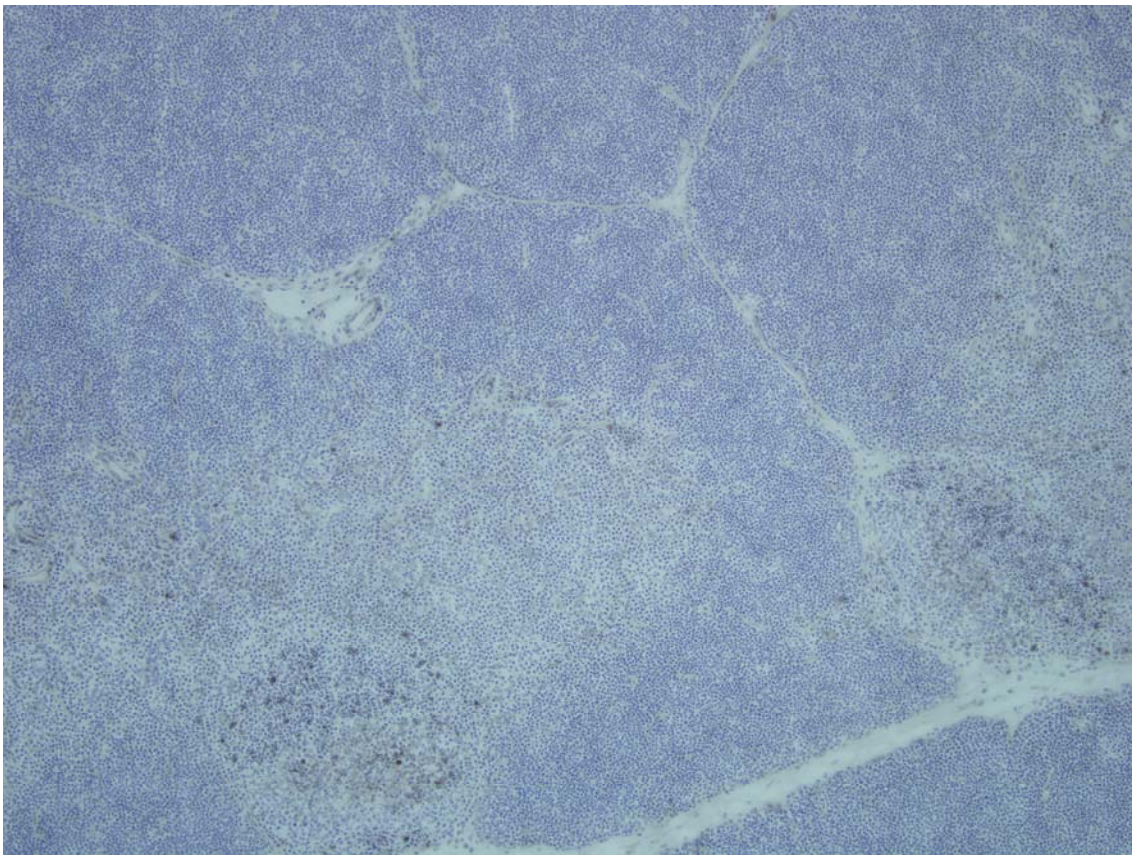

Figure 6-4. 10X. Single-label immunohistochemistry with an antibody against IFN-α performed on thymic sections from an 8-week-old kitten infected with FIV. Black IFN+ cells are clustered within germinal centers and along the thymic corticomedullary junction. The fainter homogenous brown staining was typical of germinal centers and was not considered positive when counting for IFN+ cells.

Single-label immunohistochemistry using an antibody against the p24 antigen of FIV did not stain cells within uninfected tissues. Again, the distribution of positively staining cells within the thymic sections was largely limited to lymphoid follicles with smaller numbers of cells scattered throughout the medulla. p24 staining cells were distributed evenly throughout the follicles, and the number of positive cells seemed to exceed that observed with the DLEC and IFN antibodies (Figure 6-5). p24+ cells were rare within the thymic cortex.

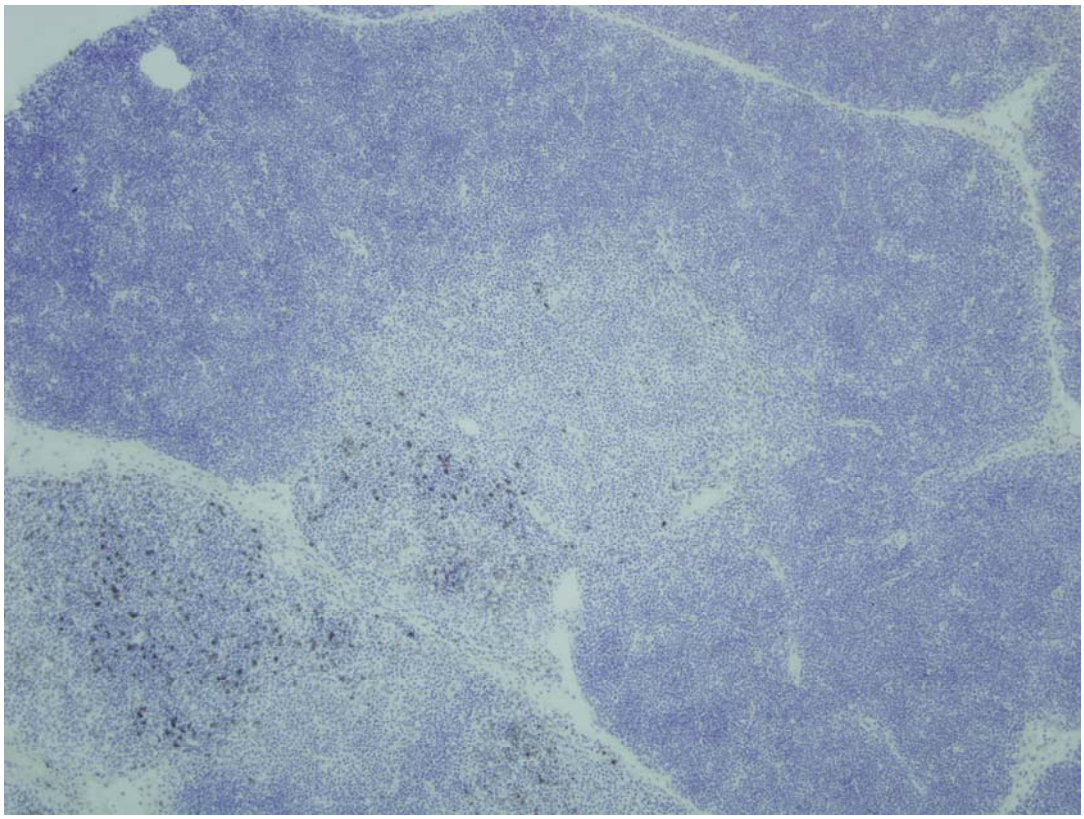

Figure 6-5. 10X. Single-label immunohistochemistry with mAb against FIV p24 performed on thymic sections from an 8-week-old kitten infected with FIV. Black p24+ cells are clustered within germinal centers and throughout the medulla.

As the tissue sections from the different animals varied in size, the area of thymus being assessed for positive staining was measured in order to standardize the data. The number of DLEC+ and IFN+ cells per unit area are summarized in Tables 6-1 and 6-2.

Table 6-1. Number of DLEC+ cells per unit of thymic area.

Animal group	Mean # positive cells/unit area
6-8-week-old cats, uninfected (n=2)	2.27×10^{-6}
6-8-week-old cats, FIV-infected (n=6)	14.49×10^{-6}
>16-week-old cats, uninfected (n=4)	2.3×10^{-6}
>16-week-old cats, FIV-infected (n=6)	5.28×10^{-6}

Table 6-2. Number of IFN+ cells per unit of thymic area.

Animal group	Mean # positive cells/unit area
6-8-week-old cats, uninfected (n=2)	1.55×10^{-6}
6-8-week-old cats, FIV-infected (n=5)	10.26×10^{-6}
>16-week-old cats, uninfected (n=2)	2.4×10^{-6}
>16-week-old cats, FIV-infected (n=5)	$7.24\ 10^{-6}$

Statistical analysis of the data showed that there was no significant differences among the groups for number of cells per unit area that stain positively for IFN-α . For tissues stained with anti-rhDLEC, 6-8-week-old FIV-infected samples contained significantly more positively staining cells than >16-week-old uninfected animals ($p=0.021$) and >16-week-old kittens infected with FIV ($p=0.0497$).

Double-Label Immunohistochemistry

In thymic tissues stained for DLEC and p24 or DLEC and IFN, the histological appearance of the positively staining cells was similar. Cells staining positively for DLEC (black) also appeared to stain positively for p24 and IFN (purple) in the respective sections (Figures 6-6 and 6-7). There were occasional cells that stained purple (FIV+ or IFN+) in the absence of co-localizing black stain. These results suggest that many

DLEC+ cells within these sections were associated with virus antigen and are producing IFN-α.

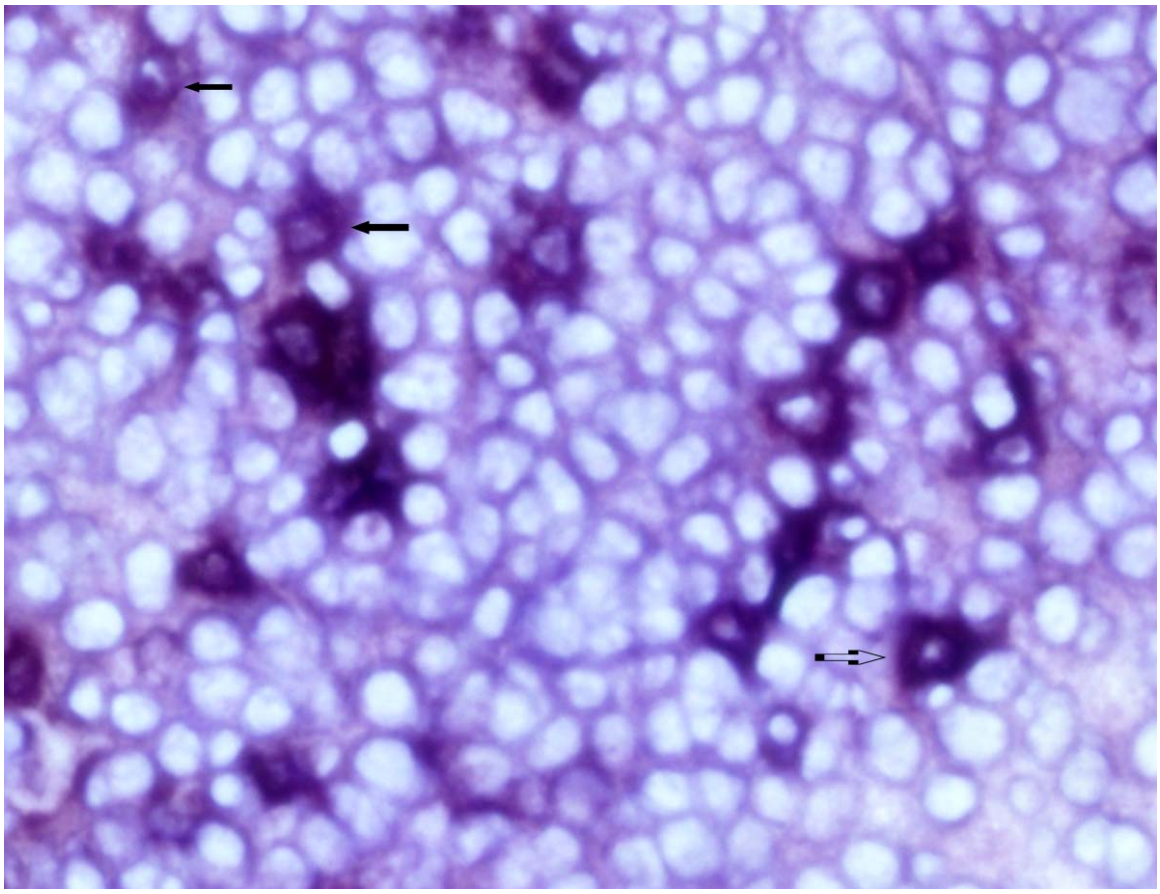

Figure 6-6. 40X. Double-label immunohistochemistry for DLEC and IFN-α performed on thymic sections from an 8-week-old kitten infected with FIV. Black staining (DLEC+) co-localizes with purple stain for IFN-α in germinal centers(open arrow). Occasional cells stain positively for IFN in the absence of DLEC expression (black arrows).

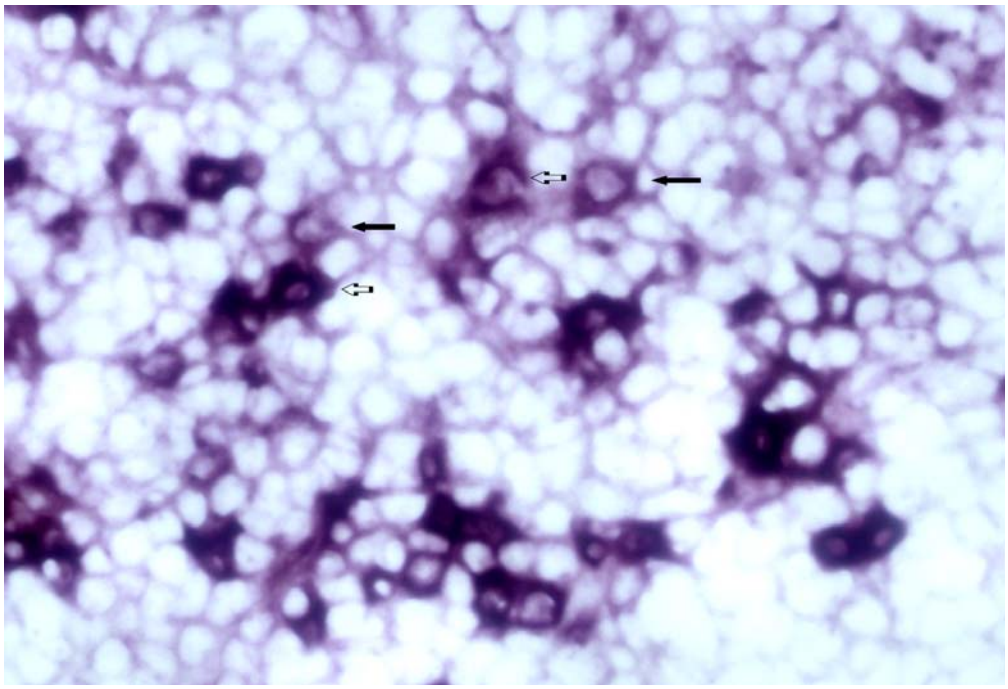

Figure 6-7. 40X. Double-label immunohistochemistry for DLEC and FIV p24 performed on thymic sections from an 8-week-old kitten infected with FIV. Black staining (DLEC+) co-localizes with purple stain for the p24 antigen of FIV in the germinal centers (open arrows). Occasional cells stain positively for p24 in the absence of DLEC expression (black arrows).

Discussion

The series of immunohistochemistry experiments in this study show that polyclonal antibody raised against rhDLEC cross-reacts with a resident subset of feline thymic cells. As the polyclonal antibody against IFN-α gave a similar histological distribution of cells within the thymus, double-label immunohistochemistry was performed on infected thymus samples to demonstrate that the same cells are staining positively for both dendritic cell antigen and are producing IFN-α. The signals did appear to co-localize, suggesting DLEC+ cells are in fact IPCs. Some IFN+ cells were not expressing DLEC, suggesting that another cell type is contributing to interferon production, or that DLEC expression within some IPCs was too low to detect by this method.

DLEC+ cells appear increased in numbers in infected thymus samples, but this proved to be only statistically significant for samples from FIV-infected 6-8-week-old kittens when compared to those of infected and uninfected 16-week-old animals. In normal animals, the distribution of these cells is limited to the corticomedullary junction, while in FIV-infected animals, DLEC+ cells are a prominent cell type within germinal centers. The distribution of IFN+ cells was similar to that of DLEC+ cells, but statistical significance was not observed between any of the animal groups.

FIV-infected p24+ cells were observed within germinal centers and scattered in smaller numbers within the thymic medulla. Given the similar distribution of infected cells to the IPCs in previous sections, dual-label immunohistochemistry for p24 and DLEC was performed. Again, there was co-localization of the p24 signal to DLEC+cells, suggesting that IPCs within the feline thymus harbor FIV.

This preliminary investigation shows that DLEC+ cells are present in the feline thymus, and appear to produce IFN-α and become infected with FIV. Isolation of this cell type and *in vitro* infection studies are necessary for definitive confirmation of these observations.

CHAPTER 7
SUSCEPTIBILITY OF THYMOCYTES TO FIV CHALLENGE IN VITRO

Introduction

Thymopoiesis and the ongoing output of viable thymocytes are crucial to the pathogenesis of lentivirus infection and are necessary for the replacement of the virally targeted T cells that are lost in the course of infection. Direct infection of the thymus by FIV is known to occur and results in a partial loss of the primary subpopulation of thymocytes, the double-positive (DP) CD4+CD8+ cells (Orandle, 1997; Orandle, 2000; Norway, 2001; Johnson, 2001). As our experiments showed that IFN-α was normally expressed in the thymus, had suppressed expression with FIV infection (Chapter 4), and that increased levels of IFN correlated with increased absolute numbers of DP thymocytes and total numbers of thymocytes (Chapter 5), we hypothesized that IFN-α may confer protective effects in thymuses against FIV infection and the loss of IFN contributes to increases thymic pathogenesis. Cell culture experiments with fetal thymocytes were undertaken to produce viral infection in thymocytes and observe the impact of IFN treatment on viral replication in thymocyte cultures. The previously characterized, pathogenic FIV molecular clone JSY3 and the open reading frame (ORF)-A-deficient clone were used in these studies.

Materials and Methods

Cell Culture

Frozen thymocytes cells were retrieved from storage in liquid nitrogen, thawed, rinsed in wash media (complete RPMI 1640 medium supplemented with 2% fetal bovine

serum), pelleted and resuspended in culture medium [cRPMI 1640 medium supplemented with 10% fetal bovine serum, 2mM L-glutamine, 10 mM HEPES, 0.075% sodium bicarbonate, 2 mM sodium pyruvate, 2-mecaptoethanol, and 100U/mL of recombinant human interleukin-2 (rhIL-2)]. Cells were plated at 2 X 10^6 viable cells per milliliter and incubated at 37ºC for the nine days of the experiment. Viral stocks of JSY3 and JSY3ΔORF-A (viral strain containing a mutation in the open reading frame A [ORF-A] gene) were used in multiple experiments at various dilutions of 50% tissue culture infectious doses ($TCID_{50}$), which ranged from 5 X 10^4 to 3 X 10^5 $TCID_{50}$. Samples of cell culture supernatant were taken at days 3, 6 and 9 for the reverse transcriptase activity assay. When viral infection was not observed, subsequent experiments included CD4E cells as a positive control cell type for viral replication. At day 9 samples of remaining cells were stained with trypan blue and viable cell counts were determined. Supernatant samples were submitted and evaluated for viral replication using an assay for reverse transcriptase (RT) activity (Johnson, 1990).

Results

Viral Replication in Thymocyte and CD4E Cell Culture Systems.

Three cell culture experiments were performed with thymocytes with multiple animal sources in an attempt to observe viral replication in this cell type. The first two experiments yielded no significant RT activity in any treatment wells at any time point regardless of infectious dose, leading to the conclusion that infection studies in this cell type were not feasible. A final cell culture experiment was undertaken in conjunction with CD4E cells as a positive cell type control, in order to confirm that the input virus strains were infectious. This third run yielded a single small peak in RT activity in thymocyte cultures infected with the JSY3 strain of FIV at day 9 and significant

replication was observed at days 6 and 9 in CD4E cells (Figure 7-2), confirming the viability of the infecting virus. The ORF-A-deficient mutant strain of FIV did not show significant replication in either cell type.

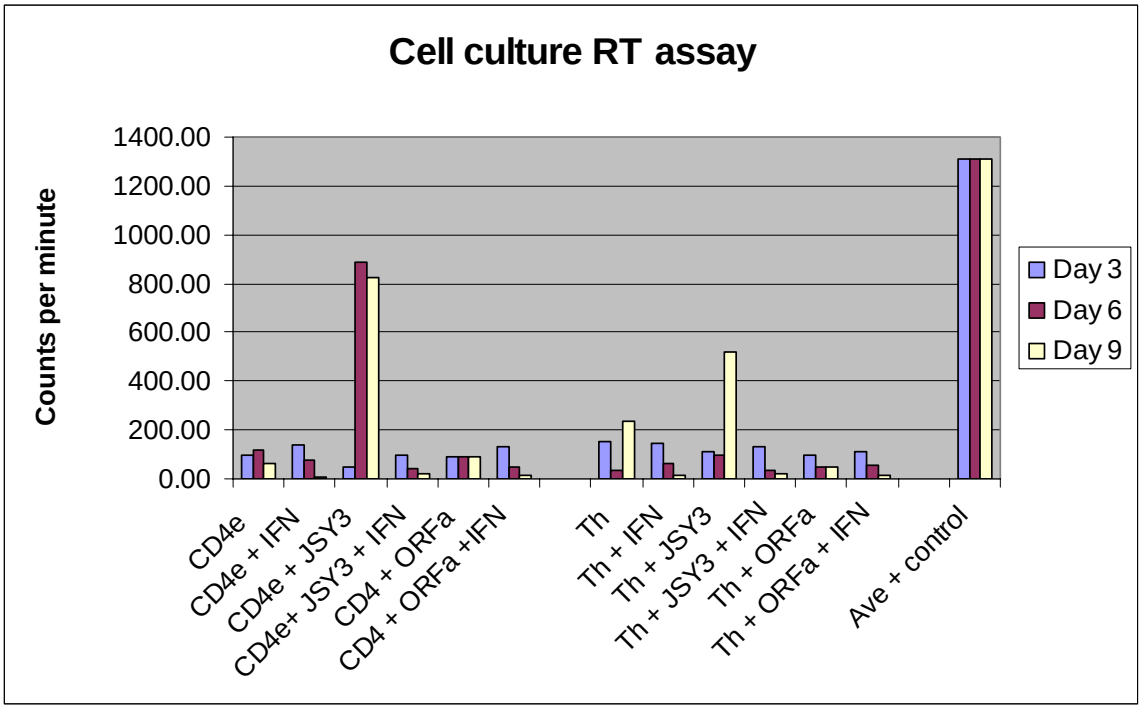

Figure 7-1. Summary of reverse transcriptase (RT) activity in cell cultures of CD4E cells and fetal thymocytes in one of three series of experiments.

Viability of Thymocytes In Vitro

The overall viability of thymocytes in culture was low by day 9 in all experiments (~10% of original numbers of plated thymocytes permeable to typan blue), and there were no determined statistical differences between wells, regardless of virus inoculation or treatment with IFN-α (Figure 7-1). The experiments using thymocytes were done in conjunction with cultures of CD4E cells for a third and final series of cell culture experiments, and wells of CD4E cells contained ten times as many viable cells at the end of the studies. Wells of uninfected CD4E cells that were treated with IFN-α had half as

many surviving cells as untreated, uninfected CD4E cells ($P = 0.01$), indicating that IFN-α may exhibit a considerable toxic effect on this cell type.

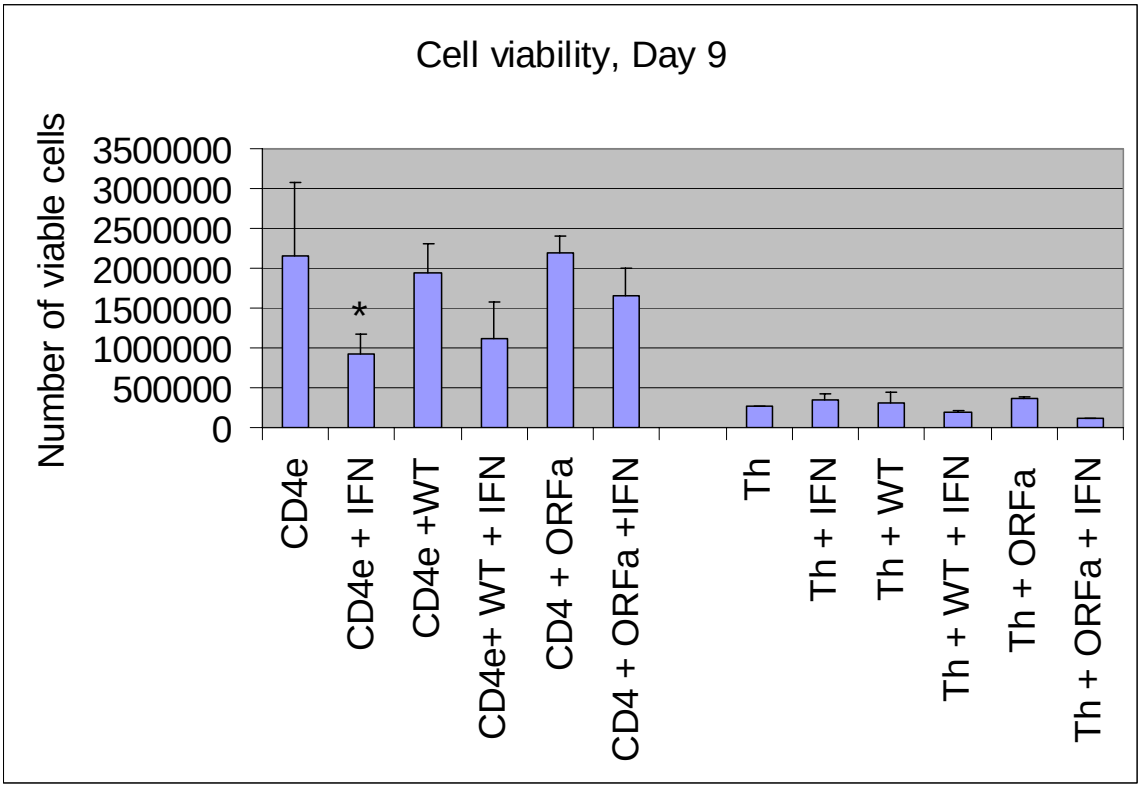

Figure 7-2. Number of viable cells on day 9 of cell culture in one of three attempted experiments. (*) denotes statistically significant differences from control wells without treatment without IFN-α.

Cytopathic Viral Effects on Thymocyte Cultures.

Photomicrographs of the cells in cell culture experiments are shown in Figures 7-3 through 7-6. Nonviable cells that have died over the course of the experiment appear dark and opaque. Treatment with IFN-α did not have any observed effects on cell morphology in CD4E cells or in thymocytes.

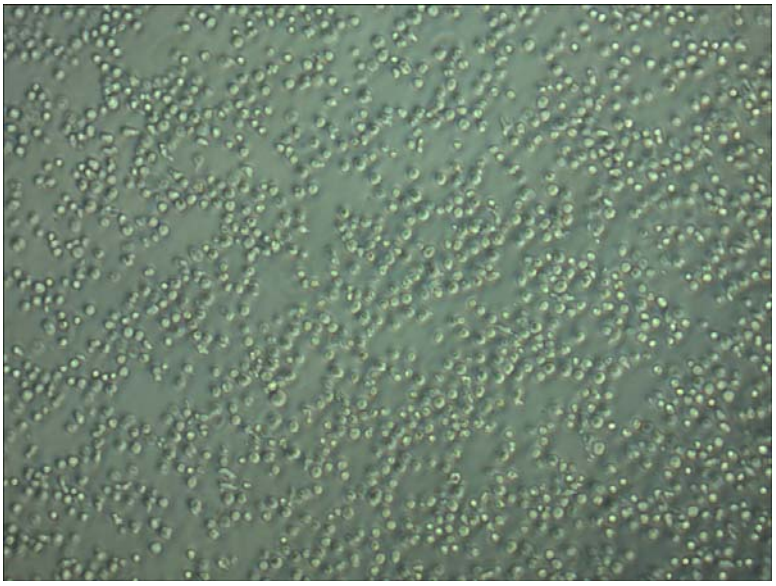

Figure 7-3. Appearance of freshly thawed CD4E cells at the outset of the cell culture experiments (20X magnification).

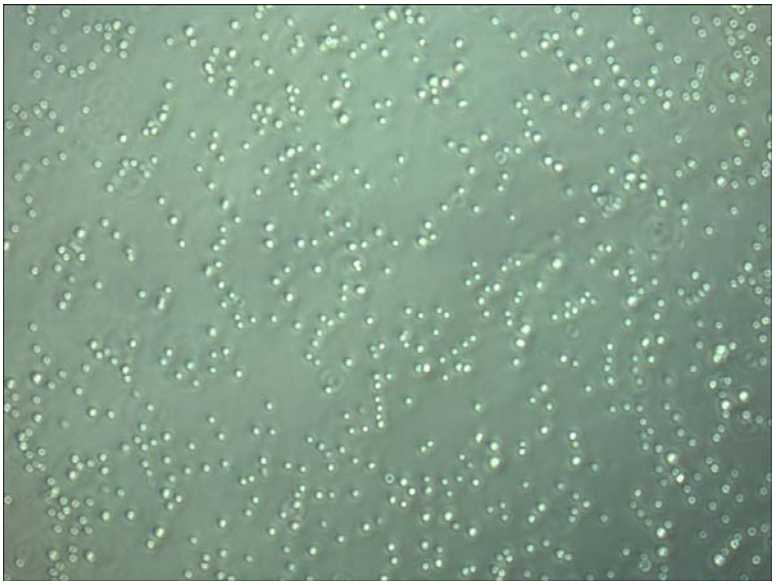

Figure 7-4. Appearance of freshly thawed thymocytes at the outset of cell culture (20X magnification).

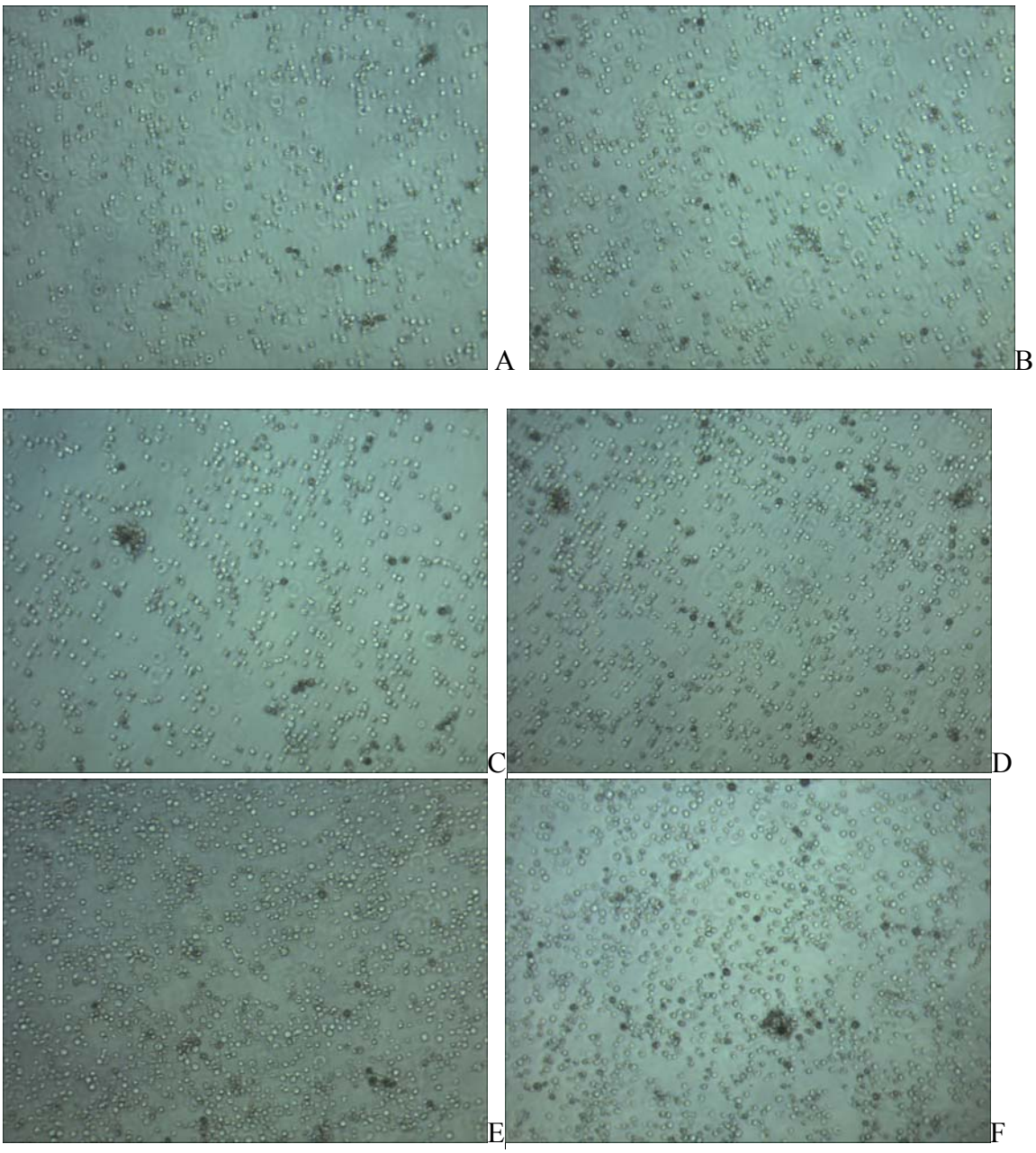

Figure 7-5. CD4E cells at Day 9 of culture experiments. A) Uninfected cells. B) Uninfected cells treated with IFN-α. C) Cells infected with JSY3 clone of FIV. D) Cells infected with JSY3 and treated with IFN-α. E) Cells infected with ORF-A deficient FIV clone. F) Cells infected with ORF-A deficient FIV clone and treated with IFN-α. (20X)

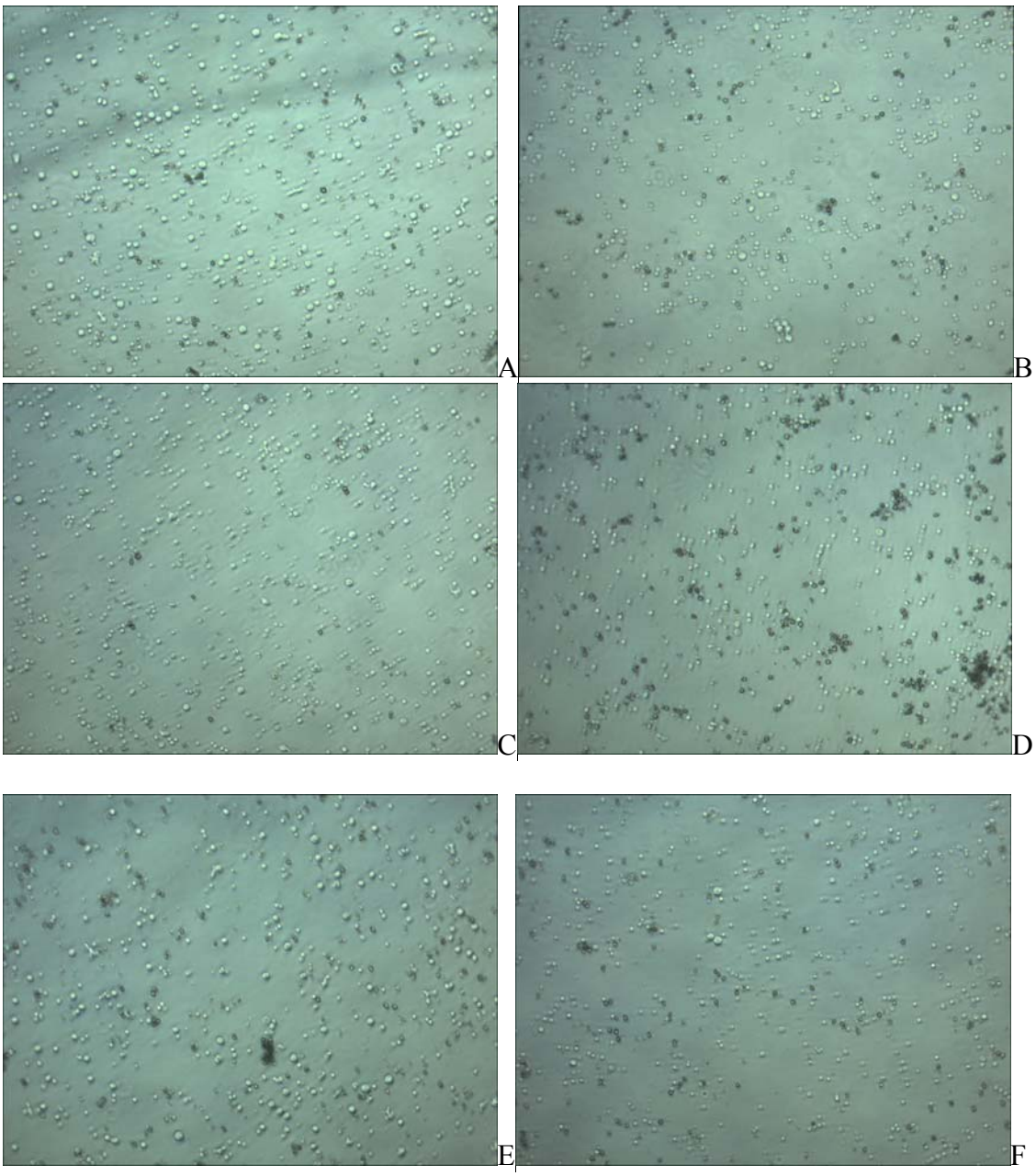

Figure 7-6. Fetal thymocyte cells at Day 9 of culture experiments. A) Uninfected cells. B) Uninfected cells treated with IFN-α. C) Cells infected with JSY3 clone of FIV. D) Cells infected with JSY3 and treated with IFN-α. E) Cells infected with ORF-A deficient FIV clone. F) Cells infected with ORF-A deficient FIV clone and treated with IFN-α. (20X)

Discussion

These attempts to infect cryopreserved fetal thymocytes with the JSY3 molecular clone of FIV were largely unsuccessful, and only a single small peak of viral RT activity was observed over the course of the experiments. Cell viability was low by the end of the cell culture trial period, making evaluation protective effects of IFN more difficult to assess. Cell death in culture precludes observations of the protective effects of IFN-α in cryopreserved thymocytes.

A recent report on optimization of cell culture recommends the usage of fresh thymocytes and co-culture with allogenic or autologous thymic epithelial cells in order to maintain thymocyte viability, function and subset distribution (Young, 2006). Preservation at -4ºC was recommended if extra time was needed to procure a source of TEC. Treatment of cultures with IL-7 caused downregulation of the IL-7 receptor, CD127.

The dosage of IFN treatment in this experiment was chosen based on previous experiments that used Type I IFN in feline cells lines in order to maximize antiviral activity without producing profound cytotoxicity (Pontzer, 1997). This goal was achieved, as the only statistically significant decrease in viable cells were seen in control CD4E cells. While we observed no apparent major cytotoxic effects of IFN in thymocytes, the overall poor viability of these cryopreserved cells precluded a definitive judgement.

Very few thymocytes stained positively for FIV p24 via immunohistochemistry (Chapter 6), instead, the viral protein was found more in the germinal centers and in the medulla, perhaps representing mature thymocytes or inflammatory cells that would not be present these under cell culture conditions. Taken together, the cell culture and IHC

experiments support the hypothesis that viral replication is largely limited to mature immune system cells that traffic the thymus in the course of viral infection, particularly interferon-producing cells. These findings indicate a need to further investigate this cell type in a future series of separate culture experiments as the cell-specific reagents become available and the cells are better accessible for manipulation.

CHAPTER 8
CONCLUSIONS

The main goal of these experiments was to determine the local changes in cytokine expression and effects of cytokines on the pathogenesis of FIV within the thymus of neonatally-infected cats. Our hypothesis was that alterations in cytokine mRNA expression occur as a result of FIV infection of the pediatric thymus, and that these changes correlate with changes in FIV viral replication, local inflammatory cell populations and T cell production by the thymus. Several experiments were executed in order to achieve this goal: 1. Discover the full-length cDNA/mRNA sequences for interleukin (IL)-7, IL-4, IL-15, interferon (IFN)-α, and IFN-γ; 2. Measure the mRNA expression levels of interleukin (IL)-7, IL-4, IL-15, interferon (IFN)-α, and IFN-γ within neonatally FIV-infected animals and age-matched controls at 3 time points correlating with acute and chronic infection, and measure corresponding levels of viral RNA expression and assess proviral load; 3. Determine cytokine alterations which correlate with changes in viral load and replication, influx of inflammatory cells and thymocyte depletion; 4. Demonstrate changes in inflammatory cell populations, IFN-α expression and viral protein distribution using immunohistochemistry; 5. Assess the antiviral activity of IFN-α in vitro. The results of the preceding chapters demonstrate the accomplishment of all of these objectives, except for the low level and inconsistent infection rate of FIV in fetal thymocyte culture experiments.

Currently feline-specific cytokine reagents are in short supply, including the feline recombinant proteins and monoclonal/polyclonal anti-cytokine antibodies. In addition,

measurement of the cytokine proteins directly is limited due to the low levels of protein expression within the tissue and therefore the large amount of tissue that would be necessary to perform these experiments. Fortunately, cytokine mRNA expression has been found to adequately reflect protein production (Blaschke, 2000; Hein, 2001), so real time RT-PCR was chosen as the protocol of choice in investigating the thymus cytokine levels.

In order to launch the subsequent experiments regarding cytokine production in the cat thymus, the full-length sequences of the feline mRNA/cDNA had to be determined. All of the sequences were successfully amplified using PCR and oligonucleotide primers and probes, which designed using consensus sequences from the available data from other species. PCR products were inserted into plasmids and used to transform bacteria in order to purify and amplify single amplicons. All the sequences were confirmed as the desired amplification product by full-length DNA sequencing and comparison to previously published cytokine data, and the homology of the feline sequences are herein reported. The full-length cDNA sequences were amplified as plasmid DNA inserts and stored for any future desired experiments where in-house cytokine protein expression would be necessary.

Cytokine levels within the thymus of FIV-infected cats and age-matched controls were successfully measured at three time points post-infection in order to represent acute (6-8 weeks), chronic (>16 weeks) and intermediate (12 weeks) infection time points, but also provide developmental immunological data for cytokine expression in the cat. For four of the five measured cytokines (IL-4, IL-7, IFN-α, IFN-γ), there was an observed peak in mRNA expression that naturally occurred after 16 weeks of age, which paralleled

absolute numbers of total thymocytes, immature double-negative CD4-CD8- thymocytes, and double-positive CD4+CD8+ thymocytes present in these subadult thymus samples. These findings taken together may suggest that this is a particularly active time point for thymopoiesis and perhaps represents a threshold for immune system maturity and competence in the cat.

The most significant impact of neonatal FIV infection was also found at the same chronic time point. For IL-4, IL-7, IFN-α, and IFN-γ, the naturally-occurring developmental peak in these cytokines was abrogated and there was a statistically significant reduction in the mRNA production of all four. In infected animals, cytokine levels were reduced 3.8-fold for IL-4, 6.3-fold for IL-7, and 4.5-fold for IFN-γ. The most profound impact of FIV infection on cytokine elaboration in the thymus was found for IFN-α, which exhibited a 149-fold reduction in expression. The decrease in IL-7 mRNA expression came as a surprise, as it was expected to be increased in infected animals in order to stimulate thymopoiesis in the face of T cell loss.

Again, interestingly, while the reduction in thymocyte parameters in this age group was not found to be statistically significant, there is a similar trend of decreases in the absolute numbers of total thymocytes, DN and DP thymocytes that can be seen in the graphical representations of the necropsy data. Regression analysis of this data was able to confirm that expression IL-7, IFN-α and IFN-γ were positively correlated, and that levels of these cytokines also had a strong positive correlation with the absolute numbers of total thymocytes, DP and DN thymocytes. Taken together, this suggests that the infection of the thymus with FIV directly or indirectly negatively influences the function of cells that elaborate these cytokines, and that expression levels of these agents is

associated with a reduction in thymopoiesis. It remains to be determined whether the loss of thymocytes is due to the loss of a survival/proliferative cytokine signal such as IL-7, or if the reduction in cytokine levels results from the loss of certain cells in the thymus due to direct viral infection and therefore measurement of the cytokine expression merely represents another pathological indicator of infection. However, given the importance of IL-7 to T cell development, the reduction in levels of this cytokine could be responsible for the loss of thymocytes seen in these animals.

IL-7 has been determined to have critical roles in thymopoiesis at multiple stages of T cell development. It has been reported that regulation of local IL-7 production is tissue-specific. Bone marrow stroma has shown to increase IL-7 synthesis with stimulation by IL-1 and tumor necrosis factor (TNF)-α (Weitzmann, 2000), while human intestinal epithelial cells failed to respond to similar cytokine treatment (Oshima, 2004). Epidermal keratinocytes were shown to produce more IL-7 in response to treatment with IFN-γ (Ariizumi, 1995), and intestinal epithelial cells increased IL-7 synthesis in the presence of IFN-γ or its inducible proteins interferon regulatory factor (IRF)-1 and IRF-2 (Oshima, 2004). IFN-α can also trigger the production of IRF-1 (Lehtonen, 2003) and IRF-2 (Zhou, 2000), so it is likely that it can produce similar IL-7 production in sensitive cell types. The known link between IFN and IL-7 production may explain the strong correlations between IFN-α, IFN-γ and IL-7 found in the current study, however, the lack of data regarding other cytokine levels such as TNF or IL-1 preclude a definitive conclusion.

The high levels of endogenous IFN-α mRNA expression and a potential link between IFN production and IL-7, a known thymopoietic cytokine, are unexpected.

While IFN-α demonstrates remarkable antiviral properties and is being investigated as a treatment for a number of disorders and cancers, side effects with this cytokine can be an issue. IFN-α exhibits a dose-dependent toxicity in developing B and T cells (Lin, 1998), and the most prevalent clinical contraindication for use of IFN-α is its well-known hematotoxicity and immunosuppressive effects (reviewed in Sleijfer, 2005). Therefore, the presence of IFN expression is unexpected and raises questions of its role in thymopoiesis and the innate immune protection of the thymus.

Our finding of a reduction of IFN-γ mRNA expression in the thymus of chronically FIV-infected cats is not consistent with previously published data. Liang et al. (2000) found increased thymic IFN-γ expression via reverse transcription-quantitative competitive PCR, however, the cats in the study were infected as adults with a different FIV strain from the current study (NCSU-1) and were sacrificed after 6-12 weeks. Dean et al. (1998) used a similar technique and found an increase in IFN-γ thymic expression after 8 weeks of infection, but study animals were 3-4 months of age at the time of inoculation with FIV-Petaluma. Orandle et al. (2000) determined that infected cats demonstrated a 10-fold increase in IFN-γ mRNA in thymus samples using reverse transcription-quantitative competitive PCR. The animal age for necropsy in this study was between 12 and 16 weeks, but contained a similar number of JSY3-infected cats for these time points. The causes for these differences in values is unclear.

IFN-γ demonstrated the only observed statistically significant positive correlation to viral replication in this study. As IFN-γ expression is generally considered indicative of an indication of a strong CD8+ T cell response to lentiviral infection and corresponding viral suppression, this finding is somewhat counterintuitive. Recombinant

feline IFN-γ was previously shown to have no effect on FIV viral replication *in vitro* (Tanabe, 2001), and the positive correlation may reflect a secondary IFN response to increased viral replication and an appropriate T cell response. Another possibility is that the increased numbers of activated IFN-producing T cells present within the infected thymus act as one of the primary sources of FIV replication, and that increased viral replication occurs secondary to a stronger inflammatory response. This latter hypothesis is supported by our immunohistochemistry findings, where viral replication was mainly observed within germinal centers.

The results for IL-15 did not lend themselves for definitive conclusions regarding the cytokine's role in lentiviral infection of the thymus. Little of the data achieved statistical significance, so only a guarded observation of the trends is reasonable based on the current analysis. Changes were limited to a slight physiologic increase in IL-15 expression at 12 weeks of age, and very mild increases as a result of FIV infection that were not significant. Regression analysis showed weak correlations between IL-15 expression and the percentage of CD8+ thymic cells, the presence of IgG+ cells and increases in viral *gag* RNA. This partially supports our hypothesis that IL-15 in the thymus is related to the inflammatory response to FIV within the thymus. IL-15 levels in the thymus did positively correlate with total white blood cells and CD8+ T cells in the peripheral blood at statistically significant levels, which may indicate that an IL-15 response within the thymus could have an ultimate beneficial effect on the peripheral immune system.

While IL-4 demonstrated a similar expression pattern as seen for IL-7, IFN-α and IFN-γ, regression analysis did not support an association between this cytokine and total

thymocytes numbers or the DN or SP thymocyte subpopulations. Expression of IL-4 showed a positive correlation to the absolute numbers of single-positive CD4+ thymic cells and a weak positive relationship to the numbers of CD8+ T cells in the peripheral blood. A positive correlation between IL-4 expression, viral replication and proviral burden was not observed as it has been seen in vitro with HIV (Pedroza-Martins, 2002). This may be due to the unexpected suppression of both IL-4 and IL-7 within the thymus of chronically infected animals, and increases in viral replication may need higher levels of these cytokines *in vivo* in order to occur.

After establishing the relevant changes in cytokine expression in the FIV-infected thymus, particular interest in the marked reduction of IFN-α prompted further investigation. Immunohistochemistry (IHC) was undertaken to provide information regarding the presence of an interferon-producing cell type (IPC) in the cat thymus. IPCs have been described in the thymus of humans and mice (Okada, 2003), and are often referred to as plasmacytoid dendritic cells (PDC) or Type II dendritic cells. PDC are considered to be the "professional" Type I interferon-producing cell type, and PDC are capable of producing large amounts of IFN in response to exposure to viral nucleotide sequences. PDC research has recently been facilitated by the identification of a cell-specific surface lectin BDCA-2 (Dzionek, 2000) and the subsequent development of a polyclonal antibody against this antigen (anti-human DLEC antibody, R&D Systems, Minneapolis, MN, USA).

Our IHC experiment was designed to first test the efficacy of this antibody for cat samples, so a single-label and a dual-label IHC protocol was developed to determine if BDCA-2/DLEC+ cells were present and also stained positively for IFN-α. The

conclusion was that staining for IFN and DLEC antigens produced a similar distribution within the sections in single-label experiments, and the signals co-localized in specific cells with the dual-label protocol. Therefore it was concluded that the antibody cross-reacted with a feline PDC lectin and appeared to identify a thymic IPC. In dual-label IHC sections, occasional cells stained for IFN but not DLEC, which may represent a PDC with low surface expression of DLEC or another cell type within the thymus that is contributing to Type I IFN production. These data remain to be confirmed in future studies, where conjugated antibody can be used for cell sorting and subsequent intracellular flow cytometry for IFN protein expression in this cell type.

DLEC+ cells within the thymus samples were predominantly located in small numbers along the corticomedullary junction of uninfected animals. This cell type appeared to be increased in numbers in infected cats at all time points, but cell counts that were corrected for unit area of thymic tissue did not reach statistical significance. In infected animals, small numbers of DLEC+ positive cells were present along the corticomedually junction, but also represented a prominent subpopulation within the inflammatory germinal centers.

IHC experiments were also performed using an antibody against the FIV p24 portion of the *gag* protein. Staining for p24 co-localized with staining for DLEC, which was interpreted as direct infection of PDC by FIV. Infection of this cell type and subsequent reduced function may be the primary cause of the reduced IFN-α mRNA expression observed in the cytokine analysis. Cell culture techniques for the derivation of PDC from CD34+ stem cells and the maintenance of this cell type *in vitro* need to be

developed in order to draw definitive conclusions regarding the impact of FIV infection on IPC function.

The distribution of the FIV p24 protein in our thymic samples was different than previously published reports. Using our single-label protocol, p24 staining primarily occurred in numerous cells within germinal centers, with a few scattered virally-infected cells present within the medulla. Woo (1997) showed virus present in cells enriched for CD1 via quantitative competitive PCR, and concluded that cortical thymocytes were infected with FIV. However, this sorted population would also contain various dendritic cell populations (Dzionek, 2000), which we have shown to harbor FIV. Orandle (1997) performed *in situ* hybridization for FIV RNA in JSY3-infected thymuses and found viral replication exclusively within the thymic cortex, which would indicate infection of immature thymocytes and not more mature thymocytes or infiltrating cells with FIV. Norway (2000) used the same anti-FIV antibody in IHC experiments, but tissue sections exhibited a similar distribution of positive cells in the thymic cortex as Orandle et al. A marked difference in our IHC protocol may account for some of this disparity. An extensive series of fixation experiments was performed at the outset of our IHC studies in order to maximize our fixation protocol and best preserve tissue architecture and antigen signal. In the course of these troubleshooting experiments, it became evident that the standard drying steps resulted in tissue damage and that the endogenous peroxidase quenching step caused a severe loss of antigen in the sections with weak or absent subsequent cellular staining, even when performed with the most mild concentrations of hydrogen peroxide and methanol. Fortunately, it was also apparent from negative control slides that background staining was not an issue, so this step was discarded for the

remainder of the experiments and confirmed by the inclusion of a negative control slide in each run. Also, we used frozen tissue sections rather than paraffin-embedded tissue, which also likely contributed to better antigen preservation. While these differences in technique can account for some of the differences in antigen staining, the reasons for a lack of positive cortical cells in our study compared to previous accounts are unexplained.

Experiments that were performed to infect fetal thymocytes with FIV were largely unsuccessful. While this was somewhat disappointing and precluded our ability to definitively confirm a protective effect of IFN-α on thymocytes, these findings ultimately supported our IHC experiments. *In vivo* thymocytes were not found to express FIV *gag*, and the absent to low levels of viral replication observed in the cell culture experiments support the conclusion that FIV largely infects the more mature and activated inflammatory cells in the thymus of neonatally infected animals.

Overall, the preceding research confirms our hypothesis and shows that several important cytokine alterations occur as a result of neonatal FIV infection within the thymus, particularly during the most physiologically active time periods for the thymus after 16 weeks of age. Changes in cytokine expression were associated with decreased numbers of certain key thymocyte subpopulations. The decrease in IL-7 expression was found to correlate with the loss of IFN mRNA, which may indicate a role for Type I and/or Type II IFN production in thymopoiesis that requires further investigation. This reduction in IFN-α proved to be the most significant cytokine alteration, and prompted IHC experiments to establish a potential cellular source for the protein that may be influenced by FIV. The IHC results supported the conclusion that an IPC exists in the

feline thymus that appears to become infected with FIV. It is suggested that future studies involving FIV in the thymus should focus on further characterization of viral effects on this cell type.

LIST OF REFERENCES

Agostini C, Zambello R, Facco M, Perin A, Piazza F, Siviero M, Basso U, Bortolin M, Trentin L, Semenzato G. CD8 T cell infiltration in extravascular tissues of patients with human immunodeficiency virus infection. Interleukin-15 upmodulates costimulatory pathways involved in the antigen-presenting cells-T cell interaction. *Blood.* 1999. **93**(4): 1277-1286.

Ahmad R, Sindhu ST, Toma E, Morisset R, Ahmad A. Studies on the production of IL-15 in HIV-infected/AIDS patients. *JClinImmunol.* 2003. **23**(2): 81-90.

Al-Harthi L and Landay A. Immune recovery in HIV disease: role of the thymus and T cell expansion in immune reconstitution strategies. *JHematotherStemCellRes*. 2002. **11**(5): 777-786.

Argyle DJ, Smith K, McBride K, Fulton R, Onions DE. Nucleotide and predicted peptide sequence of feline interferon-gamma. *DNASeq.* 1995. **5**(3): 169-171.

Ariizumi K, Meng Y, Bergstresser PR, Takashima A. IFN-gamma-dependent IL-7 regulation in keratinocytes. *JImmunol.* 1995. **154**(11): 6031-6039.

Aspinall R and Andrew D. Thymic involution in aging. *JClinImmunol*. 2000. **20**(4): 250-256.

Audige A, Schlaepfer E, Joller H, Speck RF. Uncoupled anti-HIV and immune-enhancing effects when combining IFN-alpha and IL-7. *JImmunol.* 2005. **175**(6): 3724-3736.

Badley AD, Dockrell, Simpson M, Schut R, Lynch DH, Leibson P and Paya CV. Macrophage-dependent apoptosis of $CD4^+$ T Lymphocytes from HIV-infected individuals is mediated by FasL and tumor necrosis factor. *JExpMed.* 1997. **185**(1): 55-64.

Beq S, Nugeyre MT, Fang RH, Gautier D, Legrand R, Schmitt N, Estaquier J, Barre-Sinoussi F, Hurtrel B, Cheynier R, Israel N. IL-7 induces immunological improvement in SIV-infected macaques under antiviral therapy. *JImmunol.* 2006. **176**(2): 914-922.

Blaschke V, Reich K, Blaschke S, Zipprich S, Neumann C. Rapid quantitation of proinflammatory and chemoattractant cytokine expression in small tissue samples and monocyte-derived dendritic cells: validation of a new real-time RT-PCR technology. *JImmunolMethods*. 2000. **246**(1-2): 79-90.

Burkhard MJ and Dean GA. Transmission and immunopathogenesis of FIV in cats as a model for HIV. *CurrHIVRes.* 2003. **1**(1): 15-29.

Buseyne F, Scott-Algara D, Bellal N, Burgard M, Rouzioux C, Blanche S, Riviere Y. The frequency of HIV-specific interferon-gamma-producing CD8 T cells is associated with both age and level of antigenic stimulation in HIV-1-infected children. *JInfectDis.* 2005. **192**(10): 1781-1786.

Caufour P, Le Grand R, Cheret A, Neildez O, Thiebot H, Theodoro F, Boson B, Vaslin B, Venet A, Dormont D. Longitudinal analysis of CD8+ T cell phenotype and IL-7, IL-15 and IL-16 mRNA expression in different tissues during primary simian immunodeficiency virus infection. *Microbes and Infection*. 2001. **3**: 181-191.

Cebulla CM, Miller DM, Sedmak DD. Viral inhibition of interferon signal transduction. *Intervirology*. 1999. **42**(5-6): 325-330.

Cella M, Jarrossay D, Facchetti F, Alebardi O, Nakajima J, Lanzavecchia A, Colonna M. Plasmacytoid monocytes migrate to inflamed lymph nodes and produce large amounts of type I interferon. *NatMed.* 1999. **5**(8): 919-923.

Chung E, Amrute SB, Abel K, Gupta G, Wang Y, Miller CJ, Fitzgerald-Bocarsly P. Characterization of virus-responsive plasmacytoid dendritic cells in the rhesus macaque. *ClinDiagnLabImmunol.* 2005. **12**(3): 426-435.

Colonna M, Krug A and Cella M. Interferon-producing cells: on the front line in immune responses against pathogens. *CurrOpinImmunol*. 2002. **14**: 373-379.

Correa R and Munoz-Fernandez MA. Production of new T cells by thymus in children: effect of HIV infection and antiretroviral therapy. *PediatrRes*. 2002. **52**(2): 207-212.

Corthay A. A three-cell model for activation of naïve T helper cells. *ScandJImmunol.* 2006. **64**(2): 93-96.

Crawford PC, Papadi GP, Levy JK, Benson NA, Mergia A and Johnson CM. Tissue dynamics of CD8 lymphocytes that suppress viral replication in cats infected neonatally with feline immunodeficiency virus. *JInfectDis*. 2001. **184**(6):671-81.

d'Ettorre G, Forcina G, Lichtner M, Mengoni F, D'Agonstino C, Massetti AP, Mastroianni CM, Vullo V. Interleukin-15 in HIV infection: immunological and virological interactions in anti-retroviral-naïve and –treated patients. *AIDS*. 2002. **16**: 181-188.

de la Rosa R and Leal M. Thymic involvement in recovery of immunity among HIV-infected adults on highly active antiretroviral therapy. *JAntimicrobChemother*. 2003. **52**(2): 155-158.

Dean G, Pedersen N. Cytokine response in multiple lymphoid tissues during the primary phase of feline immunodeficiency virus infection. *JVirol.* 1998. **72**(12): 9436-9440.

Dean GA, Barger A, Lavoy A. Cloning and expression of feline interleukin 15. *Cytokine*. 2005. **29**(2): 77-83.

DeLuca D and Clark DR. Interleukin-7 negatively regulates the development of mature T cells in fetal thymus organ cultures. *DevCompImmunol*. 2002. **26**: 365-384.

Dhillon NK, Sui Y, Potula R, Dhillon S, Adany I, Li Z, Villinger F, Pinson D, Narayan O, Buch S. Inhibition of pathogenic SHIV replication in macaques treated with antisense DNA of interleukin-4. *Blood*. 2005. **105**(8): 3094-3099.

Durbin JE, Fernandez-Sesma A, Lee C, Rao TD, Frey AB, Moran TM, Vukmanovic S, Garcia-Sastre A and Levy DE. Type I IFN modulates innate and specific antiviral immunity. *JImmunol.* 2000. **164**: 4220-4228.

Dzionek A, Fuchs A, Schmidt P, Cremer S, Zysk M, Miltenyi S, Buck DW, Schmitz J. BDCA-2, BDCA-3, and BDCA-4: three markers for distinct subsets of dendritic cells in human peripheral blood. *JImmunol.* 2000. **165**(11): 6037-6046.

Dzionek A, Sohma Y, Nagafune J, Cella M, Colonna M, Facchetti F, Gunther G, Johnston I, Lanzavecchia A, Nagasaka T, Okada T, Vermi W, Winkels G, Yamamoto T, Zysk M, Yamaguchi Y, Schmitz J. BDCA-2, a novel plasmacytoid dendritic cell-specific type II C-type lectin, mediates antigen capture and is a potent inhibitor of interferon alpha/beta induction. *JExpMed.* 2001. **194**(12): 1823-1834.

Feldman S, Stein D, Amrute S, Denny T, Garcia Z, Kloser P, Sun Y, Megjugorae N, Fitzgerald-Bocarsly P. Decreased interferon-alpha production in HIV-infected patients correlates with numerical and functional deficiencies in circulating type 2 dendritic cell recursors. *Clin Immunol.* 2001. **101**(2): 201-210.

Fernandez S, Nolan RC, Price P, Krueger R, Wood C, Cameron D, Solomon A, Lewin SR, French MA. Thymic function in severely immunodeficient HIV Type 1-infected patients receiving stable and effective antiretroviral therapy. *AIDSResHumRetroviruses.* 2006. **22**(2): 163-170.

Fohrer H, Audit IM, Sainz A, Schmitt C, Dezutter-Dambuyant C, Dalloul AH. Analysis of transcription factors in thymic and CD34+ progenitor-derived plasmacytoid and myeloid dendritic cells: evidence for distinct expression profiles. *ExpHemat.* 2004. **32**(1): 104-112.

Fong L, Mengozzi M, Abbey M, Herndier BG, Engleman EG. Productive infection of plasmacytoid dendritic cells with human immunodeficiency virus type 1 is triggered by CD40 ligation. *JVirol.* 2002. **76**(21): 11033-11041.

George JW, Pedersen NC and Higgins J. The effect of age on the course of experimental feline immunodeficiency virus infection in cats. *AIDS Research and Human Retroviruses*. 1993. **9**(9): 897-905.

Giordani L, Giacomini, E, Quarenta MG, Viora M. HIV-1 Nef protein inhibits the in vitro induction of a specific antibody response to Candida albicans by an early up-regulation of IL-15 production. *ClinExpImmunol.* 2000. **122**(3): 358-363.

Giulietti A, Overbergh L, Valckx D, Decallonne B, Bouillon R, Mathieu C. An overview of real-time quantitative PCR: applications to quantify cytokine gene expression. *Methods*. 2001. **25**(4): 386-401.

Gurney KB, Colantonio AD, Blom B, Spits H, Uittenbogaart CH. Endogenous IFN-alpha production by plasmacytoid dendritic cells exerts an antiviral effect on thymic HIV-1 infection. *JImmunol.* 2004. **173**(12): 7269-7276.

Haigwood NL. Predictive value of primate models of AIDS. *AIDSRev.* 2004. **6**(4): 187-198.

Hare KJ, Jenkinson EJ and Anderson G. An essential role for the IL-7 receptor during intrathymic expansion of the positively selected neonatal T cell repertoire. *JImmunol*. 2000. **165**: 2410-2414.

Hayes KA, Phipps AJ, Francke S and Mathes LE. Antiviral therapy reduces viral burden but does not prevent thymic involution in young cats infected with feline immunodeficiency virus. *AntimicrobAgentsChemother*. 2000. **44**(9): 2399-2405.

Hazra R and Mackall C. Thymic function in HIV infection. *CurrHIV/AIDS Rep*. 2005. **2**(1): 24-28.

Hein J, Schellenberg U, Bein G, Hackstein H. Quantification of murine IFN-gamma mRNA and protein expression: impact of real-time kinetic RT-PCR using SYBR green I dye. *ScandJImmunol*. 2001. **54**(3): 285-291.

Jablonowski H. IFN-alpha: therapeutic options in HIV and HIV/HCV, HIV/HBV dual infection. *Infection*. 2003. **31**(2):131-3.

Johnson CM, Bortnick SJ, Crawford PC and Papadi G. Unique susceptibility of the fetal thymus to feline immunodeficiency virus infection: an animal model for HIV infection in utero. *AmJReprodImmunol*. 2001. **45**(5): 273-288.

Johnson V, Byington R, Walker B. Reverse transcriptase (RT) activity assay. 1990. *In* AA Aldovini and BD Walker Techniques in HIV Reasearch. Stockton Press, NY, NY.

Kedzierska K, Azzam R, Ellery P, Mak J, Jaworowski A, and Crowe SM. Defective phagocytosis by human monocyte/macrophages following HIV-1 infection: underlying mechanisms and modulation by adjunctive cytokine therapy. *JClinVirol*. 2003. **26**(2):247-63.

Khoury M and A Kovacs. Pediatric HIV infection. *Clin Obstet Gynecol*. 2001. **44**(2): 243-275.

Kimata JT. HIV-1 fitness and disease progress: insights from the SIV-macaque model. *CurrHIVRes.* 2006. **4**(1): 65-77.

Klein SA, Dobmeyer JM, Dobmeyer TS, Pape M, Ottmann OG, Helm EB, Hoelzer D and Rossol R. Demonstration of the Th1 to Th2 cytokine shift during the course of HIV-1 infection using cytoplasmic cytokine detection on single cell level by flow cytometry. *AIDS.* 1997. **11**(9): 1111-1118.

Koka PS, Brooks DG, Razai A, Kitchen CM, Zack JA. HIV type 1 infection alter cytokine mRNA expression in thymus. *AIDSResHumRetroviruses.* 2003. **19**(1): 1-12.

Kopka J, Mecikovsky D, Aulicino PC, Mangano AM, Rocco CA, Bologna R, Sen L. High IL-7 plasma levels may induce and predict the emergence of HIV-1 virulent strains in pediatric infection. *JClinVirol.* 2005. **33**(3): 237-242.

Lehtonen A, Lund R, Lahesmaa R, Julkunen I, Sareneva T, Matikainen S. IFN-alpha and IL-12 activate IFN regulatory factor 1 (IRF-1), IRF-4, and IRF-8 gene expression in human NK and T cells. *Cytokine.* 2003. **24**(3): 81-90.

Lelievre JD, Petit F, Arnoult D, Ameisen JC, Estaquier J. Interleukin 7 increases human immunodefiency virus type 1 LAI-mediated Fas-induced T-cell death. *JVirol.* 2005. **79**(5): 3195-3199.

Levy JA. HIV pathogenesis: knowledge gained after two decades of research. *AdvDentRes.* 2006. **19**(1): 10-16.

Liang Y, Hudson, Levy J, Ritchey J, Tompkins W, Tompkins M. T cell overexpressing interferon-gamma and interleukin-10 are found in both the thymus and secondary lymphoid tissues of feline immunodeficiency virus-infected cats. *JInfectDis*. 2000. **181**: 564-575.

Lin Q, Dong C, Cooper M. Impairment of T and B cell development by treatment with a Type I interferon. *JExpMed.* 1998. **187**(1): 79-87.

Loré K, Smed-Sorensen A, Vasudevan J, Mascola JR, Koup RA. Myeloid and plasmacytoid dendritic cells transfer HIV-1 preferentially to antigen-specific CD4+ T cells. *JExpMed.* 2005. **201**(12): 2023-2033.

Martinez V, Costagliola D, Bonduelle O, N'go N, Schnuriger A, Theodorou I, Clauvel JP, Sicard D, Agut H, Debre P, Rouzioux C, Autran B. Combination of HIV-1-specific CD4 Th1 cell responses and IgG2 antibodies is the best predictor for persistence of long-term nonprogression. *JInfectDis.* 2005. **191**(12): 2053-2063.

McCune JM. The dynamics of $CD4^+$ T-cell depletion in HIV disease. *Nature.* 2001. **410**: 974-979.

Meissner EG, Duus KM, Loomis R, D'Agostin R and Su L. HIV-1 replication and pathogenesis in the human thymus. *CurrHIVRes*. 2003. **1**(3):275-285.

Mertsching E, Burdet C and Ceredig R. IL-7 transgenic mice: analysis of the role of IL-7 in the differentiation of thymocytes *in vivo* and *in vitro*. *IntImmunol*. 1995. **7**(3): 401-414.

Morrissey PJ, McKenna H, Widmer MB, Braddy S, Voice R, Charrier K, Williams DE and Watson JD. Steel factor (c-*kit* ligand) stimulates the *in vitro* growth of immature $CD3^-CD4^-CD8^-$ thymocytes: synergy with IL-7. *CellImmunol*. 1994. **157**(1): 118-131.

Mueller YM, Petrovas C, Bojczuk PM, Dimitriou ID, Beer B, Silvera P, Villinger F, Cairns JS, Gracely EJ, Lewis MG, Katsikis PD. IL-15 increases effector memory CD8+ T cells and NK cells in simian immunodeficiency virus-infected macaques. *JVirol.* 2005. **79**(8): 4877-4885.

Muhl H and Pfeilschifter J. Anti-inflammatory properties of pro-inflammatory interferon-gamma. *IntImmunopharmacol*. 2003. **3**(9): 1247-55.

Murphy PM, Lane CH, Gallin JI and Fauci AS. Marked disparity in incidence in bacterial infections in patients with the acquired immunodeficiency syndrome receiving interleukin-2 and interferon-gamma. *AnnInternMed.* 1988. **108**:36–41.

Nagai A, Taira O, Ishikawa M, Hiramatsu K, Hohdatsu T, Koyama H, Arai S, Sato H, Nakano K, Maehara N. Cloning of cDNAs encoding multiple subtypes of feline interferon-alpha from the feline epithelial cell line. *JVetMedSci.* 2004. **66**(6): 725-728.

Napolitano LA, Grant RM, Deeks SG, Schmidt D, De Rosa SC, Herzenberg LA, Herndier BG, Andersson J and McCune JM. Increased production of IL-7 accompanies HIV-1-mediated depletion: implications for T-cell homeostasis. *NatureMedicine*. 2001. **7**(1): 73-79.

Neben K, Heidbreder M, Müller J, Marxer A, Petry J, Didier A, Schimpl A, Hünig T and Kerkau T. Impaired thymopoietic potential of immature $CD3^-CD4^+CD8^-$ T cell precursors from SIV-infected rhesus monkeys. *IntImmunol*. 1999. **11**(9): 1509-1518.

Norway RM, Crawford PC, Johnson CM and Mergia A. Thymic lesions in cats infected with a pathogenic molecular clone or and ORF-A/2-deficient molecular clone of feline immunodeficiency virus. *JVirol.* 2001. **75**(13): 5833-5841.

Okada T, Lian ZX, Naiki M, Ansari A, Ikehara S, Gershwin M. Murine thymic plasmacytoid dendritic cells. *EurJImmunol.* 2003. **33**: 1012-1019.

Onlamoon N, Pattanapanyasat K, Ansari AA. Impaired IFN-gamma production by viral immunodominant peptide-specific tetramer+ CD8+ T cells in HIV-1 infected patients is not secondary to HAART. *ClinDevImmunol.* 2004. **11**(3-4): 287-298.

Or R, Abdul-Hai A, and Ben-Yehuda A. Reviewing the potential utility of interleukin-7 as a promoter of thymopoiesis and immune recovery. *CytokinesCellMolTher*. 1998. **4**(4): 287-294.

Orandle MS, Crawford PC, Levy JK, Udoji R, Papadi GP, Ciccarone T, Mergia A and Johnson CM. CD8+ thymic lymphocytes express reduced levels of CD8β and increased interferon-γ in cats perinatally infected with the JSY3 molecular clone of feline immunodeficiency virus. *AIDSResHumRetroviruses.* 2000. **16**(15): 1559-1571.

Orandle MS, Papadi GP, Bubenik LJ, Dailey CI and Johnson CM. Selective thymocyte depletion and immunoglobulin coating in the thymus of cats infected with feline immunodeficiency virus. *AIDSResHumRetroviruses*. 1997. **13**(7): 611-620.

Oshima S, Nakamura T, Namiki S, Okada E, Tsuchiya K, Okamoto R, Yamazaki M, Yokota T, Aida M, Yamaquchi Y, Kanai T, Handa H, Watanabe M. Interferon regulatory factor 1 (IRF-1) and IRF-2 distinctively up-regulate gene expression and production of interleukin-7 in human intestinal epithelial cells. *MolCellBiol*. 2004. **24**(14): 6298-6310.

Overbergh L, Giulietti A, Valckx D, Decallonne R, Bouillon R, Mathieu C. The use of real-time reverse transcriptase PCR for the quantification of cytokine gene expression. *JBiomolTech.* 2003. **14**(1): 33-43.

Pedroza-Martins L, Boscardin WJ, Anisman-Posner DJ, Schols D, Bryson YJ, and Uittenbogaart CH. Impact of cytokines on replication in the thymus of primary human immunodeficiency virus type 1 isolates from infants. *JVirol.* 2002. **76**(14): 6929-6943.

Phipps AJ, Hayes KA, Buck WR, Podell, and Mathes LE. Neurophysiologic and immunologic abnormalities associated with feline immunodeficiency virus molecular clone FIV-PPR DNA inoculation. *JAIDS*. 2000. **23**: 8-16.

Poli G, Biswas P and Fauci AS. Interferons in the pathogenesis and treatment of human immunodeficiency virus infection. *AntiviralRes.* 1991. **24**: 221-233.

Pontzer CH, Yamamoto JK, Bazer FW, Ott TL, Johnson HM. Potent anti-feline immunodeficiency virus and anti-human immunodeficiency virus effect of IFN-tau. *JImmnol.* 1997. **158**(9): 4351-4357.

Power C, Buist R, Johnston JB, Del Bigio MR, Ni W, Dawood MR and Peeling J. Neurovirulence in feline immunodefiency-infected neonatal cats is viral strain specific and dependent on systemic immune suppression. *JVirol*. 1998. **72**(11): 9109-9115.

Prlic M, Lefrancois, L, Jameson SC. Multiple choices: Regulation of memory CD8 T cell generation and homeostasis by Interleukin (IL)-7 and IL-15. *JExpMed.* 2002. **195**(12): F49-52.

Rajeevan M, Ranamukhaarachchi D, Vernon S, Unger E. Use of real-time quantitative PCR to validate the results of cDNA array and differential display PCR technologies. *Methods*. 2001. **25**(4): 443-451.

Reed SG, Da Silva JS, Ho JL, Koehler, Russo DM, Pihl DL and Coombs RW. Cytokine activation of human macrophages infected with HIV-1 to inhibit intracellular protozoa. *JAcquirImmunDefi Syndr.* 1992. **5**: 666–675.

Resino S, Galan I, Correa R, Pajuelo L, Bellon JM, Munoz-Fernandez MA. Homeostatic role of IL-7 in HIV-1 infected children on HAART: association with immunological and virological parameters. *ActaPaediatr.* 2005. **94**(2): 170-177.

Rethi B, Fluur C, Atlas A, Krzyzowska M, Mowafi F, Grutzmeier S, De Milito A, Bellocco R, Falk KI, Rajnavolgyi E, Chiodi F. Loss of IL-7Ralpha is associated with CD4 T-cell depletion, high interleukin-7 levels and CD28 down-regulation in HIV infected patients. *AIDS*. 2005. **19**(18): 2077-2086.

Robertson P and Poznansky MC. T-lymphocyte development and models of thymopoietic reconstitution. *TransplInfectDis*. 2003. **5**(1): 38-42.

Rodrigues DB, Correia D, Marra MD, Giraldo LE, Lages-Silva E, Silva-Vergara ML, Barata CH, Rodrigues Jr V. Cytokine serum levels in patients infected by HIV with and without Trypanosoma cruzi coinfection. *RevSocBrasMedTrop.* 2005. **38**(6): 483-487.

Saez R, Echaniz P, de Juan MD, Iribarren JA, Cuadrado E. HIV-infected progressors and long-term non-progressors differ in their capacity to respond to an A-class CpG oligodeoxynucleotide. *AIDS.* 2005. **19**(16): 1924-1925.

Samuel CE. Antiviral actions of interferons. *ClinMicrobiolRev.* 2001. **14**(4): 778-809.

Santana MA and Rosenstein Y. What it takes to become an effector T cell: the process, the cells involved, and the mechanisms. *JCellPhys.* 2003. **195**: 392-401.

Schmitt N, Nugeyre M, Scott-Algara, D, Cumont M, Barre-Sinoussi F, Pancino G, Israel N. Differential susceptibility of human thymic dendritic cell subsets to X4 and R5 HIV-1 infection. *AIDS*. 2006. **20**: 533-542.

Sen GC. Viruses and interferons. *AnnuRevMicrobiol*. 2001. **55**: 255-81.

Siegal F. Interferon-producing plasmacytoid dendritic cells and the pathogenesis of AIDS. *ResInitiatTreatAction*. 2003. **8**(2): 10-3.

Siegal FP, Kadowski N, Shodell M, Fitzgerald-Bocarsly PA, Shah K, Ho S, Antonenko S, Liu YJ. The nature of the principal type 1 interferon-producing cells in human blood. *Science*. 1999. **284**(5421): 1835-1837.

Sindhu S, Toma E, Cordeiro P, Ahmad R, Morisset R, Menezes J. Relationship of in vivo and ex vivo levels of Th1 and Th2 cytokines with viremia in HAART patients with and without opportunistic infections. *JMedVirol.* 2006. **78**(4): 431-439.

Sleijfer S, Bannink M, Van Gool A, Kruit W, Stoter G. Side effects of interferon-alpha therapy. *PharmWorldSci.* 2005. **27**(6): 423-431.

Soumelis V, Scott I, Gheyas F, Bouhour D, Cozon G, Cotte L, Huang L, Levy J, Liu L-J. Depletion of circulating natural type 1 interferon-producing cells in HIV-infected AIDS patients. *Blood.* 2001. **98**(4): 906-912.

Steffens CM, Al-Harthi L, Shott S, Yogev R, Landay A. Evaluation of thymopoiesis using T cell receptor excision circles (TRECs): differential correlation between adult and pediatric TRECs and naïve phenotypes. *ClinImmunol*. 2000. **97**(2): 95-101.

Sutton C, Gordnier P, Avery R, Casey J. Comparative replication kinetics of cytopathic feline lentiviruses ex vivo. *Virology*. 2005. **332**(2): 519-528.

Tanabe T and Yamamoto JK. Feline immunodeficiency virus lacks sensitivity to the antiviral activity of feline IFN-γ. *JInterferonCytokineRes*. 2001. **21**(12): 1039-46.

Uittenbogaart CH, Boscardin WJ, Anisman-Posner DJ, Koka PS, Bristol G and Zack JA. Effect of cytokines on HIV-induced depletion of thymocytes *in vivo. AIDS*. 2000. **14**: 1317-1325.

Uittenbogaart CH, Higashitani S, Schmid I, Vollger LW, Boone T and Clement LT. Interleukin-4 induces expression of the CD45RA antigen on human thymocyte subpopulations. *IntImmunol.* 1990. **2**(12): 1179-1187.

UNAIDS/WHO: Global summary of the HIV and AIDS epidemic, December 2005.

von Hoegen P. Synergistic role of type I interferons in the induction of protective cytotoxic T lymphocytes. *ImmunolLett.* 1995. **47**(3): 157-162.

Waldmann T. The contrasting roles of IL-2 and IL-15 in the life and death of lymphocytes: implications for the immunotherapy of rheumatological diseases. *ArthritisRes*. 2002. 4 Suppl 3: S161-167.

Wang FX, Xu Y, Sullivan J, Souder E, Argyris EG, Acheampong EA, Fisher J, Sierra M, Thomson MM, Najera R, Frank I, Kulkosky J, Pomerantz RJ, Nunnari G. IL-7 is a potent and proviral strain-specific inducer of latent HIV-1 cellular reservoirs of infected individuals of virally suppressive HAART. *JClinInvest.* 2005. **115**(1): 128-137.

Weitzmann MN, Cenci S, Rifas L, Brown C, Pacifici R. Interleukin-7 stimulates osteoclast formation by up-regulating the T-cell production of soluble osteoclastogenic cytokines. *Blood*. 2000. **96**(5): 1873-1878.

Willett BJ, Flynn JN, Hosie MJ. FIV infection of the domestic cat: an animal model for AIDS. *ImmunolToday*. 1997. **18**(4): 182-189.

Woo J, Dean G, Pedersen N, Moore P. Immunopathologic changes in the thymus during the acute stage of experimentally induced feline immunodeficiency virus infection of juvenile cats. *JVirol*. 1997. **71**(11): 8632-8641.

Wu L, Shortman K. Heterogeneity of thymic dendritic cells. *SemImmunol.* 2005. **17**(4): 304-312.

Ye P, Kirschner DE and Kourtis AP. The thymus during HIV disease: role in pathogenesis and in immune recovery. *CurrHIVRes*. 2004. **2**: 177-183.

Yin J, Shackel N, Zekry A, McGuinness P, Richards C, Putten KV, McCaughan GW, Eris J, Bishop G. Real-time reverse transcriptase-polymerase chain reaction (RT-PCR) for measurement of cytokine and growth factor mRNA expression with fluorogenic probes or SYBR Green I. *ImmunolCellBiol*. 2001. **79**(3): 213-221.

Yonezawa A, Morita R, Takaori-Kondo A, Kadowaki N, Kitawaki T, Hori T, Uchiyama T. Natural alpha interferon-producing cells respond to human immunodeficiency virus type 1 with alpha interferon production and maturation into dendritic cells. *JVirol.* 2003. **77**(6): 3777-3784.

Young CD and JB Angel. Optimization of culture and storage conditions for an in vitro system to evaluate thymocyte phenotype and function. *JImmunolMethods.* 2006. **312**(1-2): 157-166.

Young HA. Unraveling the pros and cons of interferon-gamma gene regulation. *Immunity*. 2006. **24**(5): 506-507.

Yu Q, Erman B, Bhandoola A, Sharrow SO, and Singer A. In vitro evidence that cytokine receptor signals are required for differentiation of double positive thymocytes into functionally mature CD8+ T cells. *JExpMed.* 2003. **197**(4): 475-87.

Zhou Y, Wang S, Gobl A, Oberg K. The interferon-alpha regulation of IRF-1 and IRF-2 has therapeutic implications of carcinoid tumors. *AnnOncol*. 2000. **11**(6): 707-714.

BIOGRAPHICAL SKETCH

Holly Meredith Kolenda-Roberts was born on July 6, 1973 in Cary, North Carolina. She attended Florida State University, graduating with a Bachelor of Science in Biological Sciences. She then attended the University of Florida, College of Veterinary Medicine and graduated with a Doctorate of Veterinary Medicine in 2000. She continued on at the University of Florida, pursuing a combined program for a residency in anatomic pathology and a doctoral degree in the laboratories of Drs. Calvin Johnson and Ayalew Mergia in the Department of Pathobiology, College of Veterinary Medicine. After graduation, she intends to pursue a career as a veterinary pathologist.